Strong migratory connectivity across meta-populations of sympatric North Atlantic seabirds

Benjamin Merkel[1,2,*], Sébastien Descamps[1], Nigel G Yoccoz[2], David Grémillet[3], Per Fauchald[4], Jóhannis Danielsen[5], Francis Daunt[6], Kjell Einar Erikstad[4,7], Aleksey V Ezhov[8,9], Mike P Harris[6], Maria Gavrilo[8,10], Svein-Håkon Lorentsen[11], Tone K Reiertsen[4], Geir H Systad[12], Þorkell Lindberg Þórarinsson[13], Sarah Wanless[6], Hallvard Strøm[1]

[1] Norwegian Polar Institute, Fram Centre, P.O. Box 6606 Langnes, 9296 Tromsø, Norway
[2] Department of Arctic and Marine Biology, University of Tromsø - The Arctic University of Norway, 9037 Tromsø, Norway
[3] Centre d'Ecologie Fonctionnelle et Evolutive, UMR 5175, CNRS - Université de Montpellier - Université Paul-Valéry Montpellier - EPHE, Montpellier, France & FitzPatrick Institute, DST-NRF Centre of Excellence at the University of Cape Town, Rondebosch 7701, South Africa.
[4] Norwegian Institute for Nature Research, Fram Centre, P.O. Box 6606 Langnes, 9296 Tromsø, Norway
[5] University of the Faroe Islands, Vestarabryggja 15, FO-100 Tórshavn, Faroe Islands
[6] Centre for Ecology & Hydrology, Bush Estate, Penicuik, Midlothian EH26 0QB, UK
[7] Centre for Biodiversity Dynamics, Department of Biology, Norwegian University of Science and Technology, 7491 Trondheim, Norway
[8] Association Maritime Heritage, Saint Petersburg, Russia
[9] Murmansk Marine Biological Institute, 17 str. Vladimirskaya, 183010 Murmansk, Russia
[10] National Park Russian Arctic, 57 Sovetskikh Kosmonavtove ave., Archangelsk, Russia
[11] Norwegian Institute for Nature Research, P.O. Box 5685 Sluppen, 7485 Trondheim, Norway
[12] Norwegian Institute for Nature Research, Thormøhlensgate 55, 5006 Bergen, Norway
[13] Northeast Iceland Nature Research Centre, Hafnarstétt 3, 640 Húsavík, Iceland
*Corresponding author, email: merkel.benjamin@gmail.com/ benjamin.merkel@npolar.no, phone: +47 777 50 573

Authorship: BM, HS, PF and SD designed the study; BM analysed the data with help from NGY and PF; BM wrote the paper with contributions from SD, DG, HS, PF and NGY; HS, SD, DG, JD, FD, KEE, AVE, MPH, MG, SHL, TKR, GHS, ÞLÞ, and SW provided data; All authors commented on later drafts of the manuscript.

Abstract

Identifying drivers of population trends in migratory species is difficult, as they can face many stressors while moving through different areas and environments during the annual cycle. To understand the potential of migrants for adjusting to perturbations, it is critical to study how different areas used during the annual cycle by different populations are connected via individual migration strategies (i.e. migratory connectivity). Using a large-scale tracking dataset of 662 individual seabirds from two sympatric auk meta-populations (common guillemots, *Uria aalge,* and Brünnich's guillemots, *Uria lomvia*) breeding in twelve colonies throughout the Northeast Atlantic, we found strong migratory connectivity, within and between species. This was apparent through a combination of seasonal space use and occupied environmental niches, grouping Brünnich's guillemot populations into two and common guillemot populations into five previously undescribed spatiotemporal clusters. Remarkably, common guillemot populations clustered in accordance with the variable population trends exhibited by the species, while Brünnich's guillemot populations are declining everywhere where known within the study area. Individuals from different breeding populations in both species were specialized in their space and environmental use, utilizing only a fraction of the potential species-wide range. Further, migratory connectivity varied among seasons, emphasising the variable constraints faced by both species during the different stages of their annual cycle. Our study highlights that considering spatiotemporal dynamics not only in space but also in occupied environmental niches, improves our understanding of migratory connectivity and thus population vulnerability in the context of global change.

Keywords: Environmental niche, inter-population mixing, large-scale spatiotemporal dynamics, light-level geolocation, murres, population spread, seasonality, *Uria aalge*, *Uria lomvia*

Introduction

Migration is a response to spatial and temporal fluctuations in resource availability during different phases of the annual cycle (Alerstam et al. 2003, Dingle and Drake 2007). It can be expressed by a multitude of strategies defined collectively as return journeys to one or several overwintering destinations after the breeding season (Newton 2008). Migratory animals face specific challenges in a rapidly changing world, such as loss of habitat, new physical barriers, overexploitation of seasonal food resources, and climate change impacts (Robinson et al. 2009, Wilcove and Wikelski 2008). Changes in the environment encountered by migrants outside their breeding season have the potential to affect population trends through, for example, an effect on individual survival (Gaston and Powell 2003, Webster et al. 2002). Hence, assessing the response of migratory species or populations to perturbations requires an understanding of migratory connectivity (Taylor and Norris 2010), which is the connection of different areas used by different populations during the annual cycle via migration strategies of individual migrants (Webster et al. 2002).

The concept of migratory connectivity can be divided into two spatial components: population spread and inter-population mixing (Finch et al. 2017). Population spread is a population-level trait that refers to the size of the geographic area occupied during different parts of the annual cycle, while inter-population mixing is a multi-population-level trait describing the extent to which individuals from a given breeding population mix with other populations (i.e. use the same areas) during the non-breeding period (Finch et al. 2017, Gilroy et al. 2016). Generally, higher population spread is associated with enhanced inter-population mixing (also termed “weak” connectivity) while lower population spread reduces inter-population mixing (i.e. “strong” connectivity). Strong migratory connectivity is necessary for differential population trends of geographically distinct breeding populations to be driven by factors away from the breeding sites (Kramer et al. 2018). Populations with smaller geographic spread have a limited variety of migratory movements and destinations and may thus be more vulnerable to perturbations than those with larger spread (Cresswell 2014, Gilroy et al. 2016).

The concept of migratory connectivity has so far focused on the geographic distribution of migrants but can be expanded to include their environmental niches. The niches used during the annual cycle can vary independently of the geographic area occupied as migrants move simultaneously in geographic space and among environmental conditions (Peters et al. 2017, Soberón 2007, Soberón and Nakamura 2009). Consequently, migrants moving in similar geographic space may potentially occupy different environmental niches and *vice versa* (Gómez et al. 2016, Peters et al. 2017). Populations utilizing many different environments are more likely to persist than those remaining

within similar environments regardless of the occupied geographic area (Davies et al. 2004, Lavergne et al. 2013, Thuiller et al. 2005). Consequently, whether or not the connectivity is expressed in terms of space use, realized environmental niche or both may have different consequences for the trajectories of the species. Moreover, in addition to the spatial and environmental aspects of migratory connectivity it is also important to consider its seasonal dynamics, i.e. not only *which* sites and environments are used, but also *when* they are used. This can have manifold consequences on individual fitness (e.g. through transmission of pathogens) and therefore population dynamics (Bauer et al. 2016, Eyres et al. 2017, La Sorte et al. 2018).

Migratory connectivity is increasingly being studied in different taxa (Fayet et al. 2017, Frederiksen et al. 2016, Frederiksen et al. 2012, Godley et al. 2010, Rooker et al. 2008, Russell et al. 2013) due to the growing availability of large tracking datasets (Hussey et al. 2015, Kays et al. 2015) with a main focus on terrestrial birds (reviewed in Finch et al. 2017, Hahn et al. 2013, Kramer et al. 2018, Taylor and Stutchbury 2016), where weak migratory connectivity is most commonly reported (Finch et al. 2017). However, migratory connectivity has been addressed only within species and only in terms of space use rather than with respect to temporal variability and occupied environmental niches. Here, we assessed year round spatial and environmental migratory connectivity within and between two sympatric circumpolar seabird species, the temperate common guillemot (hereafter COGU, *Uria aalge*) and the arctic Brünnich's guillemot (hereafter BRGU, *Uria lomvia*). These two auk species share similar morphology and life history (Benowitz-Fredericks and Kitaysky 2005, Gaston and Jones 1998). Their energetic costs for flight are among the highest recorded for any vertebrate (Elliott et al. 2013) suggesting severe constraints upon large-scale movement capabilities and high sensitivity towards habitat loss (Taylor and Norris 2010). Guillemots also exhibit contrasting population trends in the Atlantic, with colonies of BRGUs generally declining within the Northeast Atlantic and those of COGUs exhibiting more variable trends (table 1, Anker-Nilssen et al. 2017, Fauchald et al. 2015, Frederiksen 2010, Frederiksen et al. 2016, Garðarsson et al. 2019, JNCC 2016). Some evidence exists that population trends as well as adult survival in *Uria* spp. are associated with environmental conditions experienced during the non-breeding period (Descamps et al. 2013, Fluhr et al. 2017, Gaston and Powell 2003, Mesquita et al. 2015) and that Atlantic-wide BRGU population trends are connected to mid-winter space use (Frederiksen et al. 2016).

Divergent population trends for these congeneric seabirds make them an ideal study system to investigate the importance of space and environmental connectivity across the migratory phase (Gilroy et al. 2016, Taylor and Norris 2010, Webster et al. 2002). To characterise migratory connectivity and the potential link to population trends in *Uria* spp., we tracked the annual movements of 327 adult COGUs and 335 adult BRGUs from twelve breeding populations,

representing the entire breeding range of the Northeast Atlantic population. To evaluate migratory connectivity, in terms of inter-population mixing and population spread, within and across species we not only considered the geographic areas occupied, but also the environmental conditions experienced and their variability during different phases of the annual cycle.

Material & Methods

Study species & area

Guillemots are large (~1kg), deep diving (up to ~200m), long lived, colonial seabirds with high adult survival, high breeding philopatry, high breeding synchrony and low annual fecundity (Benowitz-Fredericks and Kitaysky 2005, Gaston and Jones 1998). Their non-breeding period can be divided into several seasons corresponding to different life history stages throughout the annual cycle. Post-breeding, successful males stay with their flightless chicks for at least a month after colony departure (Elliott et al. 2017, Harris and Wanless 1990). Further, guillemots undergo moulting of their primaries and secondaries during one to two months in the autumn post-breeding which renders them flightless during this time period (Birkhead and Taylor 1977, Bridge 2004, Elliott and Gaston 2014, Thompson et al. 1998). Both species display periodic synchronized attendances at their breeding colonies starting up to several months prior to breeding (Gaston and Nettleship 1981) which in effect restricts them to central place foraging during this period. Hence, adult guillemots are only able to move without constraints for extended periods of time after they have renewed their flight feathers and before the pre-breeding colony attendance period starts.

Research was conducted at 16 seabird colonies spanning 56°N to 80°N and 16°W to 68°E in the Northeast Atlantic (table 1, figure 1A). For the purpose of this study we combined some colonies in close spatial proximity to each other (< 160 km) which exhibited similar space use patterns. This resulted in twelve breeding populations. BRGU and COGU breed sympatrically at four of these sites (table 1).

Tracking data

We used archival light-level loggers to estimate spatiotemporal locations of guillemot individuals throughout the non-breeding period. These devices record light intensity and time which can be used to estimate approximate latitude (i.e. day length) and longitude (i.e. time of noon) positioning twice daily (estimated accuracy: ~180 km, Merkel et al. 2016). They are attached to a leg band with cable ties (logger, band, and cable ties < 0.5% adult body mass) and need to be retrieved in subsequent

years after deployment for data to be downloaded. During the summers of 2007 to 2017 we captured adult guillemots with noose poles at different sites and equipped them with geolocators which we retrieved in subsequent years (overall retrieval rate > 60%). Individuals were chosen opportunistically in most cases among birds breeding on cliff ledges on the landward edge of the colony. This resulted in 1103 annual tracks (531 BRGU, 572 COGU) of 662 individual guillemots (335 BRGU, 327 COGU, table 1). All subsequent analyses have been conducted in R 3.3.3 (R Development Core Team 2017). All loggers (Mk15: British Antarctic Survey, Cambridge, UK; Mk3006: Biotrack, Wareham, UK; F100, C250 & C330: Migrate Technology, Cambridge, UK; or L250A: Lotek, St. John's, Newfoundland, Canada) also recorded temperature and salt water immersion ("wet/dry") data which were used in combination with recorded light data to increase location accuracy. We calculated a most probable movement track for each individual and tracking year using an iterative approach utilizing probability sampling (Merkel et al. 2016 and details in SI 1). We binned the positional data into four seasons - irrespective of year tracked (assuming no inter-annual variation in the average non-breeding distributions, PAPER III) - to capture possible variability due to life history stages throughout the annual cycle. The delimitation of these seasons was based on assessment of core time periods in which little movement was observed across all individuals from all colonies and both species resulting in: autumn (10 August - 28 September), early winter (18 November - 6 January), late winter (17 January - 25 February), and spring (27 March - 25 May). We assume that autumn describes the post-breeding-moulting period; the two winter seasons capture temporal variability in movement behaviour during times without movement restrictions for most breeding populations; and spring is characterized by central place foraging restrictions due to pre-breeding attendance at most colonies.

Location estimation in both species and all breeding populations were to varying degrees affected by a lack of twilight events due to the polar night or midnight sun (table S2). Such cases concerned individuals using areas above 66°N, generally in the Barents Sea. Although sample size in some populations was potentially not sufficient to capture their entire distributional range (table 1), they nonetheless represent adequately the potential variability of exhibited migration strategies.

Environmental niche

To quantify environmental niches occupied during the non-breeding period, we used eight ecologically relevant oceanographic parameters (Fort et al. 2009, Fort et al. 2013b, McFarlane Tranquilla et al. 2015); three sea surface temperature variables, two sea surface height variables, surface air temperature, distance to the marginal sea ice zone and bathymetry (details in SI 1). The environment occupied was then assessed using the concept of environmental space (Broennimann et

al. 2012) defined as the first two axes of a principal component analysis (PCA) of all environmental parameters calibrated on the available environment. To capture the variability of the available environment, we sampled 20000 points with equal spatial coverage across the entire study area (figure S2) every two weeks for the entire study period (2007-2017). The study area was defined as 18 large marine ecoregions (hereafter ecoregions, Skjoldal et al. 2013) encompassed by the annual distribution of both guillemot species in the Atlantic (Cramp 1985, Gaston and Jones 1998) (figure 1A). Ecoregions are large regions of ocean space along coasts and continental shelfs characterised by specific ecological criteria (Skjoldal et al. 2013). To accommodate the aforementioned distributions, three additional areas in the middle of the North Atlantic away from continental shelfs were defined (Labrador Sea, Mid-Atlantic, and Central North Atlantic). All individual positions were projected onto the PCA (PC1 = 44% & PC2 = 19%, figure S3). Available and occupied environmental space were then calculated using Gaussian kernel utilization distributions (UD, standard bandwidth, 200 x 200 pixel grid, `adehabitatHR` package, Calenge 2006) following Broennimann et al. (2012).

Large-scale spatiotemporal inter-population mixing

To quantify large-scale inter-population mixing and species wide spatiotemporal movement partitions we developed species-specific movement networks using network theory (Taylor and Norris 2010). All calculated bird positions were assigned to ecoregions. We then used the proportion of locations in each ecoregion in each season in seasonal cluster analysis (complete-linkage clustering) to assign each individual to a given ecoregion. To avoid pseudo-replication we used only one year of tracking, randomly selected, for each individual with repeated tracks. Optimal number of clusters was determined using overall average silhouette width (Borcard et al. 2018) for each season. For individuals affected by midnight sun conditions during the spring season we included the proportion of locations unavailable due to a lack of twilight events in the cluster analysis. Similarly, for the few instances where individuals during early winter had no locations, due to polar night influence (table S2), birds were assumed to use the ecoregion “Barents Sea”. Each breeding population present in the network was given the same weight and considered to be a node in the network (eight per species). Next, each individual in a given population got a proportional weight based on the total available tracks from that population. These scaled movements (network edges) between ecoregions and seasons (network nodes) were combined to create species-specific movement networks.

To identify possible partitioning within each species-specific network we used a Walktrap community finding algorithm (finding clusters via random walks with five steps taking into account the proportional movement between ecoregions and seasons, `igraph` package, Csardi & Nepusz 2006).

This method also returns a modularity index that ranges from 0 to 1 (the closer to 1, the more the network exhibits clustering with respect to the given node grouping). A network is considered to exhibit significant cluster structuring above a value of 0.3 (Clauset et al. 2004). Total number and proportional use of population- and species-specific most common migration strategies were identified as unique individual movement paths through each network. A high number of strategies and low proportion of individuals following the most common strategy would indicate weak migratory connectivity (the opposite would be true for strong migratory connectivity). In addition, a species-wide Mantel correlation was used as an independent method to quantify migratory connectivity (Ambrosini et al. 2009, Cohen et al. 2018), and was computed for individual ten day centroid locations throughout the non-breeding period to assess the robustness of our results (details in SI 1).

Meso-scale inter-population mixing

Individual seasonal kernel UDs in geographic space were estimated with 25 km grid resolution in polar stereographic projection and a bandwidth of 30 based on a median least square cross-validation score of all individual- and season-specific kernel UDs. In order to test whether geographic space use is population-specific or homogenous between different populations and species in each ecoregion and season, we calculated the average overlap as Bhattacharyya's affinity (Fieberg and Kochanny 2005): 1) between four random individual kernel UDs from the same population occupying the same ecoregion, and 2) between four random individual kernel UDs of the two populations compared (two individuals each). This process was repeated 1000 times for both pairs in the comparison. We used this test for all populations of either species with at least four individuals present in the same ecoregion and season. The resulting comparisons were summed to species- (within and between species*, sp*) and cluster-specific (within and across clusters, *c*) proportions of inter-population mixing within ecoregions (*P*) for each season (*t*) ranging from 0 (populations segregate) to 1 (populations mix) using:

$$\mathrm{P}_{\mathrm{sp,c,t}} = 1 - \frac{\mathrm{N}_{\mathrm{sig,sp,c,t}}}{\mathrm{N}_{\mathrm{all,sp,c,t}}} \qquad \text{(Eq. 1)}$$

where, *N* is the number of considered comparisons, *sig* denotes only comparisons where within population overlap of either comparisons pairs is significantly greater than between population overlap (one tailed t-test with Bonferroni corrected significance level, p=0.05/number of correlation tests) and *all* denotes all comparisons. Ecoregion-, species- and season-specific Mantel correlations were calculated to assess the robustness of these results with an independent method (details in SI 1).

Intra- and inter-population mixing of occupied environmental niches

In order to quantify inter-population mixing of ecoregion-, species- and population-specific environmental niches occupied in each season we used the niche similarity test (Warren et al. 2008). This test compares two occupied niches and addresses whether niche 1 is more similar to the compared niche 2 than would be expected by chance. The niche as kernel UD in environmental space of one comparison pair was randomly relocated within the available environmental space while retaining the UD's shape (1000 permutations for each comparison pair). Overlap between observed niches as well as the randomly relocated and observed niches was than calculated using Schoener's D (Broennimann et al. 2012). If the observed overlap is greater than 95% of the randomly relocated niches, the compared environments are considered to be more similar than expected by chance. We tested similarity between ecoregion-, species- and population-specific environmental spaces in each season to assess migratory connectivity in environmental space as well as niche partitioning between species. These environmental similarities together with the proportional use of different ecoregion by populations are then integrated into an environmental similarity index (*S*). This index is ranging from 0 (all birds occupy distinct environments) to 1 (all birds occupy a similar environment) and is computed for each species (*sp*), population (*c*) and season (*t*) as:

$$S_{sp,c,t} = \frac{\max\left(PR_{sp,c,t,1\&2}\right)^2 + \sum_{sig}\left(PR_{sp,c,t,1} \times PR_{sp,c,t,2}\right)}{\max\left(PR_{sp,c,t,1\&2}\right)^2 + \sum_{all}\left(PR_{sp,c,t,1} \times PR_{sp,c,t,2}\right)} \qquad \text{(Eq. 2)}$$

where, *PR* is the proportional use of the compared nodes (*1* & *2*), *sig* denotes only comparisons with similar environments (one way is considered sufficient, i.e. $\text{niche } 1 \cong \text{niche } 2 \mid \text{niche } 2 \cong \text{niche } 1$) and *all* denotes all comparisons. As compared environmental spaces are population-, species- and in particular ecoregion-specific, we included a maximum term in equation 2 to account for the uneven distribution of a given population across ecoregions (figure S4). However, this term is not applicable and hence removed to compute the same index between populations and/or clusters (*c1* & *c2*) of the same species or between species (*sp1* & *sp2,* figure S4) resulting in:

$$S_{sp,c,t} = \frac{\sum_{sig}\left(PR_{sp1,c1,t} \times PR_{sp2,c2,t}\right)}{\sum_{all}\left(PR_{sp1,c1,t} \times PR_{sp2,c2,t}\right)} \qquad \text{(Eq. 3)}$$

Population spread

To quantify species and population spread in space and the environment we calculated the occupied geographic and environmental space as the area covered by all relevant individual and seasonal 90% kernel UD contours in each season as well as the entire non-breeding period (all seasons combined).

Results

Large-scale spatiotemporal inter-population mixing

Both species exhibited marked spatial clustering on a large spatiotemporal scale with distinct annual migration strategies and strong migratory connectivity. Five and two distinct clusters (modularity of 0.59 and 0.36 indicating significant clustering) describing the non-breeding distribution were identified for COGU and BRGU, respectively (table 1, figure 1B/C). These clusters were also visible in each season (figure 2, SI 2) and corresponded to their population trends (i.e. COGU populations whose individuals are part of the same cluster during the non-breeding season show the same trend, table 1). For BRGU - declining all over our study area- a migratory divide was seen along the western Barents Sea edge splitting Spitsbergen BRGU populations (figure 2). Breeding populations to the west of this divide spent the autumn along eastern Greenland and move towards Iceland and western Greenland during winter while birds breeding in the rest of the Barents Sea utilized the Barents and Kara Sea during autumn and generally stayed there year round, with the exception of Bjørnøya individuals (figure S3.13). Increasing COGUs populations in the Barents Sea and decreasing populations in the Greenland and Icelandic Sea also grouped into these clusters, whereas populations in the Faroe Islands (decreasing trend), and the one along the coast of Norway (increasing trend) and eastern UK (increasing trend) displayed distinct migration strategies (table 1, figure 1 & 2). Both species exhibited little inter-population mixing between their identified clusters and COGU even less so than BRGU (table S4). An exception was visible for COGU in the Barents Sea where a varying proportion of birds from all breeding populations (except Iceland) congregated during autumn (figure 1B & 2A). Species-wide Mantel correlation was also high (> 0.5) throughout the entire non-breeding period for both species (figure S5) confirming the identified strong migratory connectivity.

Each species utilized only a small fraction of potential migration strategies (indicating strong migratory connectivity) with BRGUs (60 unique strategies = 16% of possible paths through the network given the sample size) displaying more strategies than COGUs (40 = 9%) while both species combined only displayed 91 unique strategies (11%) on this large spatiotemporal scale. At the breeding population-level, a variable, but low amount of migration strategies were displayed with birds from the North-East and North Sea clusters showing little variability (table 1). Most tracked individuals followed the most common population-specific strategy. Most variability in spatiotemporal use was visible for individuals in the Mid-West cluster, in particular for BRGUs (table 1, SI 3).

Meso-scale inter-population mixing

Individuals from a given population and species were more likely to encounter conspecifics from their own population than an individual from a different population and/or species, which occupied the same ecoregion (figure 3). During autumn, BRGUs from all populations showed population-specific space use, while COGUs mixed to some extent (figure 1B, 3). Most homogenous space use (mixing) was visible within species for individuals from the Mid-West cluster (around Greenland and Iceland). Here, principally during winter, individuals from different populations mixed within the same ecoregion occupied. Most between species-mixing was apparent during spring (figure 3), particularly for sympatrically breeding populations (figure S6). Ecoregion-specific Mantel correlation analysis corroborated these results (figure S5).

Environmental intra- and inter-population mixing and species segregation

Both species were composed of populations and clusters occupying distinct environments and hence, exhibited little inter-population mixing in occupied environmental niches. Individuals from the same population and species occupied similar environments with most variability present during winter (figure 4). BRGU populations in the Mid-West cluster - utilizing a vast area - inhabited similar environments (figure 4). In contrast, BRGU populations in the North-East cluster inhabited distinct environments throughout the non-breeding period. COGU clusters generally occupied cluster-specific environments with most variability displayed for populations in the Mid-West cluster. Differential segregation between the two sympatrically breeding species in space and sometimes environment experienced was to a variable extent displayed during all seasons, except spring (figure 4 & S6). But, the two congeneric species in the Mid-West cluster exhibited more environmental niche mixing than in the North-East cluster.

Population spread

The observed strong migratory connectivity in geographic and environmental space was also visible in species and population spread in both spaces. Compared to COGUs, BRGUs dispersed over a wider area which is characterized by more heterogeneous environments in all seasons (figure 5). For none of the breeding populations did individuals ever utilize the entire space or environment occupied by a species. However, BRGU populations generally spread out over more space and environments compared to COGU populations (figure 5). Both species exhibited more concentrated space use during autumn and spring and spread out more in the winter seasons. This pattern was also apparent at the population-level. Finally, neither species utilized its entire annual occupied range in space or the environment during any given season (figure 5).

Discussion

Our analysis of meta-population-level migratory connectivity for the genus *Uria* revealed that COGUs exhibit strong migratory connectivity - in terms of low inter-population mixing and low population spread - with population space use during the non-breeding period corresponding to their population trends. Populations of BRGUs - which are generally declining in the Northeast Atlantic (Anker-Nilssen et al. 2017, Frederiksen et al. 2016) - also show rather strong migratory connectivity and cluster into two distinct groups which have not been described previously (Frederiksen et al. 2016). Compared to COGUs, the BRGU meta-population spreads out into a wider space, characterized by more heterogeneous environments (McFarlane Tranquilla et al. 2015) and exhibits more mixing between the study populations also within ecoregions. Further, in all populations where the two species breed sympatrically, they segregate in space and often in environmental use during the non-breeding period. Generally, guillemot space use as well as environments occupied were species- and population-specific with low spatiotemporal variability. This suggests that both species are comprised of space and environmental niche specialist populations. Overall, a strong seasonal pattern in space use and environmental spread was apparent. This pattern was likely driven by life history stages of the annual cycle of the two species.

The correlation between population trends and identified migration strategy clusters in *Uria* spp. (shown for COGU in this study and for BRGU in Frederiksen et al. 2016) as well as the spatial and to some extent environmental isolation between these clusters suggests that their population trends are linked to their non-breeding distributions (Desprez et al. 2018). Alternatively, population trends might be affected by conditions during the breeding period (through a change in breeding success and propensity), although this is unlikely due to the large distance between breeding populations (Frederiksen et al. 2016). Intra- and inter-specific competition for food are predicted to play a key role in shaping population and meta-population-scale migratory strategies (Svanbäck and Bolnick 2007). Such competition may explain why the studied populations exhibited such strong connectivity and in addition seldom travelled towards the Grand Banks and the Labrador shelf during the non-breeding periods. These areas have already been identified as major seabird wintering hotspots (Fayet et al. 2017, Fort et al. 2013a, Frederiksen et al. 2012, Montevecchi et al. 2012) in particular for Canadian and West Greenland guillemot populations (Frederiksen et al. 2016, McFarlane Tranquilla et al. 2013). Guillemots breeding in the Northeast Atlantic may avoid these areas to limit the competition for food. Alternatively, the Grand Banks and Labrador shelf may be outside the migratory range for these populations. Due to extremely high flight costs (Elliott et al. 2013), *Uria* spp. have a theoretical maximum migratory range of ~3400 km from their respective breeding sites (Watanabe 2016). The Grand Banks and Labrador would thus be outside this range for all populations

included in this study, with the exception of the Icelandic population. Only ten BRGU annual tracks (~2% of all BRGU tracks) and no COGU track exceeded the theoretical migration range. These ten tracks were mainly from individuals utilizing the Grand Banks and the Labrador Shelf; range: 3500 - 4600 km). This supports the hypothesis that migration distance is a limiting factor for guillemots.

The relative location of colonies to prevailing surface currents might influence breeding population-specific migration strategies, especially during autumn when both sexes are flightless and successfully breeding males accompany a flightless chick (Frederiksen et al. 2016). However, we have a poor understanding of the ontogeny of individual migration patterns and the relative roles of genetics (Liedvogel et al. 2011) and social learning therein (Jesmer et al. 2018, Keith and Bull 2017, Senner et al. 2015). Culturally acquired knowledge (Grémillet et al. 2004, Guilford et al. 2011) or the lack thereof of different historically adequate staging areas (Thorup et al. 2017, Van Moorter et al. 2016) during different seasons coupled with high flight costs (Elliott et al. 2013) and a morphologically determined maximum migration range (Watanabe 2016) as well as density-dependent competition (Alerstam and Hedenström 1998, Svanbäck and Bolnick 2007) could explain the high population-specificity and low diversity of COGU and BRGU migration strategies. In order to test this, it is essential to combine information about movement patterns of immatures and their parents, and to enhance knowledge about potential genetic differences between breeding populations. In addition, to what extent individual migration patterns are fixed or adaptive to environmental changes over an individual's life time needs to be further investigated (Senner et al. 2015) in order to test inter-annual repeatability in individual migratory behaviour (McFarlane Tranquilla et al. 2014), and in turn to better assess population level impacts of environmental change (Irons et al. 2008).

Migratory strategies evolved in order to take advantage of seasonal, energetically favourable food resources and in order to avoid unfavourable conditions (Bridge et al. 2015). Different prey species or populations might be targeted by individuals with different strategies. These in turn might be influenced by different environmental conditions and changes in these conditions (Beaugrand and Kirby 2018, Carscadden et al. 2013, Fossheim et al. 2015, Rose 2005) resulting in migration strategies linked to specific population trends, as recently documented in Atlantic puffins (*Fratercula arctica*, Fayet et al. 2017), *Vermivora* warblers (Kramer et al. 2018) and Wood thrushes (*Hylocichla mustelina*, Taylor and Stutchbury 2016). Migratory plasticity is predicted to buffer populations against perturbations at local and regional scales (Betini et al. 2015, Cresswell 2014, Gilroy et al. 2016). Here, we demonstrated strong migratory connectivity and often little variability among individual migration strategies across all study populations and both species suggesting only limited capacity to buffer against local and regional perturbations. We also demonstrated that individuals from the

same breeding population and occupying different spaces tended to occupy environments with similar abiotic conditions, which may explain their general susceptibility to regional (e.g. sea level pressure, Mesquita et al. 2015, Vader et al. 1990) and large-scale climatic features (e.g. the North Atlantic subpolar gyre, Descamps et al. 2013, Fluhr et al. 2017). Variability in environmental space is implied within the population spread component of migratory connectivity, when larger spread is assumed to be associated with more diverse environments experienced by a population (Finch et al. 2017, Gilroy et al. 2016). However, we showed that variability in geographic area does not necessarily lead to variability in environmental space. Hence, an assessment of environmental variability in addition to migratory connectivity is needed to evaluate population responses to perturbations. In both species space use was most restricted during autumn and spring, with concomitantly low variability in environmental characteristics. This suggests critically low capacity to adjust to perturbations during these periods, under the constraints set by the breeding cycle (such as molt of their flight feathers and pre-breeding colony attendance, Desprez et al. 2018, Dias et al. 2011).

Conclusion

We provide evidence of strong migratory connectivity within and between two congeneric seabird species at an ocean basin scale and highlight the importance of considering not only space use, but also its seasonality and occupied environmental niches. Birds from different populations and species are specialized in both their seasonal space and environmental use, utilizing only a fraction of the potential species-wide range. Crucially, these spatiotemporal dynamics are concordant to population trends. This emphasizes the importance of migratory connectivity and the environmental conditions experienced during the non-breeding period as drivers of population dynamics in migratory species, particularly in the context of global change.

Acknowledgments

Funding for this study was provided by the Norwegian Ministry for Climate and the Environment, the Norwegian Ministry of Foreign Affairs and the Norwegian Oil and Gas Association through the SEATRACK project (www.seapop.no/en/seatrack) as well as from the Research Council of Norway (project 216547), TOTAL E&P Norway and the TOTAL Foundation and the UK Natural Environment Research Council's National Capability. We would like to thank Børge Moe, Hálfdán Helgi Helgason and Vegard Sandøy Bråthen for the logistical support within SEATRACK. This work would not have

444 been possible without the combined effort and long term engagement of many researchers as well
445 as numerous field assistants all across the Northeast Atlantic.

446

447 Supplementary information

448 • SI 1: Additional method information, results & Mantel correlation analysis
449 • SI 2: Species- and breeding population-specific seasonal distributions in geographic and environmental
450 space
451 • SI 3: Species- and breeding population-specific large-scale spatiotemporal movement networks

452

453 References

454 Alerstam and Hedenström 1998. The Development of Bird Migration Theory. — Journal of Avian
455 Biology 29: 343-369.
456 Alerstam et al. 2003. Long-distance migration: evolution and determinants. — Oikos 103: 247-260.
457 Amante and Eakins 2009. ETOPO1 1 Arc-Minute Global Relief Model: Procedures, Data Sources and
458 Analysis. NOAA Technical Memorandum NESDIS NGDC-24. National Geophysical Data Center,
459 NOAA. .
460 Ambrosini et al. 2009. A quantitative measure of migratory connectivity. — Journal of Theoretical
461 Biology 257: 203-211.
462 Anker-Nilssen et al. 2017. Sjøfugl i Norge 2017. — In: Anker-Nilssen, T. (ed), Resultater fra SEAPOP
463 programmet. pp. 1-28.
464 Bauer et al. 2016. Timing is crucial for consequences of migratory connectivity. — Oikos 125: 605-
465 612.
466 Beaugrand and Kirby 2018. How Do Marine Pelagic Species Respond to Climate Change? Theories
467 and Observations. — Annual Review of Marine Science 10: 169-197.
468 Benowitz-Fredericks and Kitaysky 2005. Benefits and costs of rapid growth in common murre chicks
469 Uria aalge. — Journal of Avian Biology 36: 287-294.
470 Betini et al. 2015. Experimental evidence for the effect of habitat loss on the dynamics of migratory
471 networks. — Ecology Letters 18: 526-534.
472 Birkhead and Taylor 1977. MOULT OF THE GUILLEMOT *URIA AALGE*. — Ibis 119: 80-85.
473 Borcard et al. 2018. Numerical ecology with R. — Springer.
474 Bridge 2004. The effects of intense wing molt on diving in alcids and potential influences on the
475 evolution of molt patterns. — Journal of Experimental Biology 207: 3003-3014.
476 Bridge et al. 2015. Do molt-migrant songbirds optimize migration routes based on primary
477 productivity? — Behavioral Ecology 27: 784-792.
478 Broennimann et al. 2012. Measuring ecological niche overlap from occurrence and spatial
479 environmental data. — Global Ecology and Biogeography 21: 481-497.
480 Calenge 2006. The package “adehabitat” for the R software: A tool for the analysis of space and
481 habitat use by animals. — Ecological Modelling 197: 516-519.

Carscadden et al. 2013. A comparison of recent changes in distribution of capelin (*Mallotus villosus*) in the Barents Sea, around Iceland and in the Northwest Atlantic. — Progress in Oceanography 114: 64-83.
Clauset et al. 2004. Finding community structure in very large networks. — Physical Review E 70: 066111.
Cohen et al. 2018. Quantifying the strength of migratory connectivity. — Methods Ecol. Evol. 9: 513-524.
Cramp 1985. The Birds of the Western Palearctic.Vol. IV. — Oxford University Press.
Cresswell 2014. Migratory connectivity of Palaearctic–African migratory birds and their responses to environmental change: the serial residency hypothesis. — Ibis 156: 493-510.
Csardi and Nepusz 2006. The igraph software package for complex network research. — InterJournal, Complex Systems 1695: 1-9.
Davies et al. 2004. A SYNERGISTIC EFFECT PUTS RARE, SPECIALIZED SPECIES AT GREATER RISK OF EXTINCTION. — Ecology 85: 265-271.
Descamps et al. 2013. Decline of an arctic top predator: synchrony in colony size fluctuations, risk of extinction and the subpolar gyre. — Oecologia 173: 1271-1282.
Desprez et al. 2018. Linking oceanographic conditions, migratory schedules and foraging behaviour during the non-breeding season to reproductive performance in a long-lived seabird. — Functional Ecology 32: 2040-2053.
Dias et al. 2011. Breaking the routine: individual Cory's shearwaters shift winter destinations between hemispheres and across ocean basins. — Proceedings of the Royal Society B-Biological Sciences 278: 1786-1793.
Dingle and Drake 2007. What is migration? — Bioscience 57: 113-121.
Elliott and Gaston 2014. Dive behavior and daily energy expenditure in Thick-billed Murres Uria lomvia after leaving the breeding colony. — Mar Ornithol 42: 183-189.
Elliott et al. 2017. Variation in Growth Drives the Duration of Parental Care: A Test of Ydenberg's Model. — The American Naturalist 189: 526-538.
Elliott et al. 2013. High flight costs, but low dive costs, in auks support the biomechanical hypothesis for flightlessness in penguins. — Proceedings of the National Academy of Sciences 110: 9380-9384.
Eyres et al. 2017. Quantification of climatic niches in birds: adding the temporal dimension. — Journal of Avian Biology 48: 1517-1531.
Fauchald et al. 2015. The status and trends of seabirds breeding in Norway and Svalbard. — In: Fauchald, P. (ed), NINA Rapport. NINA, pp. 1-84.
Fayet et al. 2017. Ocean-wide Drivers of Migration Strategies and Their Influence on Population Breeding Performance in a Declining Seabird. — Current Biology 27: 3871-3878.
Fieberg and Kochanny 2005. QUANTIFYING HOME-RANGE OVERLAP: THE IMPORTANCE OF THE UTILIZATION DISTRIBUTION. — The Journal of Wildlife Management 69: 1346-1359.
Finch et al. 2017. Low migratory connectivity is common in long-distance migrant birds. — Journal of Animal Ecology 86: 662-673.
Fluhr et al. 2017. Weakening of the subpolar gyre as a key driver of North Atlantic seabird demography: a case study with Brünnich's guillemots in Svalbard. — Marine Ecology Progress Series 563: 1-11.

Fort et al. 2013a. Multicolony tracking reveals potential threats to little auks wintering in the North Atlantic from marine pollution and shrinking sea ice cover. — Diversity and Distributions 19: 1322-1332.
Fort et al. 2009. Thermodynamic modelling predicts energetic bottleneck for seabirds wintering in the northwest Atlantic. — The Journal of Experimental Biology 212: 2483-2490.
Fort et al. 2013b. Energetic consequences of contrasting winter migratory strategies in a sympatric Arctic seabird duet. — Journal of Avian Biology 44: 255-262.
Fossheim et al. 2015. Recent warming leads to a rapid borealization of fish communities in the Arctic. — Nature Climate Change 5: 673.
Frederiksen 2010. Seabirds in the North East Atlantic. Summary of status, trends and anthropogenic impact. — TemaNord 21-24.
Frederiksen et al. 2016. Migration and wintering of a declining seabird, the thick-billed murre *Uria lomvia*, on an ocean basin scale: Conservation implications. — Biol. Conserv. 200: 26-35.
Frederiksen et al. 2012. Multicolony tracking reveals the winter distribution of a pelagic seabird on an ocean basin scale. — Diversity and Distributions 18: 530-542.
Garðarsson et al. 2019. The numbers of large auks on the cliffs of Iceland in 2006-2008. — Bliki 33: 35-46.
Gaston and Jones 1998. Bird families of the world. The Auks Alcidae. Oxford University Press, Oxford.
Gaston and Nettleship 1981. The thick-billed murres of Prince Leopold Island. — Canadian Wildlife Service Ottawa.
Gaston and Powell 2003. SYNCHRONOUS FLUCTUATIONS OF THICK-BILLED MURRE (URIA LOMVIA) COLONIES IN THE EASTERN CANADIAN ARCTIC SUGGEST POPULATION REGULATION IN WINTER. — The Auk 120: 362-370.
Gilroy et al. 2016. Migratory diversity predicts population declines in birds. — Ecology Letters 19: 308-317.
Godley et al. 2010. Unravelling migratory connectivity in marine turtles using multiple methods. — Journal of Applied Ecology 47: 769-778.
Gómez et al. 2016. Niche-tracking migrants and niche-switching residents: evolution of climatic niches in New World warblers (*Parulidae*). — Proceedings of the Royal Society B: Biological Sciences 283:
Grémillet et al. 2004. Offshore diplomacy, or how seabirds mitigate intra-specific competition: a case study based on GPS tracking of Cape gannets from neighbouring colonies. — Marine Ecology Progress Series 268: 265-279.
Guilford et al. 2011. A Dispersive Migration in the Atlantic Puffin and Its Implications for Migratory Navigation. — PLoS One 6: e21336.
Hahn et al. 2013. Strong migratory connectivity and seasonally shifting isotopic niches in geographically separated populations of a long-distance migrating songbird. — Oecologia 173: 1217-1225.
Harris and Wanless 1990. Breeding Status and Sex of Common Murres (Uria aalge) at a Colony in Autumn. — The Auk 107: 603-605.
Hussey et al. 2015. Aquatic animal telemetry: A panoramic window into the underwater world. — Science 348:
Irons et al. 2008. Fluctuations in circumpolar seabird populations linked to climate oscillations. — Global Change Biology 14: 1455-1463.

569 Jakobsson et al. 2012. The International Bathymetric Chart of the Arctic Ocean (IBCAO) Version 3.0.
570 — Geophysical Research Letters 39:
571 Jesmer et al. 2018. Is ungulate migration culturally transmitted? Evidence of social learning from
572 translocated animals. — Science 361: 1023-1025.
573 JNCC 2016. Seabird Population Trends and Causes of Change: 1986-2015 Report. — In: JNCC (ed),
574 Joint Nature Conservation Committee.
575 Kays et al. 2015. Terrestrial animal tracking as an eye on life and planet. — Science 348:
576 Keith and Bull 2017. Animal culture impacts species' capacity to realise climate-driven range shifts. —
577 Ecography 40: 296-304.
578 Kramer et al. 2018. Population trends in *Vermivora* warblers are linked to strong migratory
579 connectivity. — Proceedings of the National Academy of Sciences 115:
580 La Sorte et al. 2018. Seasonal associations with novel climates for North American migratory bird
581 populations. — Ecology Letters 21: 845-856.
582 Lavergne et al. 2013. Are species' responses to global change predicted by past niche evolution? —
583 Philosophical Transactions of the Royal Society B: Biological Sciences 368:
584 Liedvogel et al. 2011. The genetics of migration on the move. — Trends Ecol. Evol. 26: 561-569.
585 McFarlane Tranquilla et al. 2014. Individual Winter Movement Strategies in Two Species of Murre
586 (*Uria* spp.) in the Northwest Atlantic. — PLoS One 9:
587 McFarlane Tranquilla et al. 2013. Multiple-colony winter habitat use by murres *Uria* spp. in the
588 Northwest Atlantic Ocean: implications for marine risk assessment. — Marine Ecology
589 Progress Series 472: 287-303.
590 McFarlane Tranquilla et al. 2015. Ecological segregation among Thick-billed Murres (*Uria lomvia*) and
591 Common Murres (*Uria aalge*) in the Northwest Atlantic persists through the nonbreeding
592 season. — Canadian Journal of Zoology 93: 447-460.
593 Merkel et al. 2016. A probabilistic algorithm to process geolocation data. — Movement Ecology 4: 26.
594 Mesquita et al. 2015. There is more to climate than the North Atlantic Oscillation: a new perspective
595 from climate dynamics to explain the variability in population growth rates of a long-lived
596 seabird. — Frontiers in Ecology and Evolution 3:
597 Montevecchi et al. 2012. Tracking seabirds to identify ecologically important and high risk marine
598 areas in the western North Atlantic. — Biol. Conserv. 156: 62-71.
599 Newton 2008. The Migration Ecology of Birds. — Academic Press.
600 Peters et al. 2017. Migration in geographic and ecological space by a large herbivore. — Ecological
601 Monographs 87: 297-320.
602 R Development Core Team 2017. R: A language and environment for statistical computing. R
603 Foundation for Statistical Computing.
604 Robinson et al. 2009. Travelling through a warming world: climate change and migratory species. —
605 Endangered Species Research 7: 87-99.
606 Rooker et al. 2008. Natal Homing and Connectivity in Atlantic Bluefin Tuna Populations. — Science
607 322: 742-744.
608 Rose 2005. On distributional responses of North Atlantic fish to climate change. — ICES J. Mar. Sci.
609 62: 1360-1374.
610 Russell et al. 2013. Uncovering the links between foraging and breeding regions in a highly mobile
611 mammal. — Journal of Applied Ecology 50: 499-509.
612 Senner et al. 2015. An ontogenetic perspective on individual differences. — Proceedings of the Royal
613 Society B: Biological Sciences 282:

614 Skjoldal et al. 2013. Large Marine Ecosystems (LMEs) of the Arctic area - Revision of the Arctic LME
615 map
616 Soberón 2007. Grinnellian and Eltonian niches and geographic distributions of species. — Ecology
617 Letters 10: 1115-1123.
618 Soberón and Nakamura 2009. Niches and distributional areas: Concepts, methods, and assumptions.
619 — Proceedings of the National Academy of Sciences 106: 19644-19650.
620 Svanbäck and Bolnick 2007. Intraspecific competition drives increased resource use diversity within a
621 natural population. — Proceedings of the Royal Society B: Biological Sciences 274: 839-844.
622 Taylor and Norris 2010. Population dynamics in migratory networks. — Theoretical Ecology 3: 65-73.
623 Taylor and Stutchbury 2016. Effects of breeding versus winter habitat loss and fragmentation on the
624 population dynamics of a migratory songbird. — Ecological Applications 26: 424-437.
625 Thompson et al. 1998. An Unusual Sequence of Flight-Feather Molt in Common Murres and Its
626 Evolutionary Implications. — The Auk 115: 653-669.
627 Thorup et al. 2017. Resource tracking within and across continents in long-distance bird migrants. —
628 Science Advances 3: e1601360.
629 Thuiller et al. 2005. Niche properties and geographical extent as predictors of species sensitivity to
630 climate change. — Global Ecology and Biogeography 14: 347-357.
631 Vader et al. 1990. Differential responses of common and thick-billed murres to a crash in the capelin
632 stock in the southern Barents Sea. — Studies in Avian Biology 14: 175-180.
633 Van Moorter et al. 2016. Movement is the glue connecting home ranges and habitat selection. —
634 Journal of Animal Ecology 85: 21-31.
635 Warren et al. 2008. Environmental Niche Equivalency versus Conservatism: Quantitative Approaches
636 to Niche Evolution. — Evolution 62: 2868-2883.
637 Watanabe 2016. Flight mode affects allometry of migration range in birds. — Ecology Letters 19: 907-
638 914.
639 Webster et al. 2002. Links between worlds: unraveling migratory connectivity. — Trends Ecol. Evol.
640 17: 76-83.
641 Wilcove and Wikelski 2008. Going, Going, Gone: Is Animal Migration Disappearing. — PLOS Biology 6:
642 e188.

643

Tables and figures

Table 1. Available tracking data, published population trends, identified migration clusters, number of annual movement strategies (as unique paths through the networks in figure 1) and relative use of most common migration strategy for each breeding population and species. Some colonies (in parentheses if applicable) have been merged into populations for the purpose of this study. Tracking years denote first and last year of tracking and include gap years in many cases.

breeding population (colonies)	acronym	location	breeding population ecoregion	Common guillemot (COGU)				Brünnich's guillemot (BRGU)				cluster	# of unique strategy		% using most common strategy	
				population trend	tracking years	annual tracks	unique birds	population trend	tracking years	annual tracks	unique birds		COGU	BRGU	COGU	BRGU
Isle of May	IM	56.18°N, 2.58°W	North Sea	increasing[1,7]	2011-16	70	39	-	-	-	-	North Sea	5	-	90 %	-
Faroe Islands (Lonin)	FA	61.95°N, 6.80°W	Faroe Plateau	decreasing[2,7]	2015-16	5	5	-	-	-	-	Faroe Islands	4	-	40 %	-
Sklinna	SK	65.22°N, 10.97°E	Norwegian Sea	increasing[3,8]	2011-16	63	39	-	-	-	-	Norwegian coast	10	-	56 %	-
North-East Iceland (Grimsey, Langanes)	IC	66.44°N, 15.80°W	Iceland Shelf & Sea	decreasing[4,9]	2014-16	27	22	decreasing[4,9]	2014-16	27	24	Mid-West	6	12	78 %	46 %
Jan Mayen	JM	71.02°N, 8.52°W	Greenland Sea	decreasing[5,10]	2011-16	70	39	decreasing[5,10]	2011-16	94	54	Mid-West	15	18	24 %	29 %
Western Spitsbergen (Diabasodden, John Scottfjellet, Ossian Sarsfjellet)	WSP	78.75°N, 13.20°E	Barents Sea	-	-	-	-	decreasing[5,8]	2007-16	104	74	Mid-West	-	18	-	51 %
Hjelmsøya	HJ	71.07°N, 24.72°E	Barents Sea	increasing[5,8]	2011-16	41	27	-	-	-	-	North-East	3	-	90 %	-
Southern Barents Sea (Cape Gorodetskiy, Hornøya)	SBS	69.98°N, 32.04°E	Barents Sea	increasing[5,8]	2011-16	120	75	decreasing[6,8]	2009-16	97	64	North-East	4	15	93 %	78 %
Bjørnøya	BI	74.50°N, 18.96°E	Barents Sea	increasing[5,8]	2007-16	176	81	decreasing[5,8]	2007-16	134	59	North-East	1	13	100 %	34 %
Eastern Spitsbergen (Alkefjellet)	ESP	79.59°N, 18.46°E	Barents Sea	-	-	-	-	unknown	2015-17	14	13	North-East	-	2	-	79 %
Northern Novaya Zemlya (Oranskie islands)	NNZ	77.07°N, 67.64°E	Barents Sea	-	-	-	-	unknown	2016-17	6	6	North-East	-	2	-	74 %
Southern Novaya Zemlya (Kara Gate)	SNZ	70.59°N, 55.02°E	Barents Sea	-	-	-	-	unknown	2015-17	55	41	North-East	-	2	-	67 %

[1] (JNCC 2016), [2] (Frederiksen 2010), [3] other colonies along the Norwegian coast are decreasing as well as increasing (Fauchald *et al.* 2015; Anker-Nilssen *et al.* 2017), [4] (Frederiksen 2010; Garðarsson *et al.* in press), [5] (Fauchald *et al.* 2015; Frederiksen *et al.* 2016; Anker-Nilssen *et al.* 2017), [6] based on declining trend of Hjelmsøya BRGUs (Fauchald *et al.* 2015; Frederiksen *et al.* 2016; Anker-Nilssen *et al.* 2017), [7] 15 year trend, [8] 10 year trend, [9] 20 year trend, [10] 7 year trend

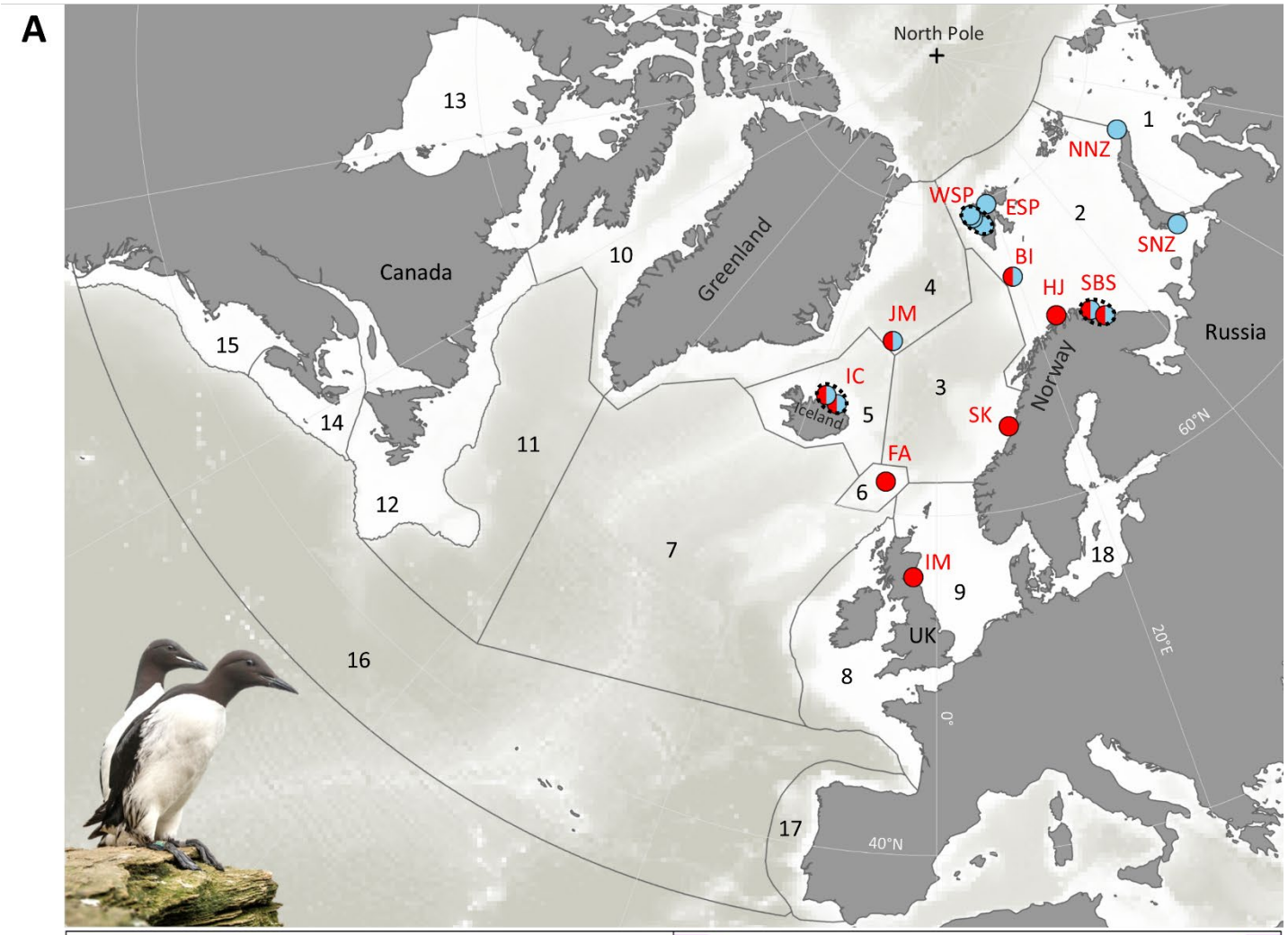
A
North Pole
13
1
NNZ
WSP
ESP
2
SNZ
10
Canada
Greenland
BI
4
HJ
SBS
JM
Russia
15
IC
3
Norway
Iceland
5
SK
60°N
14
11
FA
6
12
7
IM
18
9
UK
16
8
20°E
0°
17
40°N

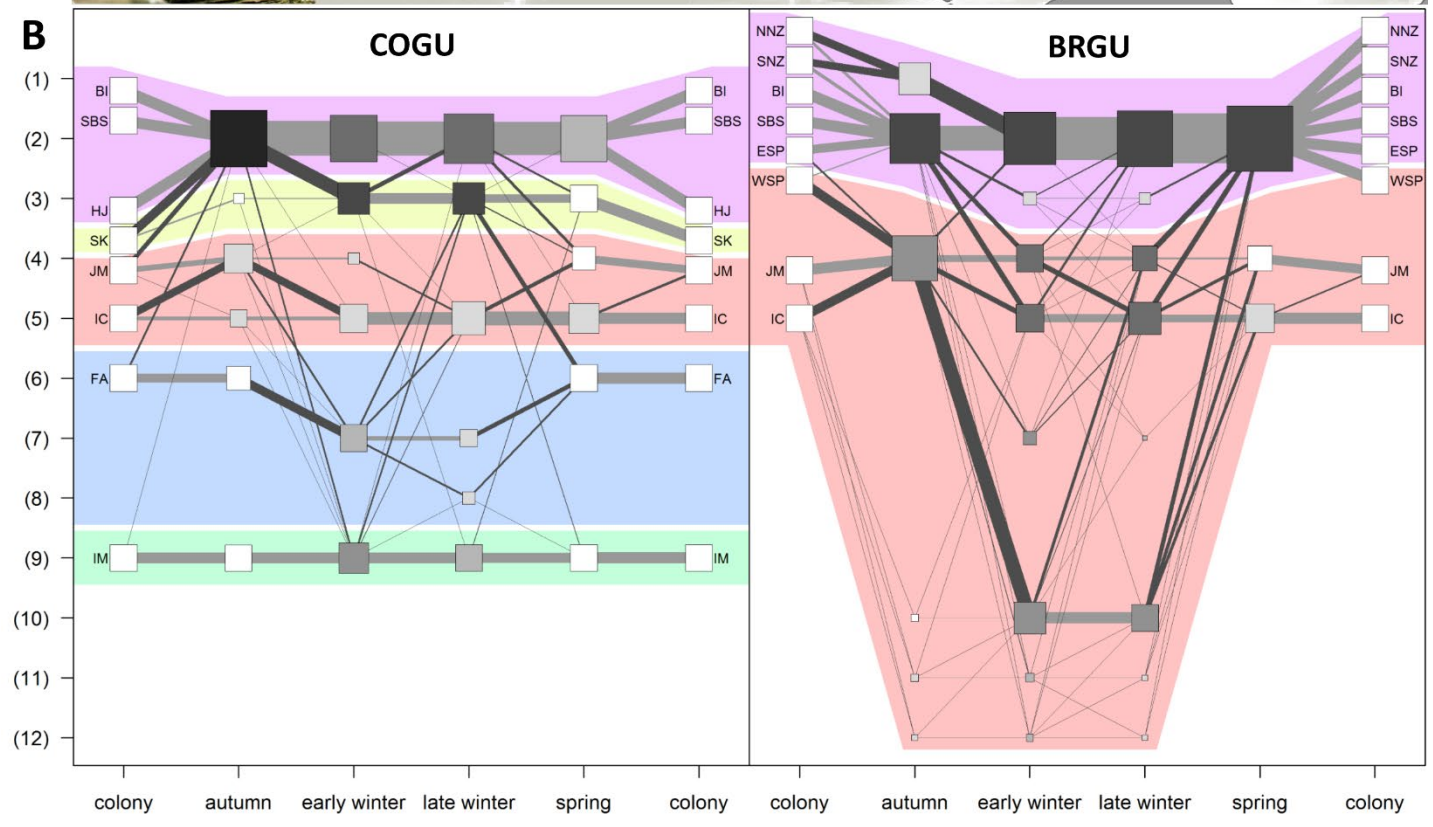
B
COGU
BRGU
(1)
(2)
(3)
(4)
(5)
(6)
(7)
(8)
(9)
(10)
(11)
(12)
BI
SBS
HJ
SK
JM
IC
FA
IM
NNZ
SNZ
ESP
WSP
colony
autumn
early winter
late winter
spring
colony

Figure 1. Panel A displays the **s**tudy area (in polar stereographic projection) with bathymetry (Amante & Eakins 2009; Jakobsson *et al.* 2012) and all large marine ecoregions included in the study. Circles denote study colonies with different colours indicating the presence of the two species (red = COGU, blue = BRGU, names detailed in table 1). Colonies combined for the purpose of this study are encircled with dashed ellipsoids. Panel B displays movement networks for both guillemot species by ecoregion (numbering corresponds to Panel A) and season. Each breeding population is scaled to the same size, while all nodes (squares) and edges (lines) are scaled to their proportional usage accordingly. Nodes are color-coded by number of populations present from white (only individuals from one population present) to black (8). Coloured areas in the background display identified clusters (5 for COGU, 2 for BRGU).

Ecoregions: 1 = Kara Sea, 2 = Barents Sea, 3 = Norwegian Sea, 4 = Greenland Sea, 5 = Iceland Sea & Shelf, 6 = Faroe Plateau, 7 = Central North Atlantic, 8 = Celtic-Biscay Shelf, 9 = North Sea, 10 = West Greenland & Canada East Arctic, 11 = Labrador Sea, 12 = Newfoundland & Labrador Shelf (including the Grand Banks), 13 = Hudson Bay Complex, 14 = Scotian Shelf, 15 = Northeast US Continental Shelf, 16 = Mid-Atlantic, 17 = Iberian Coastal, 18 = Baltic Sea.

Figure 2. Seasonal distributions (in polar stereographic projection) for COGU and BRGU during autumn, early winter, late winter and spring. Kernel utilization distributions (UD) show seasonal space use by breeding population as composite of individual UDs scaled to their respective population sample size. High colour intensity indicate use by several populations. Dots display colony locations. Dotted and solid circles indicate areas where location estimation was affected by or impossible due to polar night or midnight sun, respectively. Grey stippled and solid areas display 15% and 90% ten year seasonal median sea ice concentration, respectively. Insets in bottom left of each panel display seasonal environmental space occupied by each individual and breeding population (darker colours) as centre (dots) with variance (crosses). Stippled lines represent 100% and 50% kernel UD contours of available environmental space in the North Atlantic over 11 years. Colours correspond to spatiotemporal clusters identified by network analysis (figure 1).

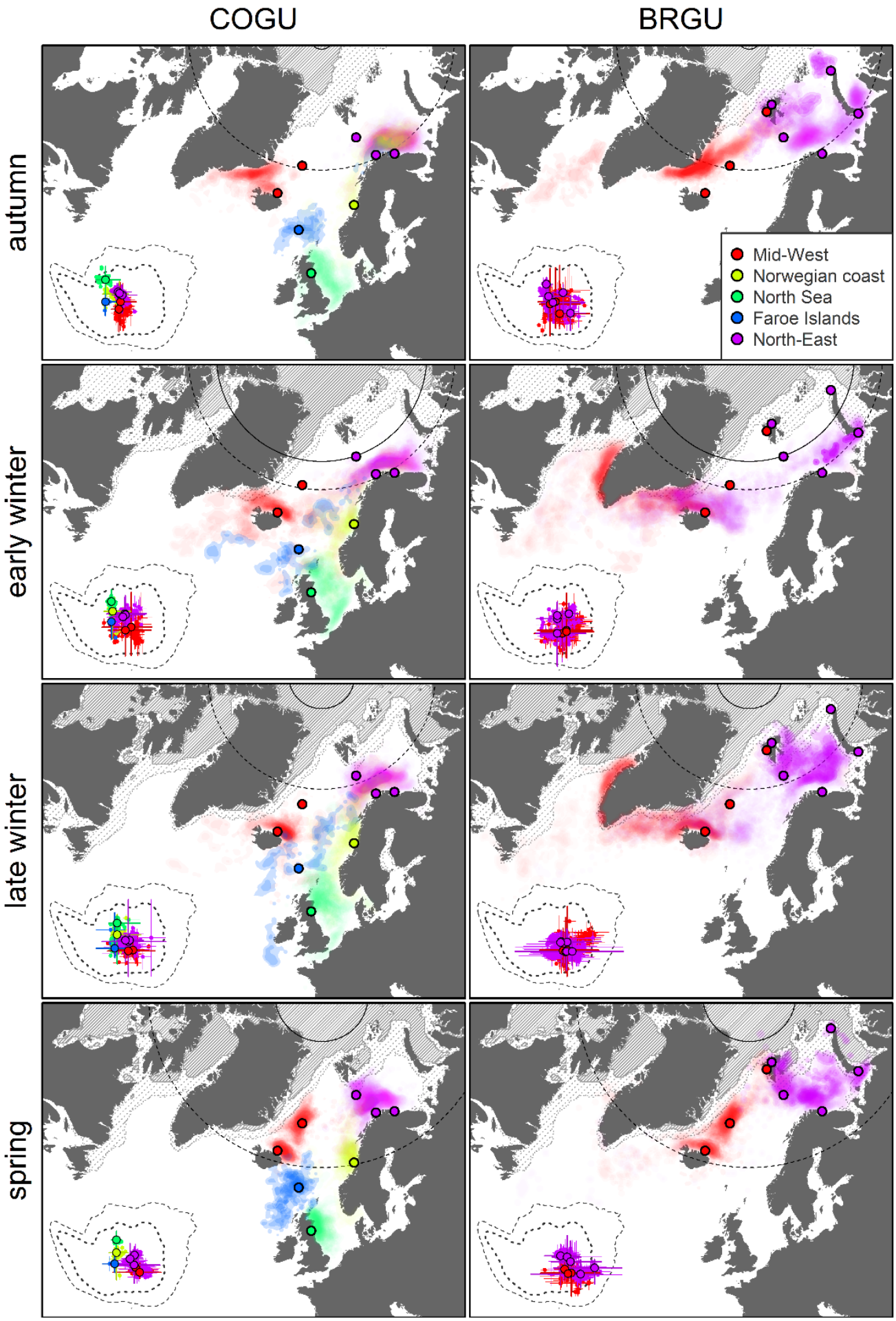
COGU
BRGU
autumn
early winter
late winter
spring
Mid-West
Norwegian coast
North Sea
Faroe Islands
North-East

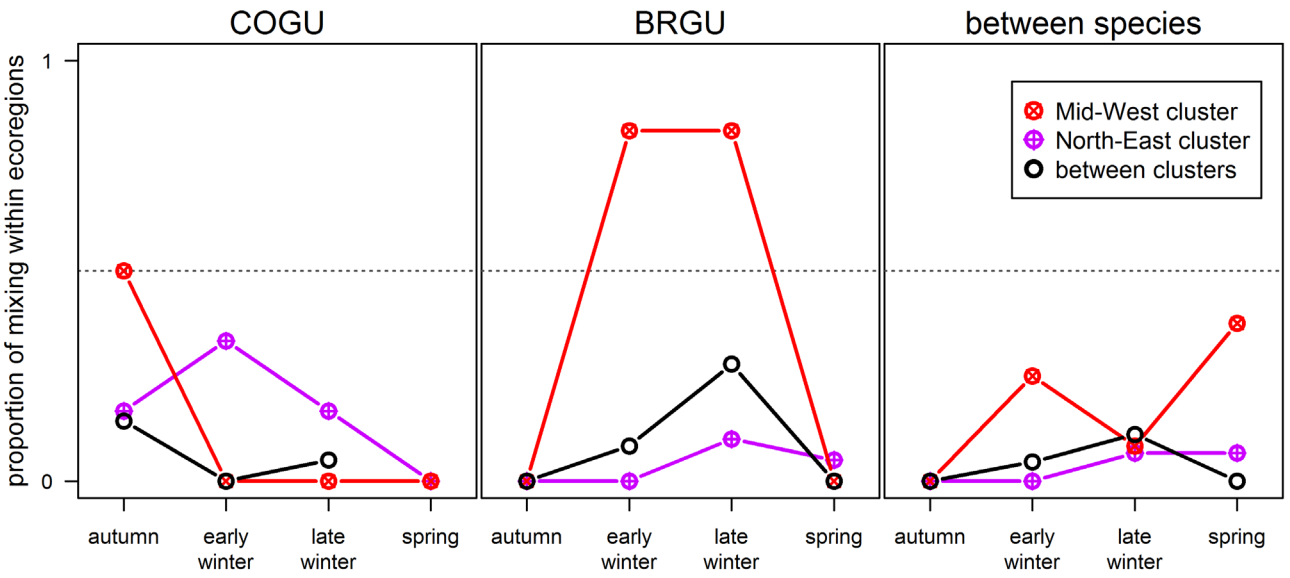

Figure 3. Overall seasonal proportion of inter-population mixing of individuals from different populations occupying the same ecoregion and belonging to the same species or different species (Equation 1). This index ranges from 0 (individuals from different populations and occupying the same ecoregion segregate) to 1 (individuals from different populations and occupying the same ecoregion mix). Colours denote comparisons within and between identified clusters. No COGU populations belonging to different clusters occupied the same ecoregion during spring (figure 1). Consequently, no proportion of mixing could be estimated. Inter-population mixing could only be calculated for the Mid-West and the North-East clusters as the other three clusters only consist of one population each.

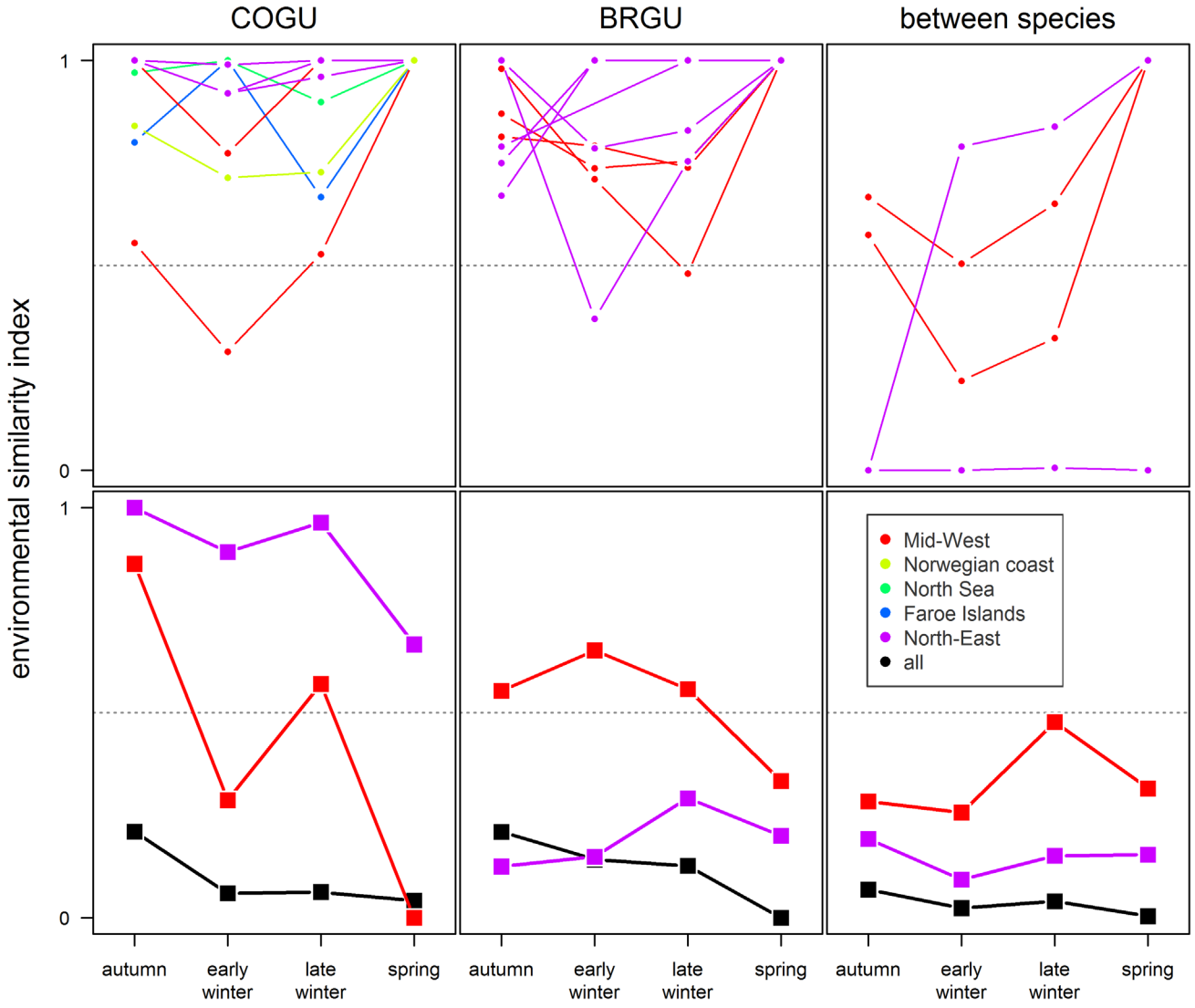

Figure 4. Environmental similarity index by season within and between species. This index is ranging from 0 (all birds occupy distinct environments) to 1 (all birds occupy a similar environment) and quantifies the seasonal inter-population mixing of ecoregion-, species- and population-specific environmental niches. Top panels (with small circles) show single population estimates, while bottom panels (with bigger squares) show comparative environmental similarities within clusters (i.e. between populations) or for all clusters combined (black).

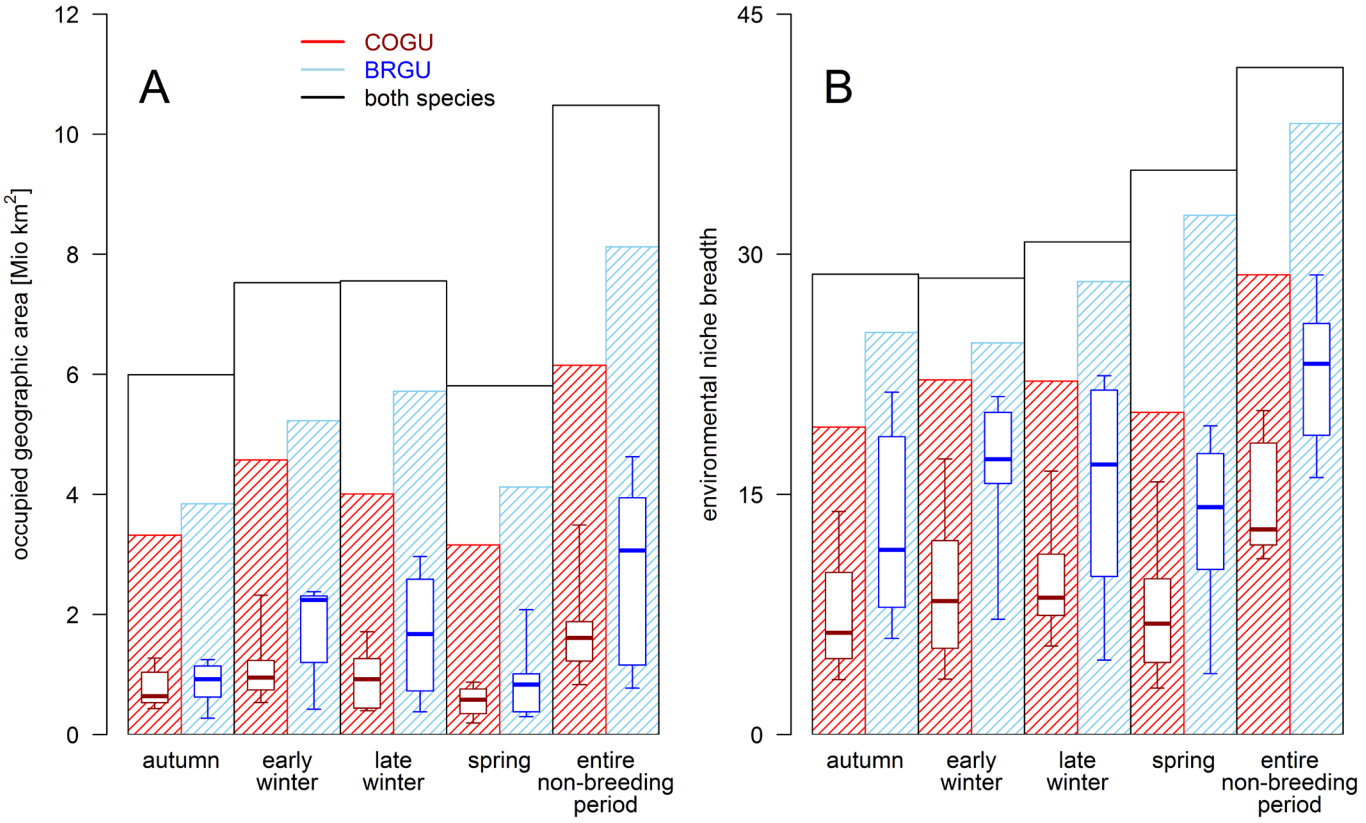

Figure 5. Size of the occupied geographic (A) and environmental space (B) in each season and both species combined as well as for COGU and BRGU. Bar plots denote the size of the entire occupied seasonal space (meta-population spread) while each boxplot displays the range of area occupied by each breeding population. Box plots illustrate 25th, 50th (median), and 75th percentiles, and error bars represent minimum and maximum values.

Supplementary information 1

Supplementary Methods

Location estimation from light-level loggers

Estimated timings of sunrise and sunset (transition times) were computed from light data using TransEdit2 (British Antarctic Survey/BAS, Cambridge, UK), and the `twilightCalc` function (`GeoLight` package; Lisovski & Hahn 2012) in R 3.3.3 (R Development Core Team 2017) for BAS, Migrate Technology and Biotrack loggers. Transition times were visually inspected for loggers retrieved during 2014-2017 by the same person. Lotek loggers did not retain raw light intensity data, but rather calculated and recorded latitudes and longitudes based on an on-board algorithm which has been shown to be biased (Frederiksen *et al.* 2016). Therefore we used these threshold method (Lisovski & Hahn 2012) derived positions to back calculate transition times using the `lotek_to_dataframe` function (`probGLS` package; Merkel *et al.* 2016). Daily experienced sea surface temperature (SST) was estimated from raw logged temperature data using the `sst_deduction` function (`probGLS` package) with a possible range of -2 to 20°C for Lotek loggers and -2 to 40°C for all other brands.

A most probable track for each individual and tracking year was calculated using an iterative method utilizing probability sampling detailed in Merkel *et al.* (2016) and implemented in the `prob_algorithm` function (`probGLS` package). Input data were logger recorded transition times, salt water immersion data as well as calculated daily recorded SST data. Daily optimal interpolated high resolution satellite derived SST, SST uncertainty estimates and sea ice concentration data for the algorithm with a 0.25° resolution were provided by NOAA (Boulder, Colorado, US; Reynolds *et al.* 2007). To improve precision we included land avoidance, an inability to enter the Baltic Sea (except for Common guillemots from the Isle of May) and an evasion of heavy pack ice (>90% sea ice concentration). Each movement path incorporated parameter values based on the ecology of the species and the oceanographic conditions in the North Atlantic (table S1). Usually, it is not possible to estimate latitude during times of equinox as day length (the proxy for latitude) is very similar everywhere on earth. However, this methodology is able to estimate locations also during times of equinox by among other things utilizing the recorded temperature data and comparing them to satellite derived sea surface temperature (SST) fields. Due to small north-south gradients in SST in certain areas of the North Atlantic (e.g. the Gulf Stream along the Norwegian coast) we limited the boundary box parameter in `prob_algorithm` for certain individuals and colonies after initial

assessment of their movement track (table S1). Each computed track was afterwards visually inspected and erroneous locations particularly around polar night and midnight sun were removed (<1 % of all locations).

Environmental parameters

All chosen environmental parameters used to calculate the environmental space and their rational are listed in table S3. Fronts in sea surface temperature (SST) and sea surface height anomaly fields were calculated using a canny edge detector (package `imager`, low & high threshold at 90% & 98%, respectively). Bathymetry was log-transformed and all distance measurements were capped at 500 km as well as square root-transformed. Predictability in SST was calculated as the sum of constancy and contingency following Colwell (1974) over a ten year time period (2007-2016) with 10 equal bins using the `hydrostats` package (figure S1). All variables have been standardized (variance = 1, mean = 0).

Mantel correlation analysis

Following Cohen *et al.* (2018) we calculated species-specific Mantel correlations to validate our migratory connectivity results with an independent method. All individual annual tracks were split into 10 day bins starting 1 July. A resolution of 10 days was chosen to retain a sufficient number of locations for each bin for further analysis. Migratory connectivity for each species was quantified using Mantel correlation tests with 1000 permutations (Ambrosini *et al.* 2009). More specifically, the distance between individual breeding locations was compared to the distance between their current locations throughout the non-breeding season for each 10 day bin (as central location in each 10 day bin). For this analysis only data from the last three years of tracking was used (2014/15 - 2016/17). To avoid pseudo-replication only one year of tracking for each repeat track individual was used. Further, ecoregion- and season-specific Mantel correlation tests were computed - for ecoregions with individuals from more than one population present during the focal time period - to assess the area and season specific connectivity for each species. Results are illustrated in figure S3.

Supplementary references

Amante, C. & Eakins, B.W. (2009). ETOPO1 1 Arc-Minute Global Relief Model: Procedures, Data Sources and Analysis. NOAA Technical Memorandum NESDIS NGDC-24. National Geophysical Data Center, NOAA. Last accessed 17.07.2015.

Ambrosini, R., Møller, A.P. & Saino, N. (2009). A quantitative measure of migratory connectivity. *Journal of Theoretical Biology*, 257, 203-211.

Berrisford, P., Dee, D., Poli, P., Brugge, R., Fielding, K., Fuentes, M. *et al.* (2011). The ERA-Interim archive Version 2.0, ERA Report Series 1, ECMWF, Shinfield Park. *Reading, UK*, 13177.

Biotrack (2013). M-Series Geolocator User Manual V11.
Cavalieri, D.J., Parkinson, C.L., Gloersen, P., Comiso, J.C. & Zwally, H.J. (1999). Deriving long-term time series of sea ice cover from satellite passive-microwave multisensor data sets. *Journal of Geophysical Research: Oceans*, 104, 15803-15814.
Cohen, E.B., Hostetler, J.A., Hallworth, M.T., Rushing, C.S., Sillett, T.S. & Marra, P.P. (2018). Quantifying the strength of migratory connectivity. *Methods Ecol. Evol.*, 9, 513-524.
Colwell, R.K. (1974). Predictability, Constancy, and Contingency of Periodic Phenomena. *Ecology*, 55, 1148-1153.
Elliott, K.H. & Gaston, A.J. (2005). Flight speeds of two seabirds: a test of Norberg's hypothesis. *Ibis*, 147, 783-789.
Fort, J., Porter, W.P. & Grémillet, D. (2009). Thermodynamic modelling predicts energetic bottleneck for seabirds wintering in the northwest Atlantic. *The Journal of Experimental Biology*, 212, 2483-2490.
Frederiksen, M., Descamps, S., Erikstad, K.E., Gaston, A.J., Gilchrist, H.G., Grémillet, D. *et al.* (2016). Migration and wintering of a declining seabird, the thick-billed murre *Uria lomvia*, on an ocean basin scale: Conservation implications. *Biol. Conserv.*, 200, 26-35.
Jakobsson, M., Mayer, L., Coakley, B., Dowdeswell, J.A., Forbes, S., Fridman, B. *et al.* (2012). The International Bathymetric Chart of the Arctic Ocean (IBCAO) Version 3.0. *Geophysical Research Letters*, 39.
Lisovski, S. & Hahn, S. (2012). GeoLight – processing and analysing light-based geolocator data in R. *Methods Ecol. Evol.*, 3, 1055-1059.
Lisovski, S., Hewson, C.M., Klaassen, R.H.G., Korner-Nievergelt, F., Kristensen, M.W. & Hahn, S. (2012). Geolocation by light: accuracy and precision affected by environmental factors. *Methods Ecol. Evol.*, 3, 603-612.
Lumpkin, R. & Johnson, G.C. (2013). Global ocean surface velocities from drifters: Mean, variance, El Niño–Southern Oscillation response, and seasonal cycle. *Journal of Geophysical Research: Oceans*, 118, 2992-3006.
Merkel, B., Phillips, R.A., Descamps, S., Yoccoz, N.G., Moe, B. & Strøm, H. (2016). A probabilistic algorithm to process geolocation data. *Movement Ecology*, 4, 26.
R Development Core Team (2017). R: A language and environment for statistical computing. R Foundation for Statistical Computing Vienna, Austria.
Reynolds, R.W., Smith, T.M., Liu, C., Chelton, D.B., Casey, K.S. & Schlax, M.G. (2007). Daily High-Resolution-Blended Analyses for Sea Surface Temperature. *Journal of Climate*, 20, 5473-5496.
Scales, K.L., Miller, P.I., Hawkes, L.A., Ingram, S.N., Sims, D.W. & Votier, S.C. (2014). REVIEW: On the Front Line: frontal zones as priority at-sea conservation areas for mobile marine vertebrates. *Journal of Applied Ecology*, 51, 1575-1583.

Supplementary Tables and Figures

Table S1. `probGLS` algorithm input parameters used to compute locations. standard deviation = sd

algorithm parameter	description	value used
`particle.number`	number of particles computed for each point cloud	2000
`iteration.number`	number of track iterations	100
`loess.quartile`	remove outliers in transition times based on local polynomial regression fitting processes (Lisovski & Hahn 2012)	used with k = 10
`sunrise.sd & sunset.sd`	shape, scale and delay values describing the assumed uncertainty structure for each twilight event following a log normal distribution	2.49/ 0.94/ 0[1]
`range.solar`	range of solar angles used	-7° to -1° (except for C250 logger from SK: -4° to -2°)
`boundary.box`	the range of longitudes and latitudes likely to be used by tracked individuals	90°W to 120°E & 40°N to 81°N; except for 91% COGU tracks from IM with 40°N to 62°N; all COGU from BI and 94% COGU SK tracks with 60°N to 77°N; 6% SK tracks with 50°N to 77°N
`day.around.spring.equinox` & `days.around.fall.equinox`	number of days before and after an equinox event in which a random latitude will be assigned	spring: 21 days before & 14 days after autumn: 14 days before & 21 days after
`speed.dry`	fastest most likely speed, speed sd and maximum speed allowed when the logger is not submerged in sea water	17/ 4/ 30 m/s[2]
`speed.wet`	fastest most likely speed, speed sd and maximum speed allowed when the logger is submerged in sea water	1/ 1.3/ 5 m/s[3]
`sst.sd`	logger-derived sea surface temperature (SST) sd	0.5°C[4]
`max.sst.diff`	maximum tolerance in SST variation	3°C
`east.west.comp`	compute longitudinal movement compensation for each set of twilight events (Biotrack 2013)	used

[1] These parameters are chosen as they resemble the twilight error structure of open habitat species in Lisovski *et al.* (2012).
[2] inferred from GPS tracks (unpublished data) and (Elliott & Gaston 2005)
[3] North Atlantic current speed up to fast current speeds (i.e. East Greenland current) (Lumpkin & Johnson 2013) as the tagged animal is assumed to not actively move when the logger is immerged in seawater
[4] logger temperature accuracy

Table S2. Proportion of locations missing in each season mainly due to lack of twilight events caused by midnight sun (seasons: autumn and spring) or polar night (early and late winter) for each breeding population as well as mean and standard deviation (sd) across populations. Breeding populations: SNZ = Southern Novaya Zemlya, NNZ = Northern Novaya Zemlya, ESP = Eastern Spitsbergen, WSP = Western Spitsbergen, BI = Bjørnøya, SBS = Southern Barents Sea, HJ = Hjelmsøya, SK = Sklinna, JM = Jan Mayen, IC = Northeast Iceland, FA = Faroe Islands, IM = Isle of May

species	season	breeding populations											mean	sd
		IM	FA	SK	IC	JM	WSP	HJ	BI	SBS	ESP	SNZ	NNZ		
BRGU	autumn	-	-	-	15 %	13 %	39 %	-	29 %	15 %	58 %	11 %	47 %	29 %	17 %
	early winter	-	-	-	6 %	1 %	1 %	-	5 %	36 %	100 %	20 %	97 %	33 %	39 %
	late winter	-	-	-	0 %	2 %	1 %	-	3 %	4 %	29 %	1 %	8 %	6 %	9 %
	spring	-	-	-	30 %	45 %	73 %	-	63 %	45 %	91 %	51 %	81 %	60 %	19 %
COGU	autumn	1 %	2 %	10 %	0 %	8 %	-	12 %	14 %	4 %	-	-	-	6 %	5 %
	early winter	1 %	1 %	9 %	0 %	5 %	-	51 %	34 %	39 %	-	-	-	18 %	19 %
	late winter	1 %	0 %	1 %	1 %	3 %	-	2 %	5 %	2 %	-	-	-	2 %	2 %
	spring	4 %	12 %	14 %	31 %	46 %	-	44 %	48 %	27 %	-	-	-	28 %	16 %

Table S3. Parameter chosen to describe the environmental space.

parameter	temporal resolution	spatial resolution	rational	data source
bathymetry	static	0.25°	predictable productivity on continental shelfs	ETOPO1 & IBCAO[1]
surface air temperature	daily	0.75°	influences energy requirements[2]	ECMWF[3]
sea surface temperature (SST)	daily	0.25°	water mass indicator & physiological constraint[2]	NOAA OI SST V2[4]
SST predictability (figure S2)	static	0.25°	identifier of spatially variable SST features across seasons and years (e.g. persistent frontal systems[5])	NOAA OI SST V2[4]
minimum distance to 15%, 50% & 90% sea ice concentrations	daily	0.25°	descriptor of marginal sea ice zone	NSIDC[6]
sea surface height (SSH)	daily	0.25°	descriptor of the locations of large-scale features such as gyres and fronts	AVISO[7]
distance to SSH anomaly gradients	daily	0.25°	distance to meso-scale eddies as spatially dynamic sources of upwelling	AVISO[7]
distance to SST gradient	daily	0.25°	distance to meso- and large-scale temperature fronts[5]	NOAA OI SST V2[4]

[1] (Amante & Eakins 2009; Jakobsson *et al.* 2012), [2] (Fort *et al.* 2009), [3] (Berrisford *et al.* 2011), [4] (Reynolds *et al.* 2007), [5] (Scales *et al.* 2014), [6] (Cavalieri *et al.* 1999), [7] Aviso, with support from Cnes (http://www.aviso.altimetry.fr/)

Table S4. Large-scale movement network metrics. P-values derived by two tailed t-tests. Displayed values denote mean ± standard deviation (minimum & maximum in brackets), if not labelled otherwise. df = degree of freedom

network metric	COGU	BRGU	p-value	df
# of nodes	24	25	-	-
# of populations present at a node	2.7 (1-7)	3.5 (1-6)	0.13	46
node size	17±14% (2-56%)	16±20% (0.4-75%)	0.89	42
node size by population	**49±40% (1-100%)**	**37±38% (1-100%)**	**0.05**	**134**
total degrees (connections per node)	**6.9 (2-21)**	**10.8 (2-26)**	**0.03**	**60**
edge size	7±8% (0.2-38%)	5±8% (0.1-55%)	0.14	157
edge size by population	**36±38% (1-100%)**	**22±32% (1-100%)**	**0.001**	**202**
# of unique ecoregions used by population	3.5 (2-6)	4.8 (2-8)	0.24	12
# of unique ecoregions used by individuals	**1.5±0.7 (1-4)**	**2.3±0.9 (1-4)**	**<0.001**	**156**

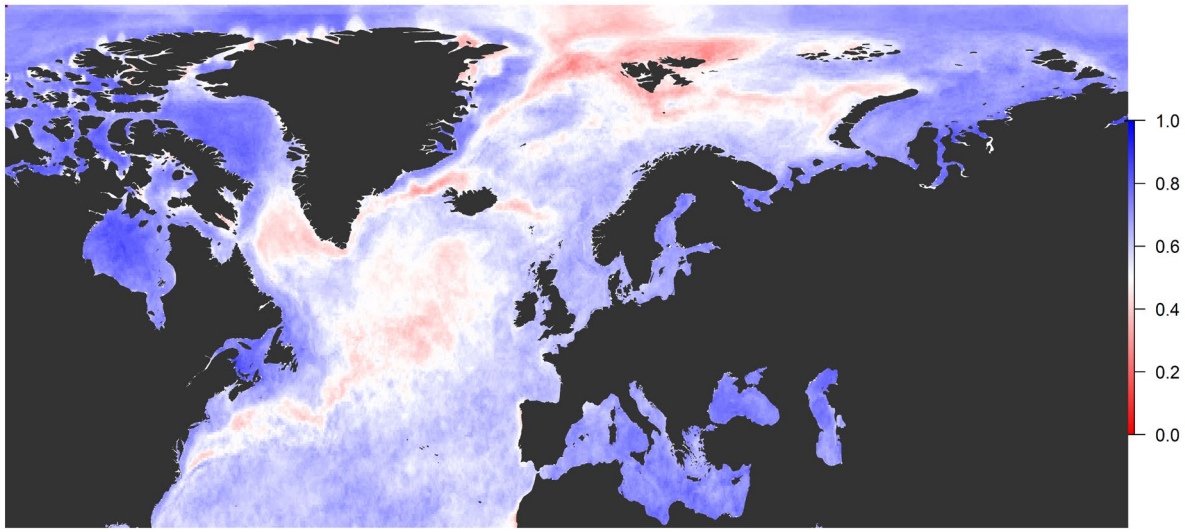

Figure S1. Distribution of SST predictability in the North Atlantic with a scale from 0 (no predictability) to 1 (very predictable).

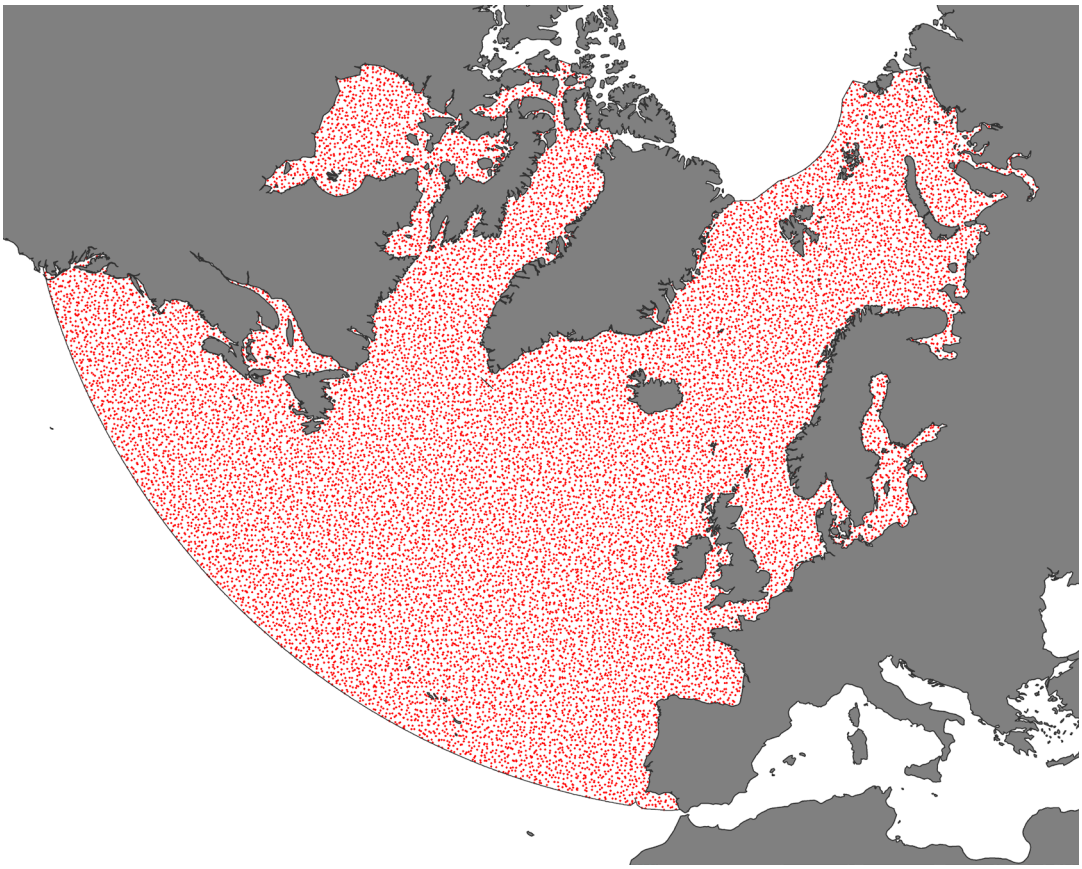

Figure S2. Map (in polar stereographic projection) displaying the study region including the 20000 stratified points (in red) used to estimate the available environmental space.

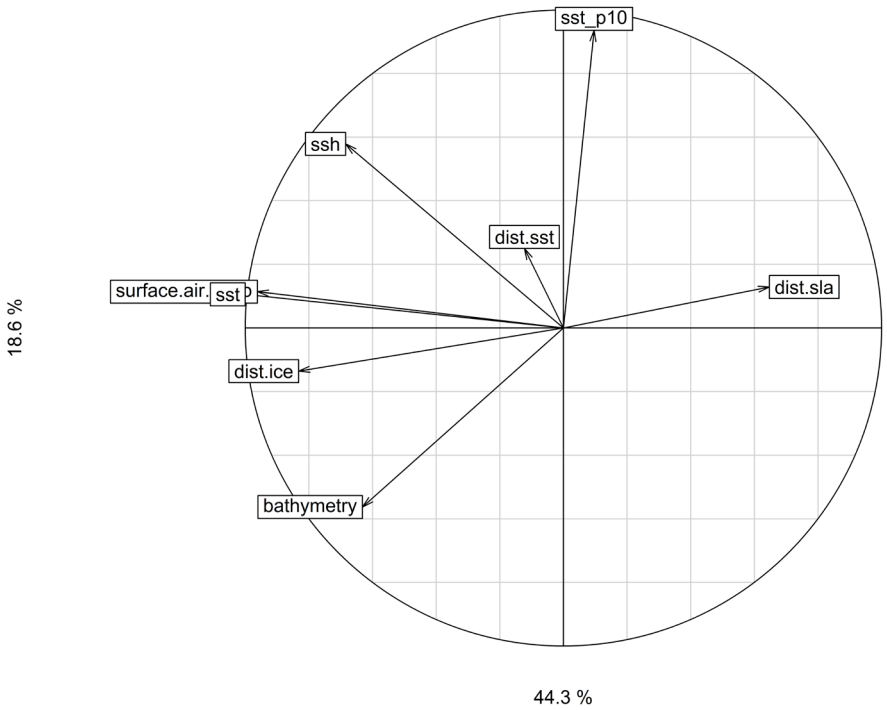

Figure S3. PCA correlation circle for the environmental space representing the North-Atlantic over the entire study period. dist.sla = distance to mesoscale eddies, dist.ice = distance to marginal sea ice zone, surface.air.temp = surface air temperature, sst = sea surface temperature, ssh = sea surface height, dist.sst = distance to temperature fronts, sst_p10 = SST predictability

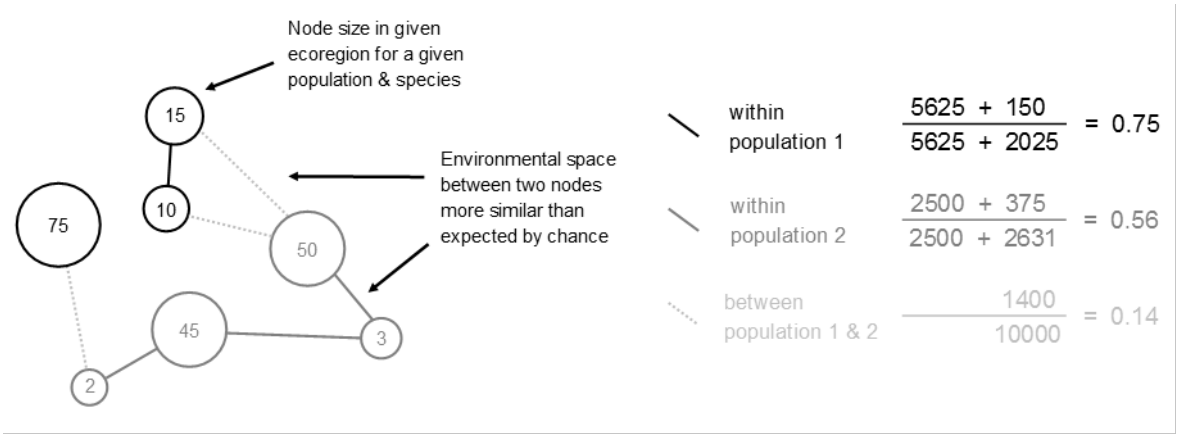

Figure S4. A schematic detailing the environmental similarity index (S) calculations in equation 1 (within example populations, solid lines) and equation 2 (between two example populations, dashed lines) using two example populations (in black and grey). The symbols denote ecoregion-, species- and breeding population-specific environmental space use. Its size corresponds to the proportional use as visualised in figure 1. Lines connect environmental spaces which are similar based on the environmental niche similarity test (one way is considered sufficient, i.e. $1 \cong 2 \mid 2 \cong 1$).

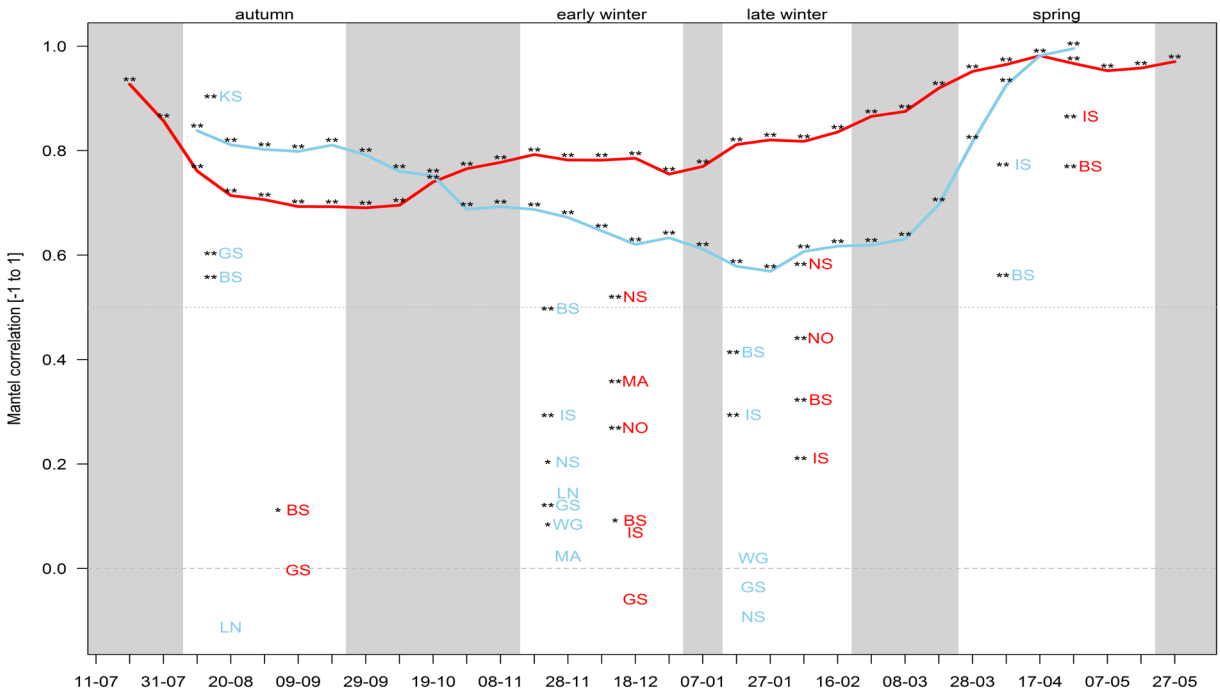

Figure S5. Species-specific mantel correlation through time (10 day bins) for all data from 2014-2017. BRGU in blue and COGU in red. Labels in each season (white boxes) denote season-specific mantel correlation values for each particular ecoregion with birds from more than one breeding population present. Significance levels based on 1 000 permutations: ** = <0.001, * = <0.05; Ecoregion abbreviations: BS = Barents Sea, KS = Kara Sea, GS = Greenland Sea, IS = Iceland Shelf & Sea, WG = West Greenland, NO = North Sea, MA = Central North Atlantic, NS = Norwegian Sea, LN = Labrador shelf & Newfoundland

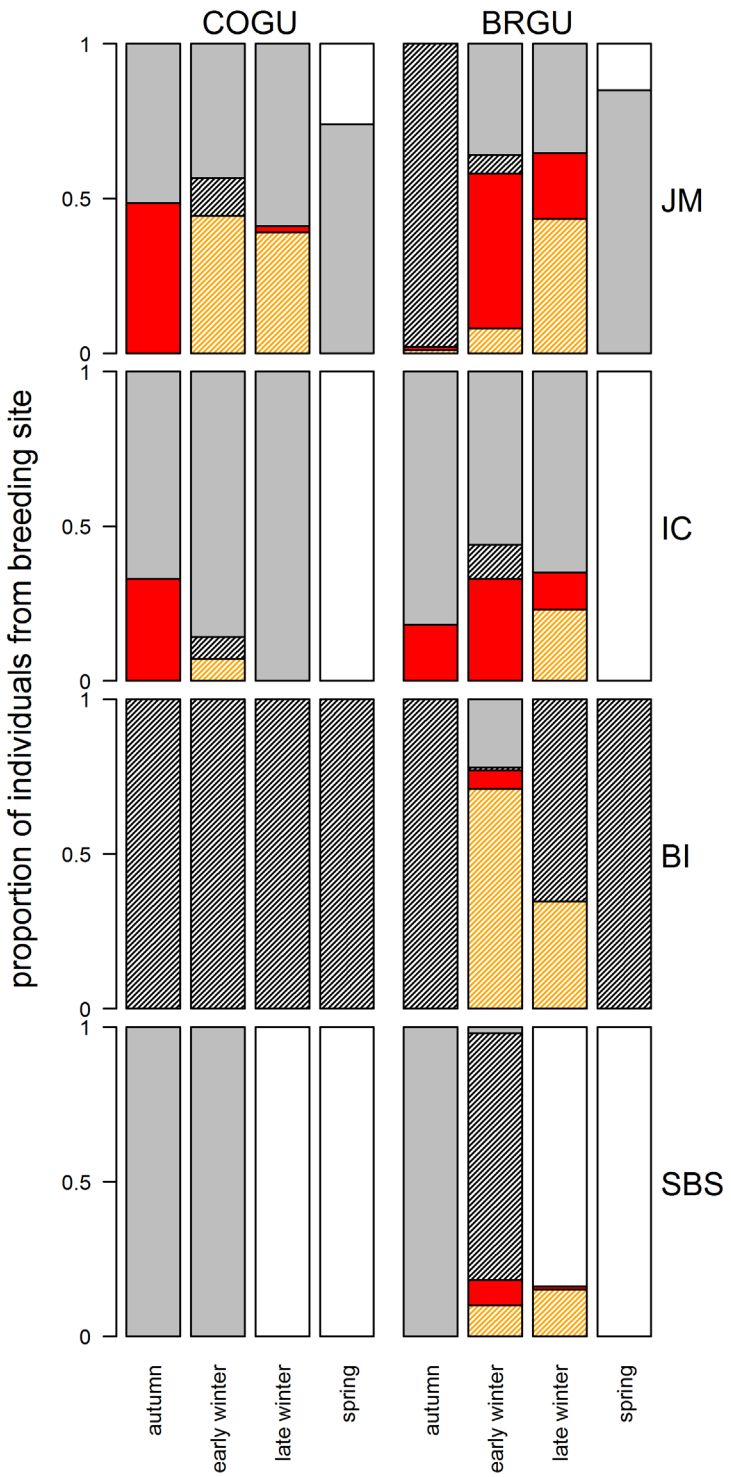

Figure S6. Seasonal proportional comparative space and environmental niche use between both species breeding sympatric at four breeding locations (JM = Jan Mayen, IC = North-East Iceland, BI = Bjørnøya & SBS = Southern Barents Sea). The proportion of the population occupying the same ecoregion with the other sympatric species breeding at the same location is indicated in white-grey-black colours while red-orange colours indicate different ecoregions used. Dark colours (grey & black) correspond to species-specific within ecoregion space use while white illustrates mixing between the species within ecoregions. Solid colours (white, grey & red) indicate similar environmental niches occupied while shaded colours denote distinct environments used (black & orange).

Supplementary information 2

Species- and breeding population-specific seasonal distributions (in polar stereographic projection) in geographic (A, C, E, G) and environmental space (B, D, F, H) during autumn (A, B), early winter (C, D), late winter (E, F) and spring (G, H). Common guillemot (COGU) breeding population distributions are displayed in figure S2.1-8 and Brünnich's guillemot (BRGU) breeding population distributions in figure S2.9-16. Colours correspond to spatiotemporal clusters identified by network analysis (figure 1).

In geographic space, kernel utilization distributions (UD) show seasonal space use as composite of individual UDs scaled to their respective population sample size. Symbols display colony locations. Dotted and solid circles indicate areas where location estimation was affected by or impossible due to polar night or midnight sun, respectively. Grey stippled and solid areas display 15% and 90% ten year seasonal median sea ice concentration, respectively.

In environmental space, each seasonal track is displayed as centre with variance. Darker crosses denote the median of all locations and the total variance displayed. Stippled lines represent 100% and 50% kernel UD contours of available environmental space in the North Atlantic over 11 years.

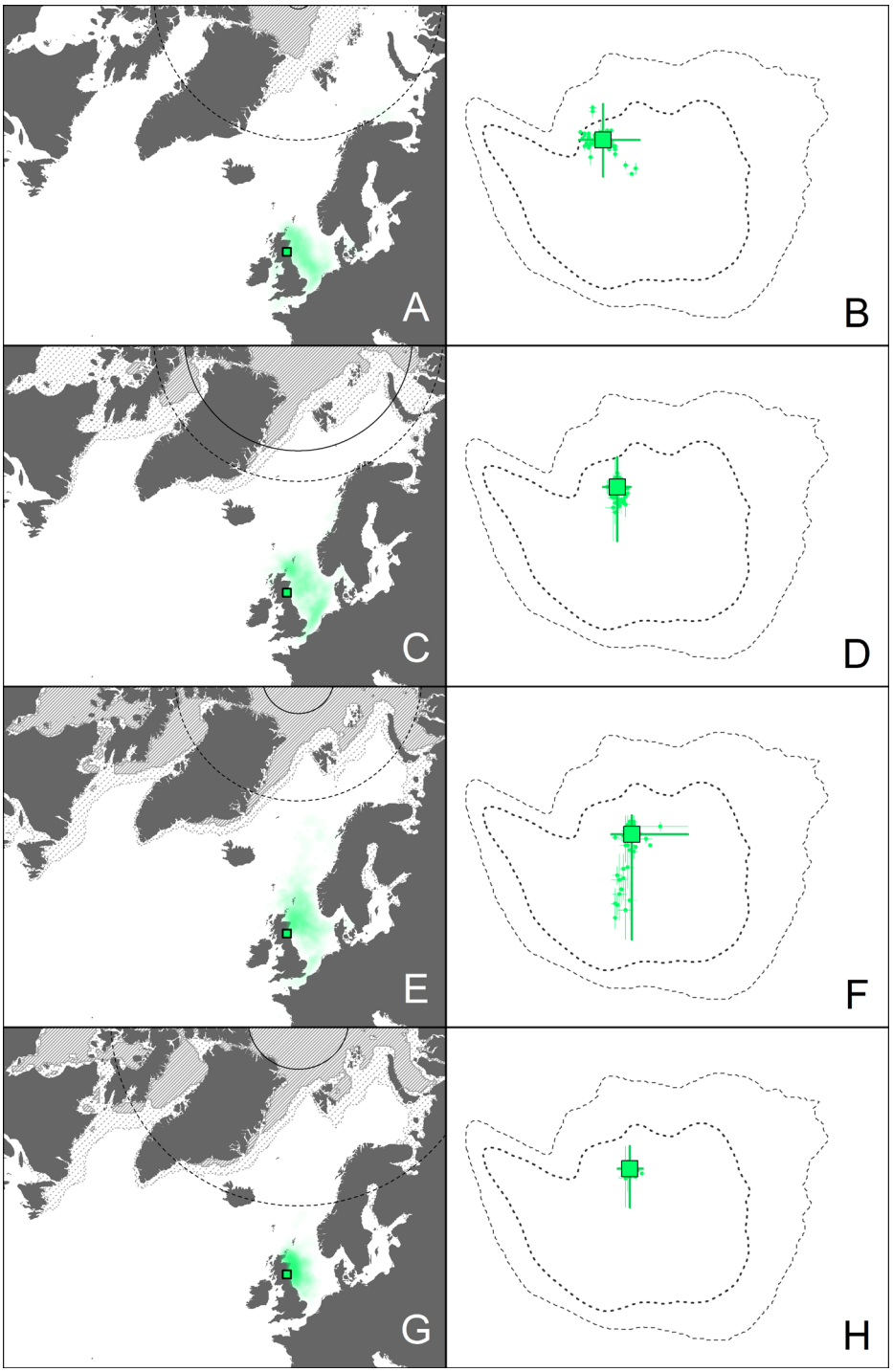

Figure S2.1. Common guillemots, Isle of May

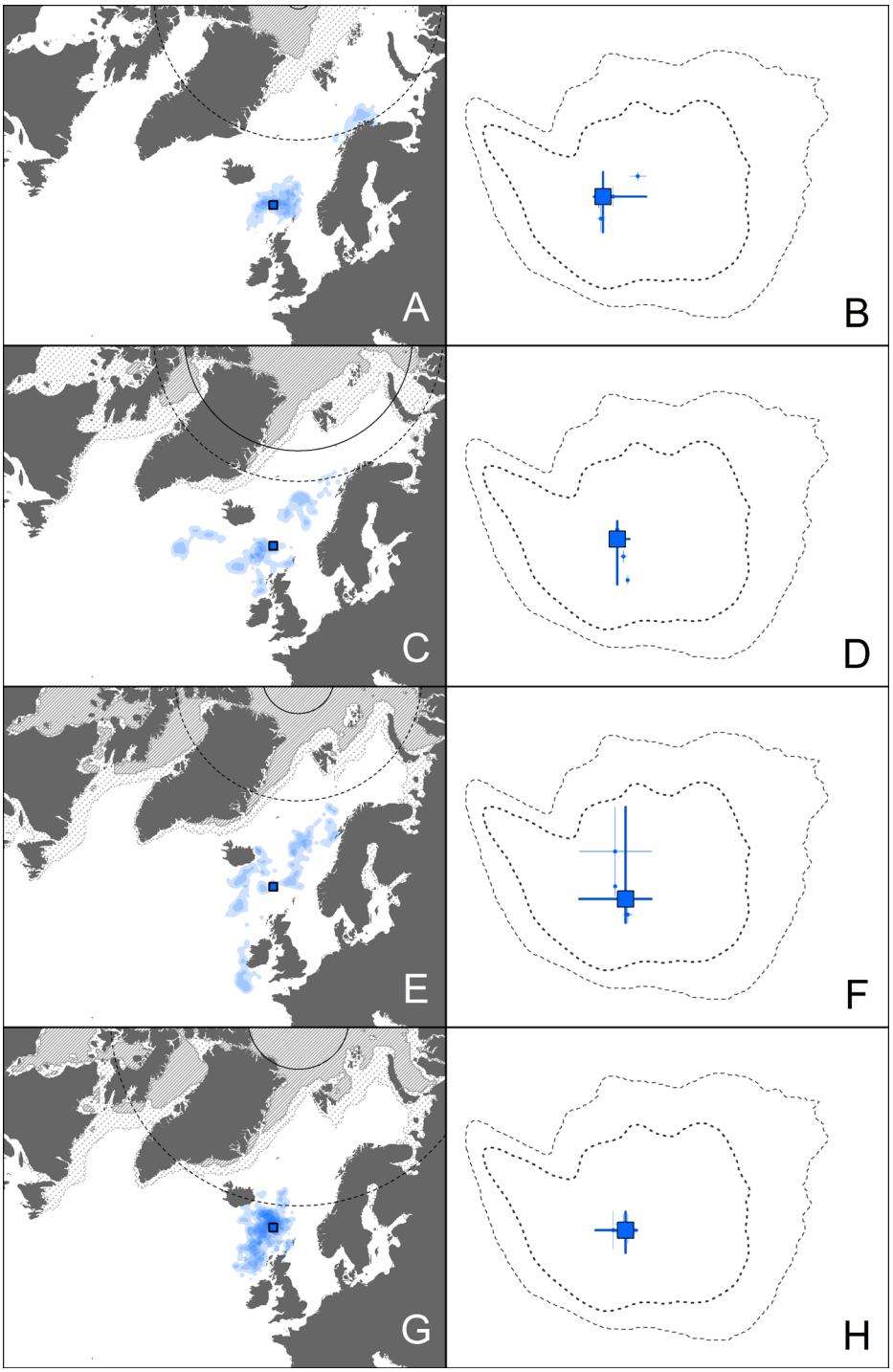

Figure S2.2. Common guillemots, Faroe Islands

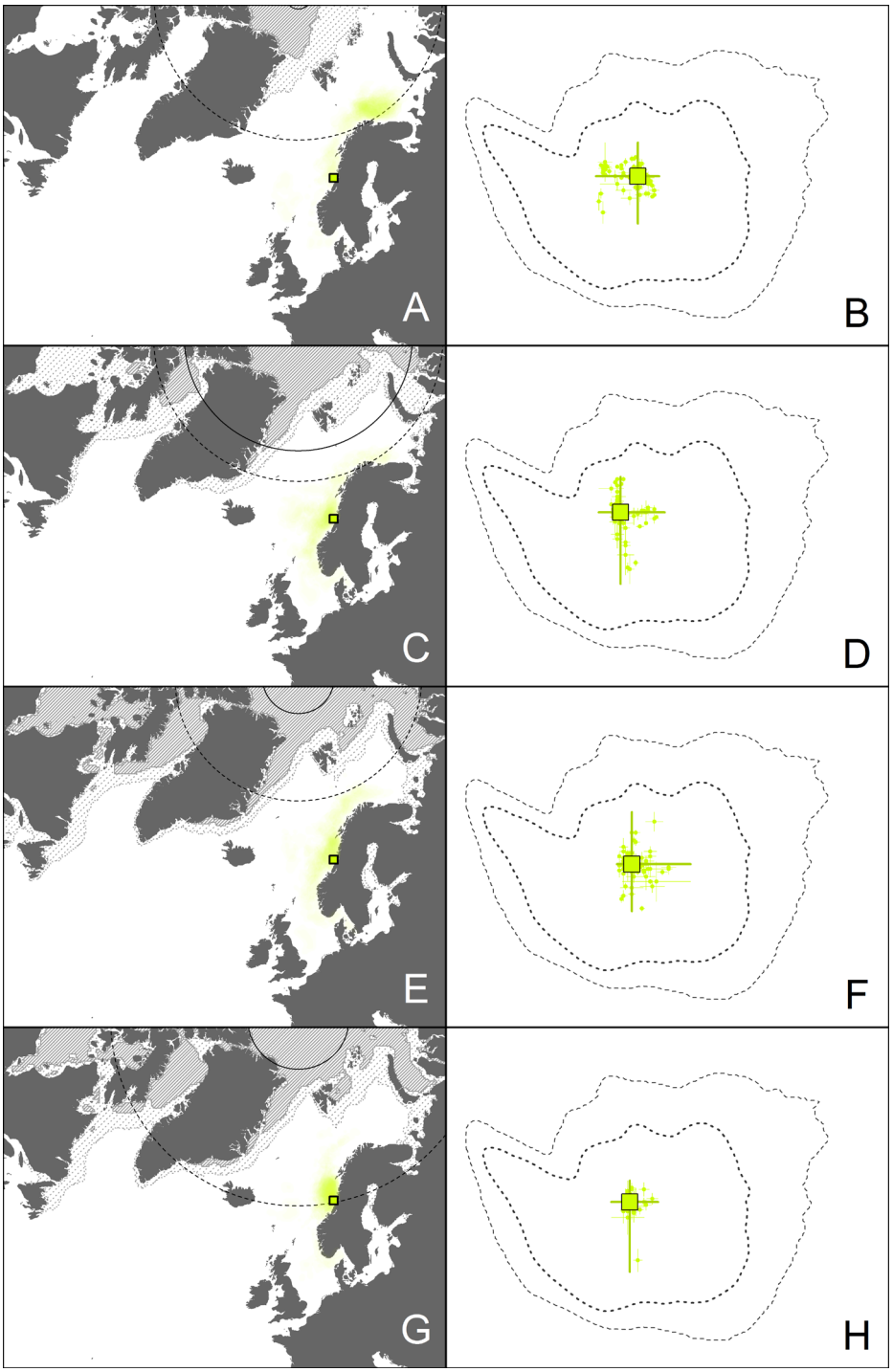

Figure S2.3. Common guillemots, Sklinna

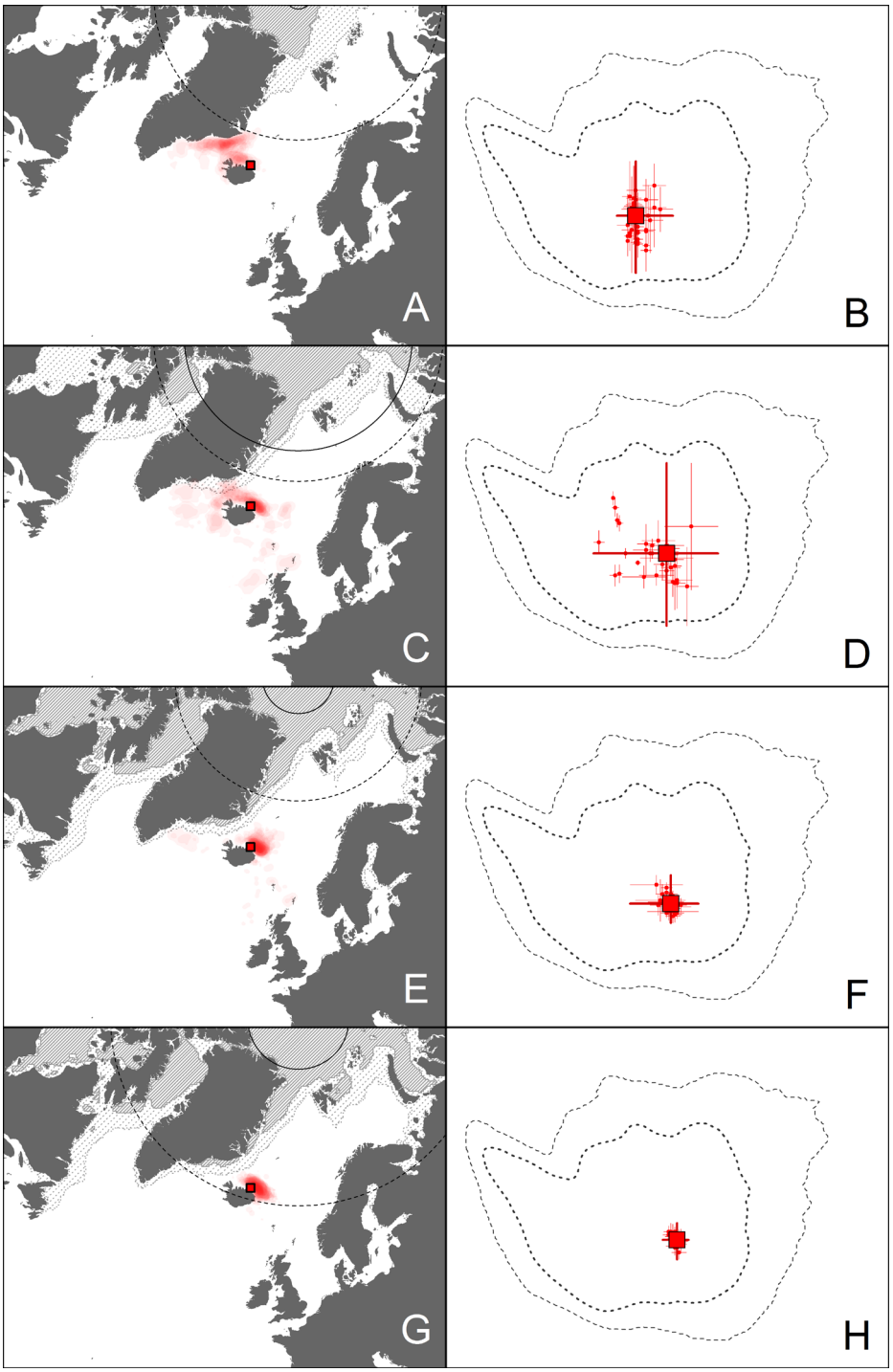

Figure S2.4. Common guillemots, North-East Iceland (Grimsey, Langanes)

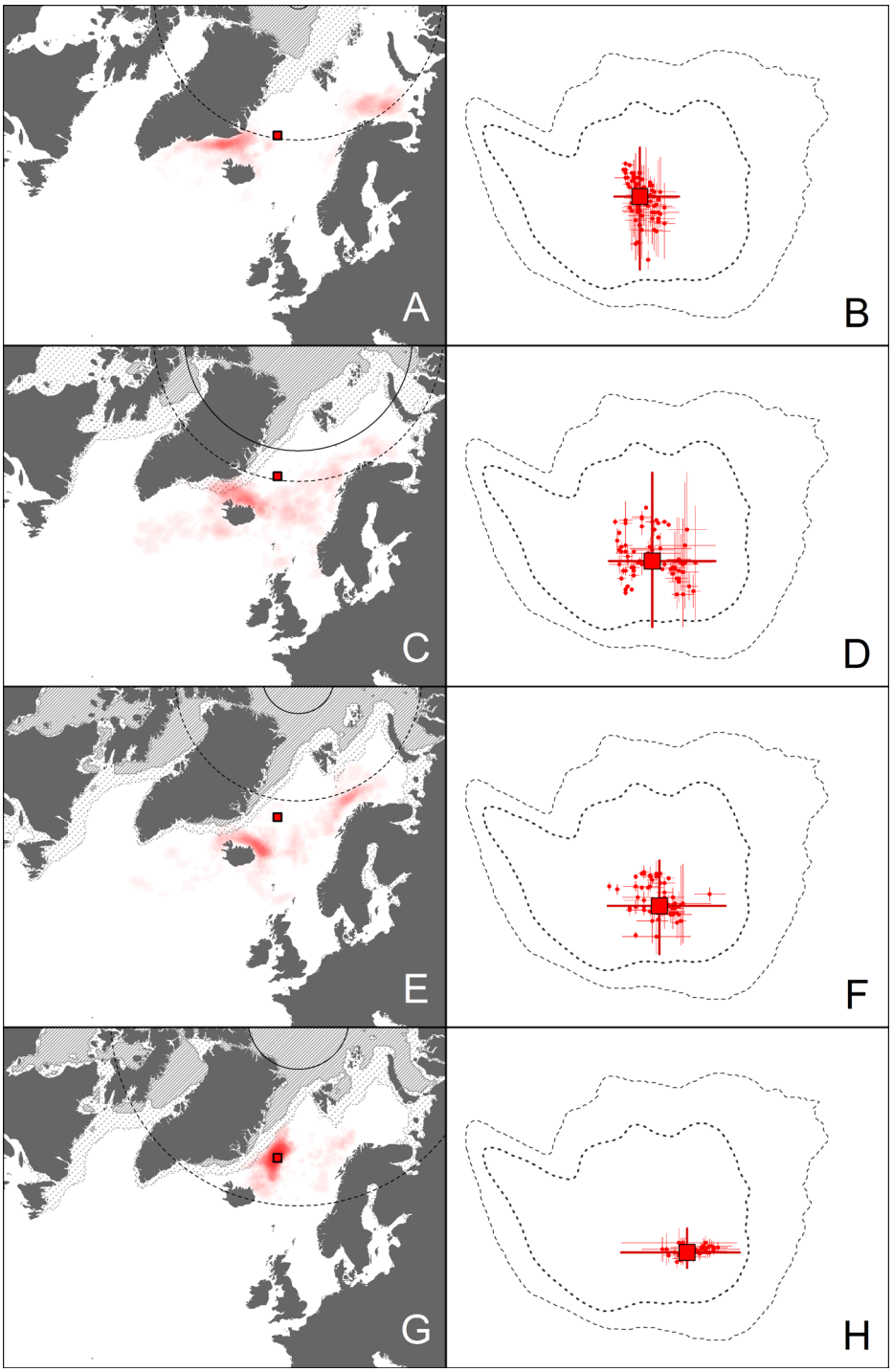

Figure S2.5. Common guillemots, Jan Mayen

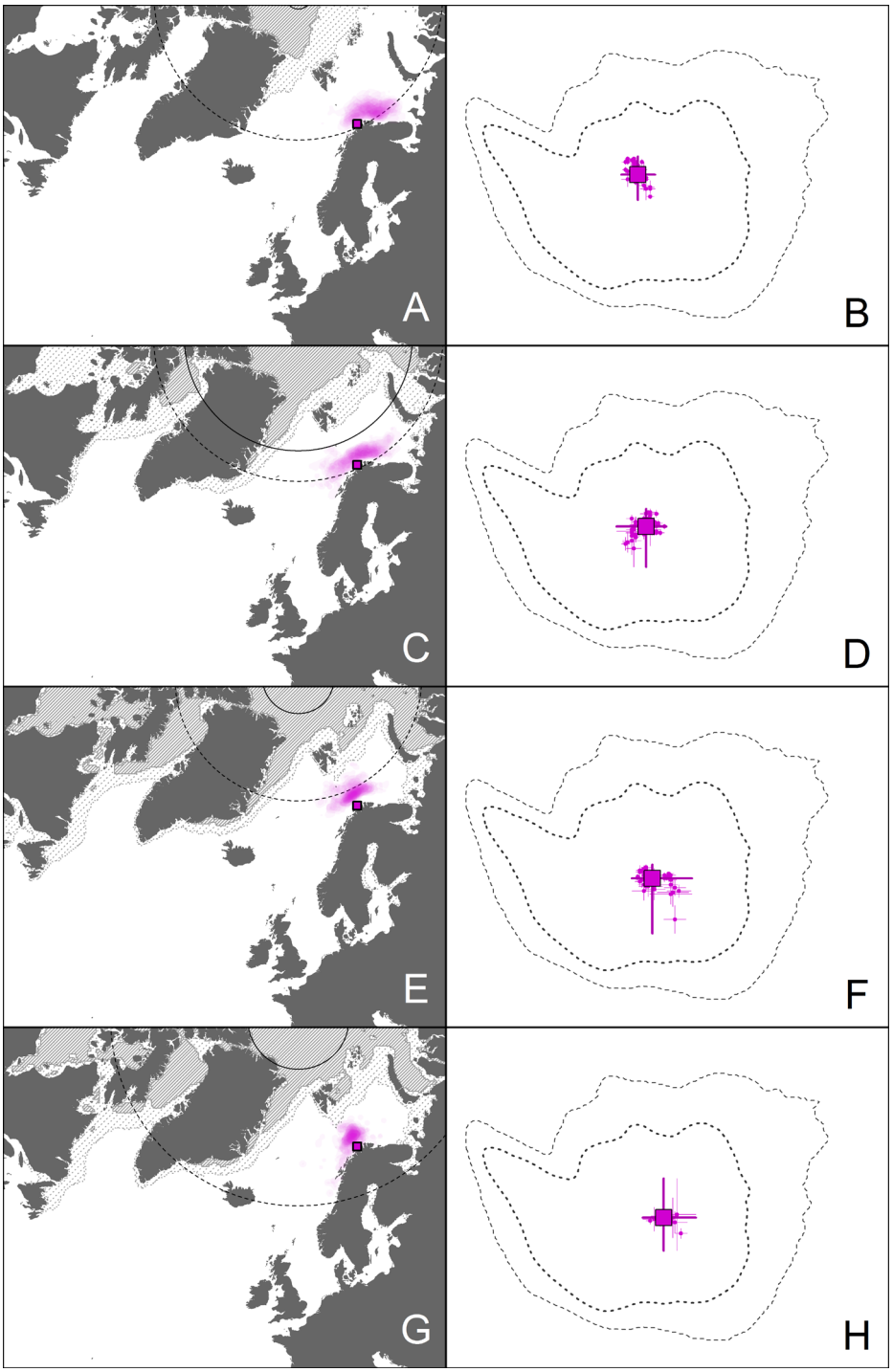

Figure S2.6. Common guillemots, Hjelmsøya

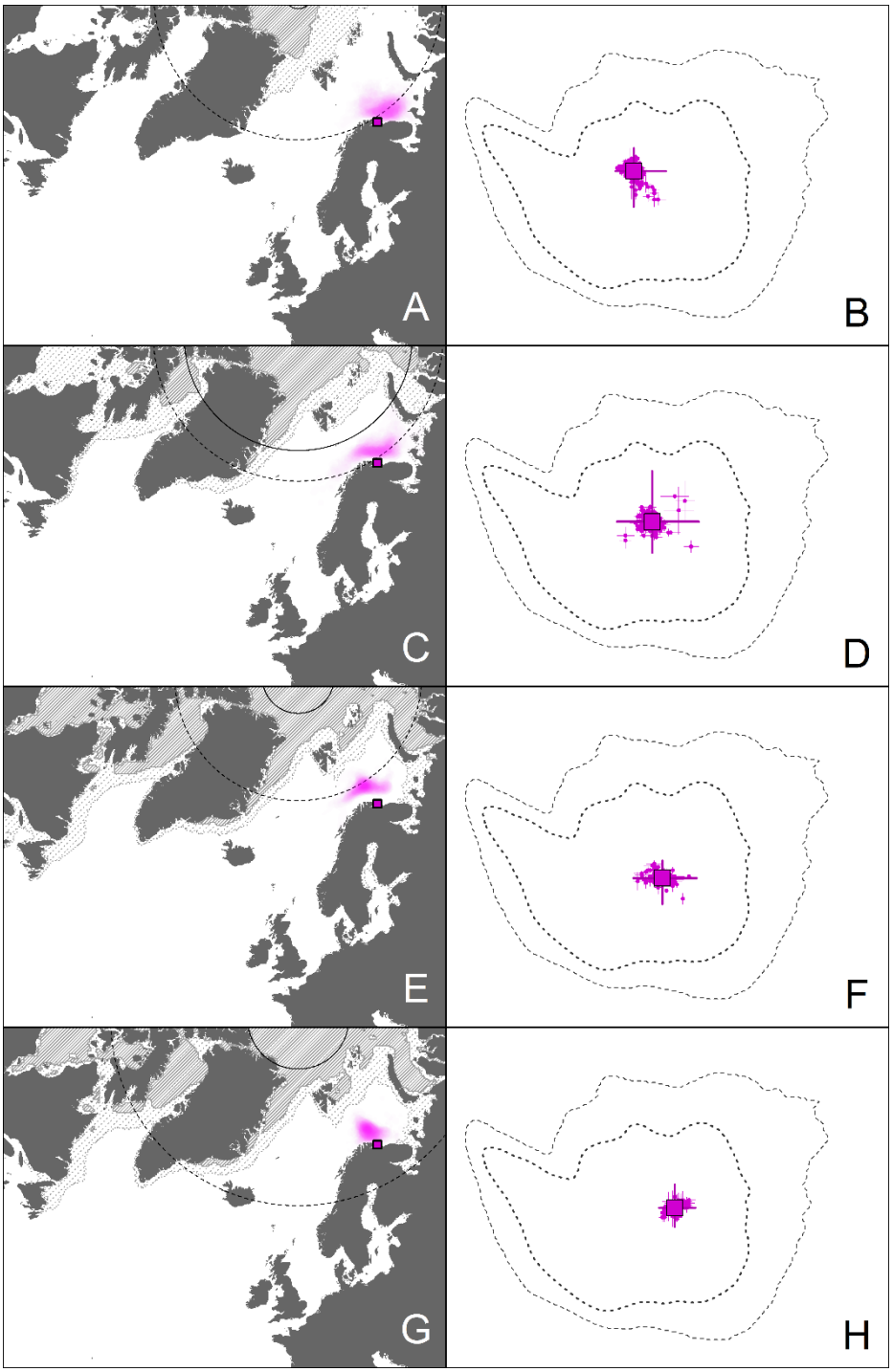

Figure S2.7. Common guillemots, Southern Barents Sea (Hornøya and Cape Gorodetskiy)

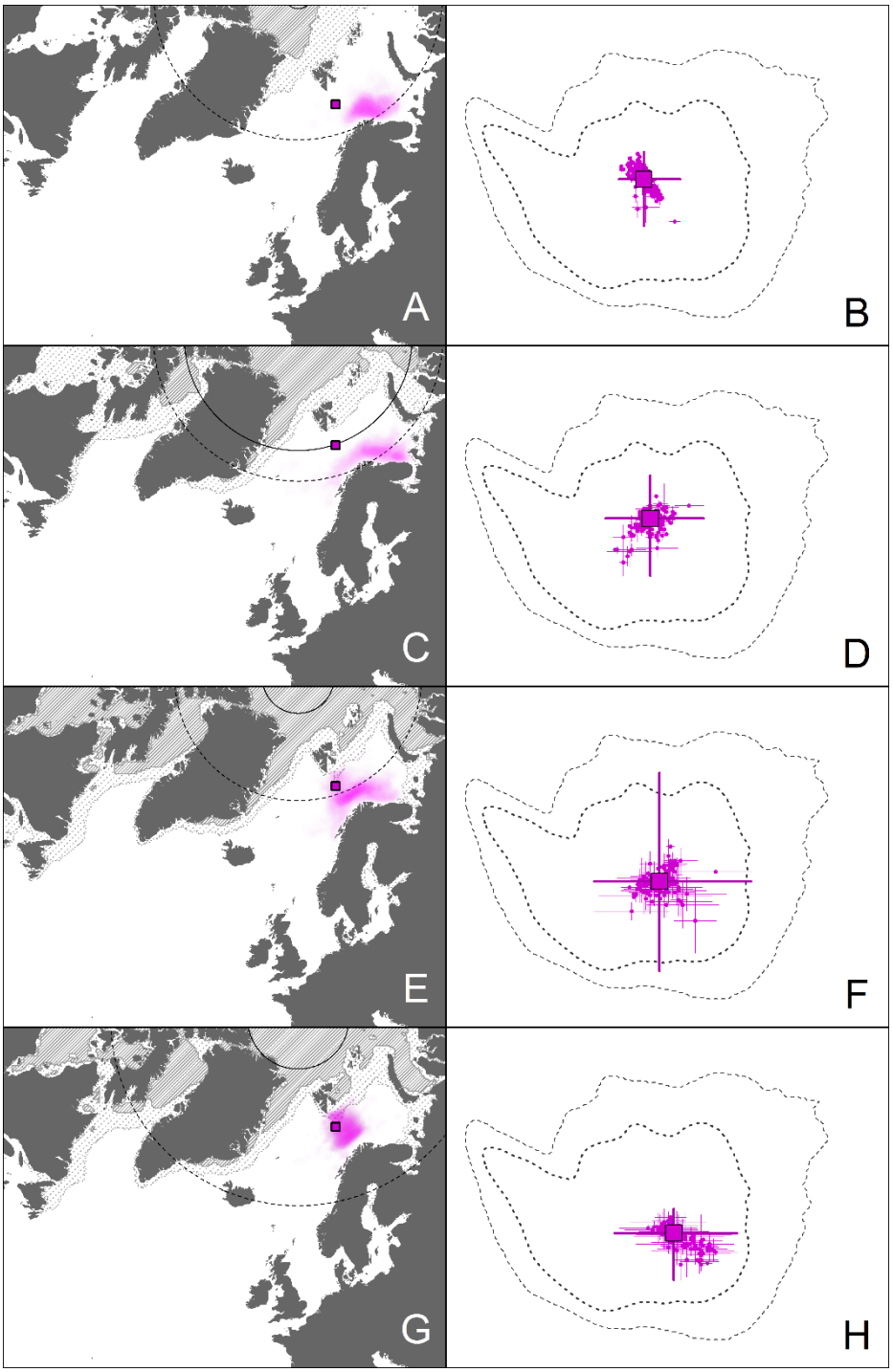

Figure S2.8. Common guillemots, Bjørnøya

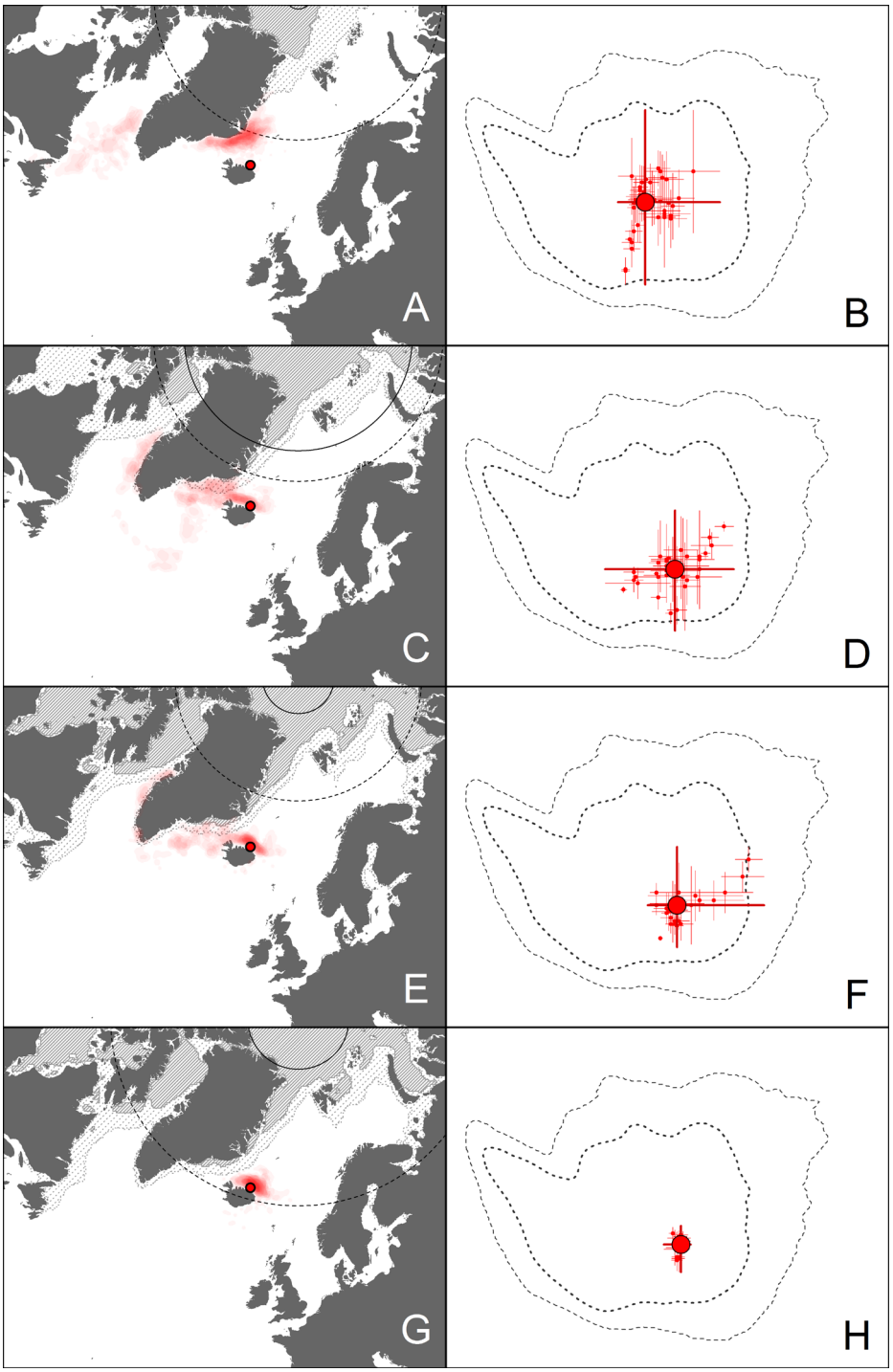

Figure S2.9. Brünnich's guillemots, North-East Iceland (Grimsey, Langanes)

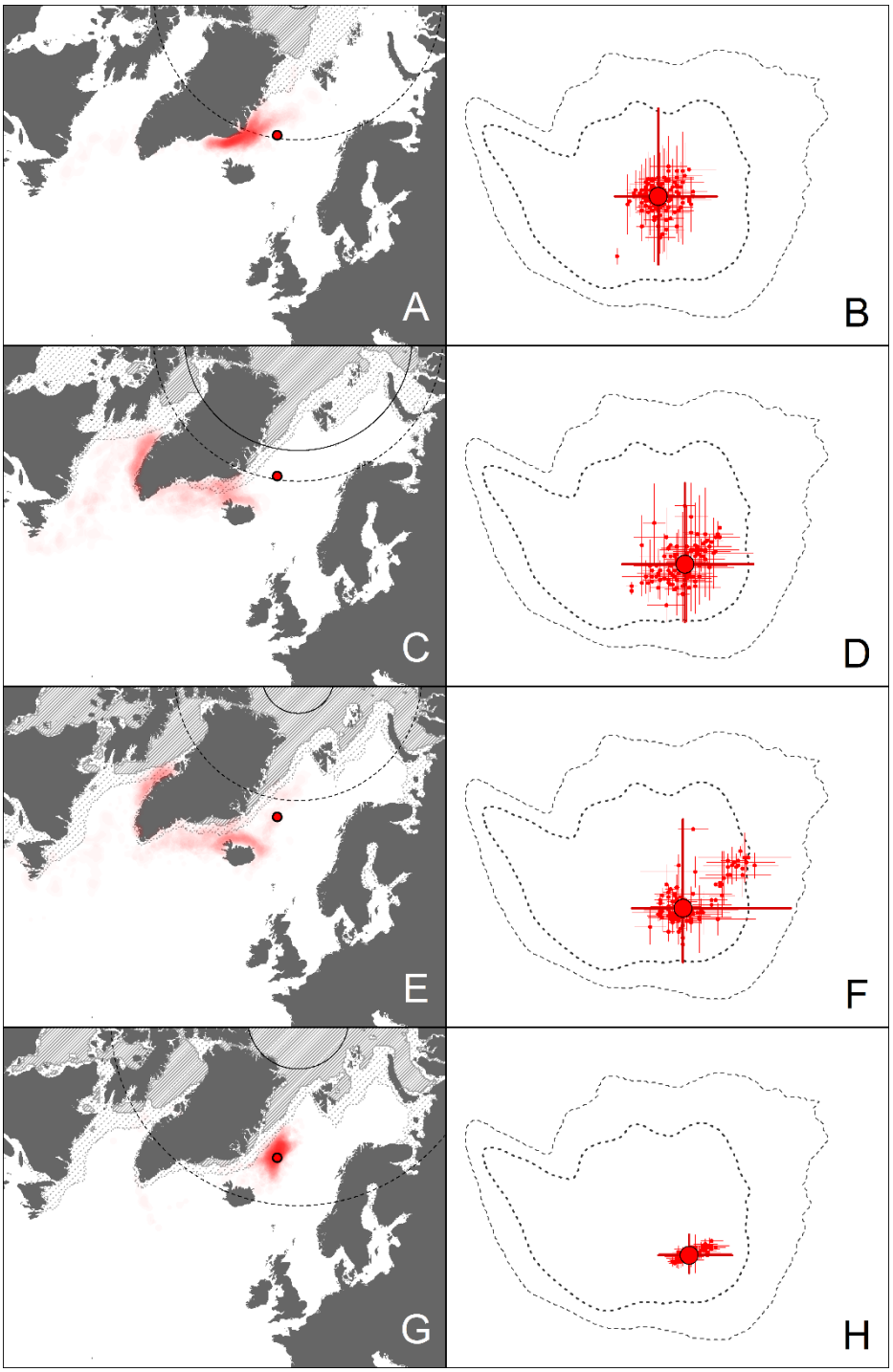

Figure S2.10. Brünnich's guillemots, Jan Mayen

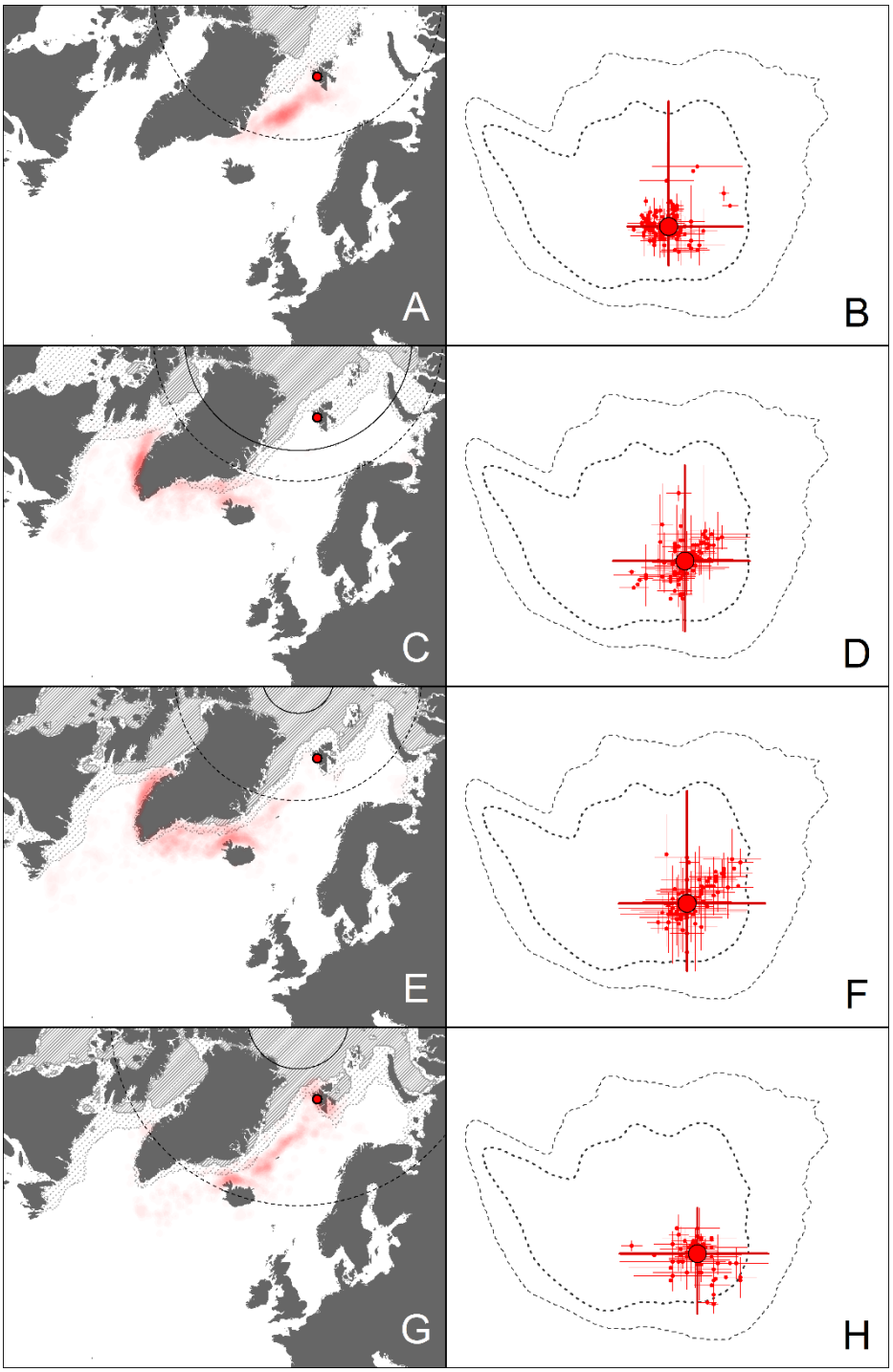

Figure S2.11. Brünnich's guillemots, Western Spitsbergen (Diabas, Ossian Sarsfjellet and John Scottfjellet)

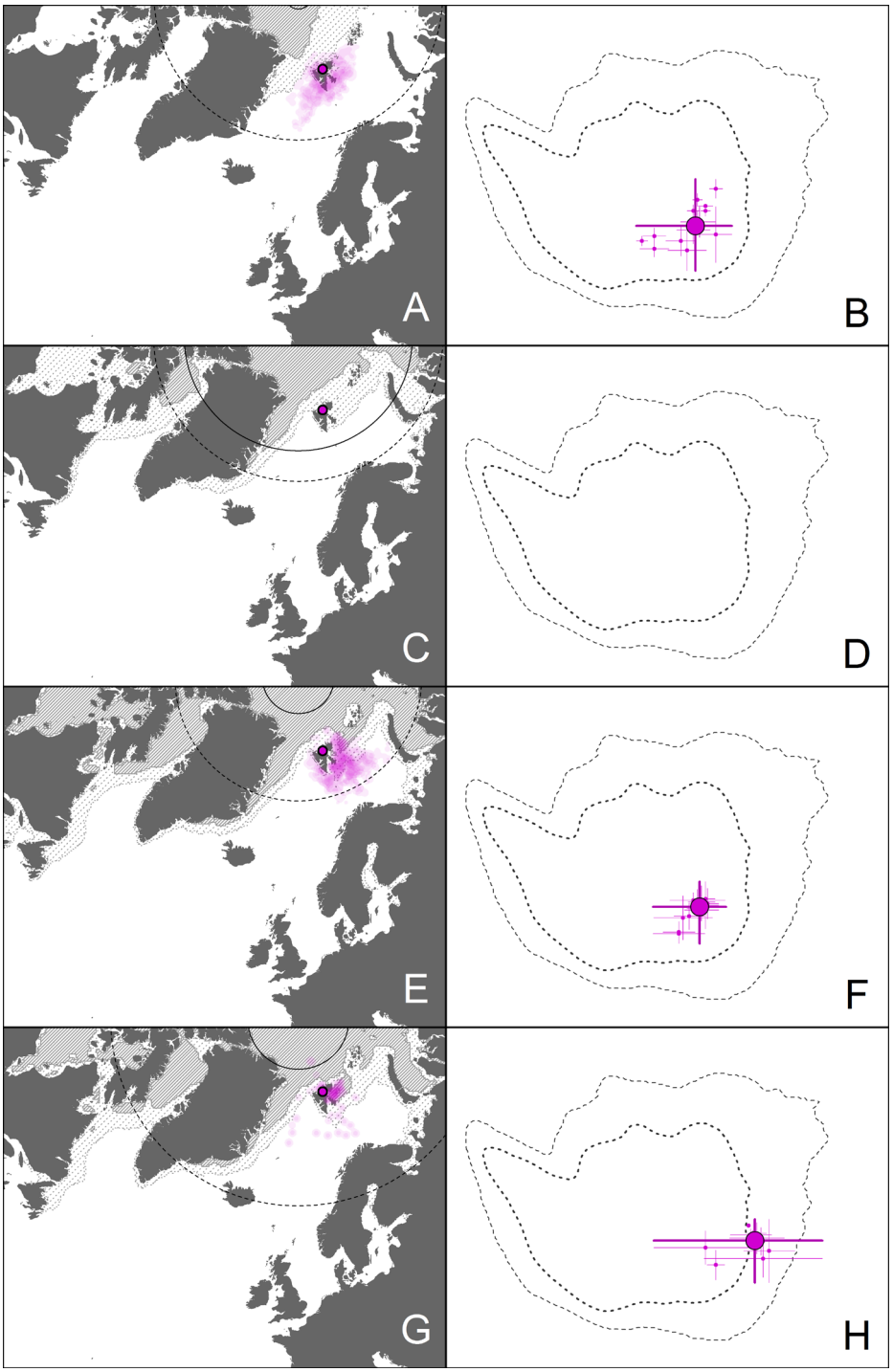

Figure S2.12. Brünnich's guillemots, Eastern Spitsbergen (Alkefjellet)

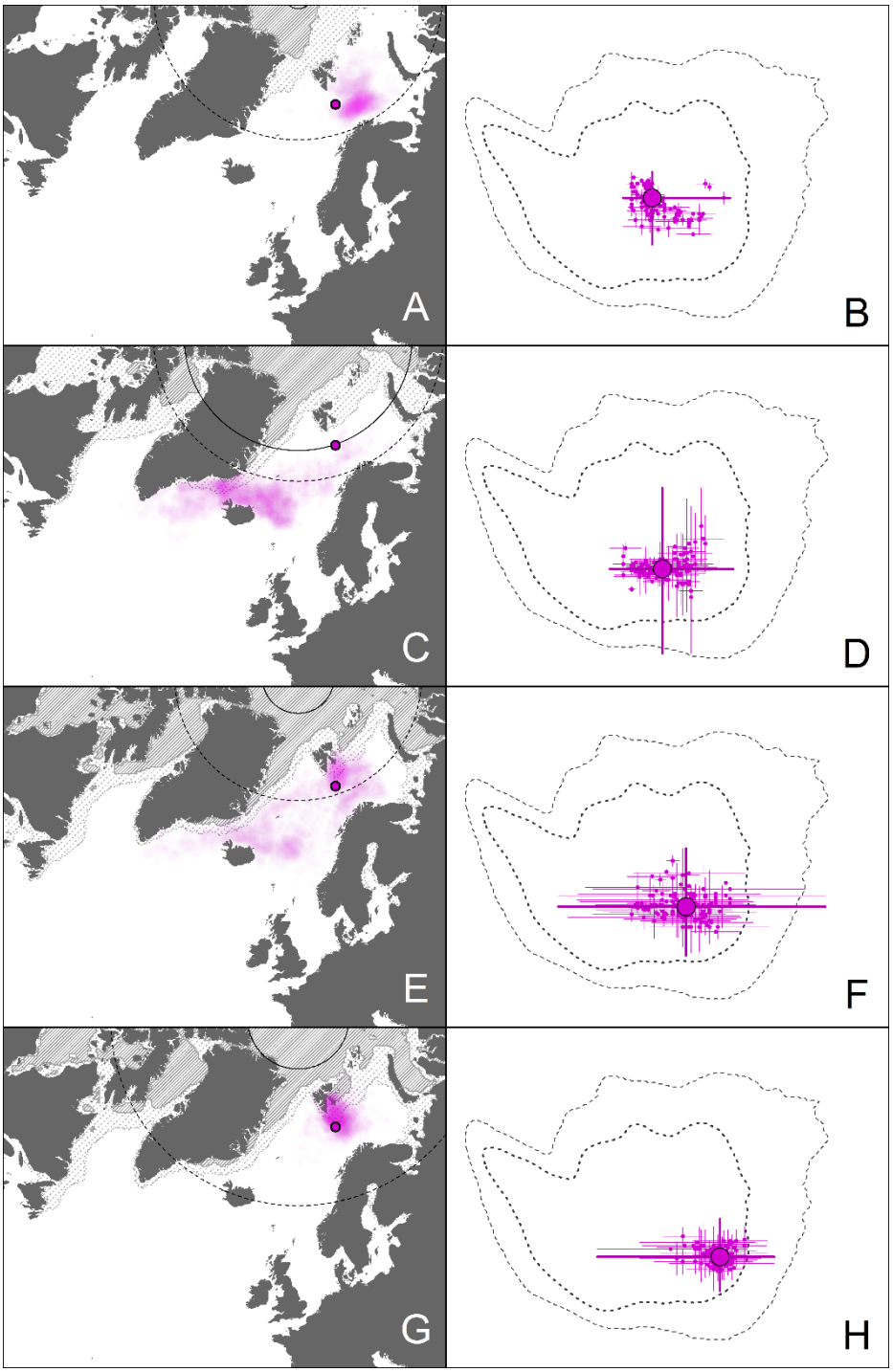

Figure S2.13. Brünnich's guillemots, Bjørnøya

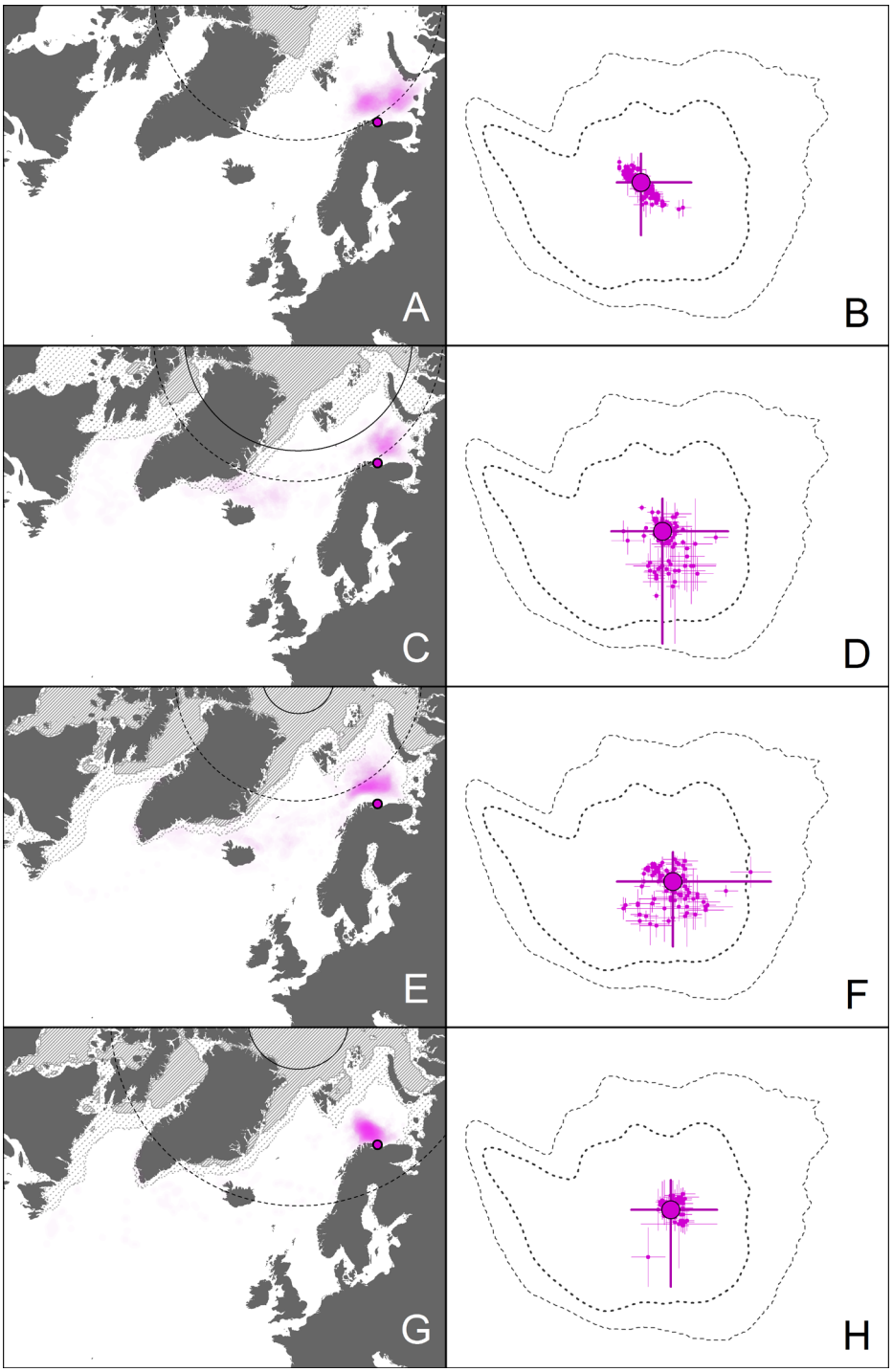

Figure S2.14. Brünnich's guillemots, Southern Barents Sea (Hornøya and Cape Gorodetskiy)

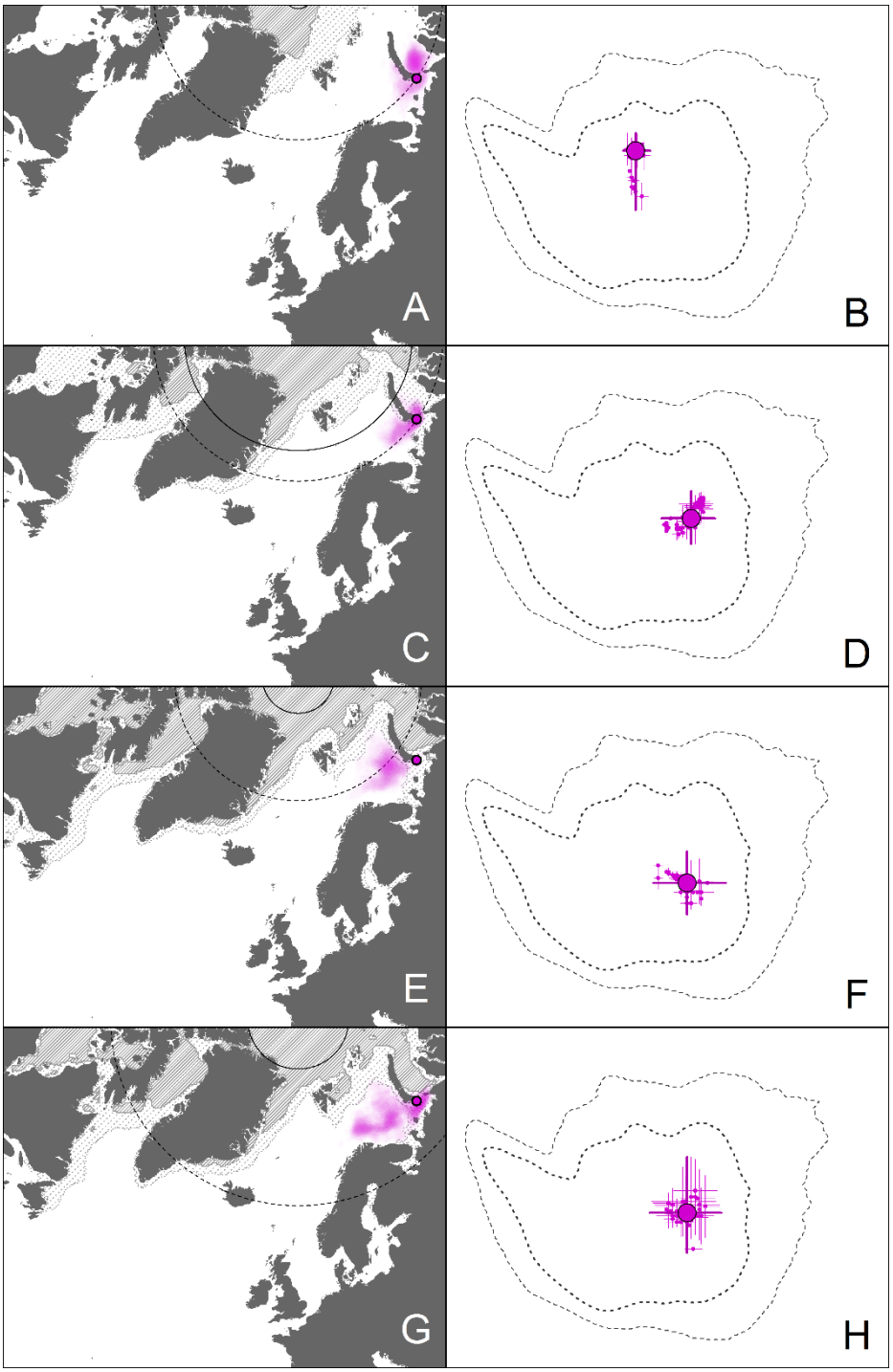

Figure S2.15. Brünnich's guillemots, Southern Novaya Zemlya (Kara Gate)

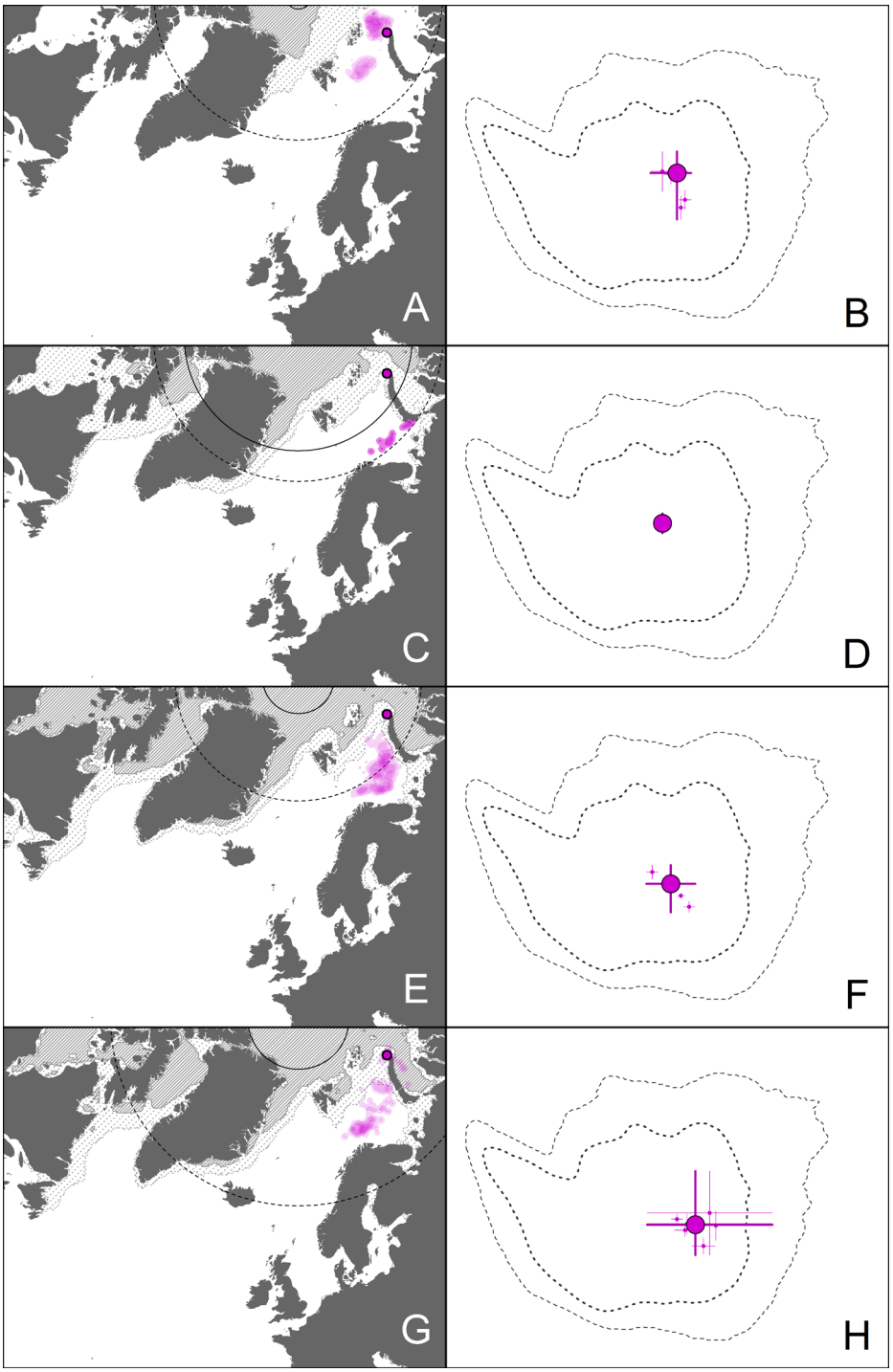

Figure S2.16. Brünnich's guillemots, Northern Novaya Zemlya (Oranskie islands)

Supplementary information 3

Species- and population-specific movement networks by large marine ecoregion (y axis) and season (x axis). Each population is scaled to the same size and all nodes (squares) and edges (lines) are scaled to their usage accordingly. The entire species-specific movement network is plotted in grey scale in each plot and each breeding population-specific network is displayed on top. Common guillemot movement networks are displayed in figure S3.1-8 and Brünnich's guillemot movement networks in figure S3.9-16.

Dark grey bars at the bottom of each figure denote the number of ecoregions used during each season by the entire network while dark red bars show population-specific use (scale on the left). Bars at the bottom of the figure between seasons denote the proportion of movement between (grey = entire network, black = population-specific) and within (light grey =entire network, yellow = population-specific) ecoregions with scale on the right.

Breeding population names: SNZ = Southern Novaya Zemlya, NNZ = Northern Novaya Zemlya, ESP = Eastern Spitsbergen, WSP = Western Spitsbergen, BI = Bjørnøya, SBS = Southern Barents Sea, HJ = Hjelmsøya, SK = Sklinna, JM = Jan Mayen, IC = North-East Iceland, FA = Faroe Islands, IM = Isle of May

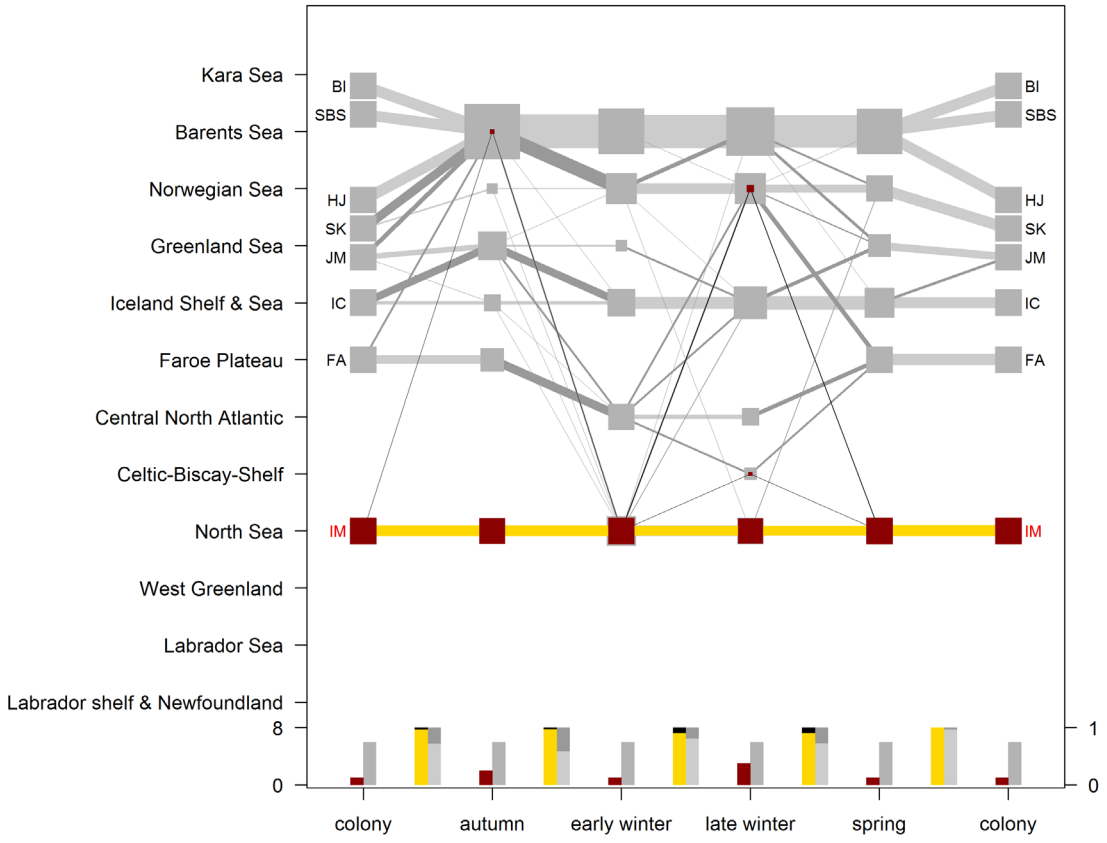

Figure S3.1. Common guillemots, Isle of May

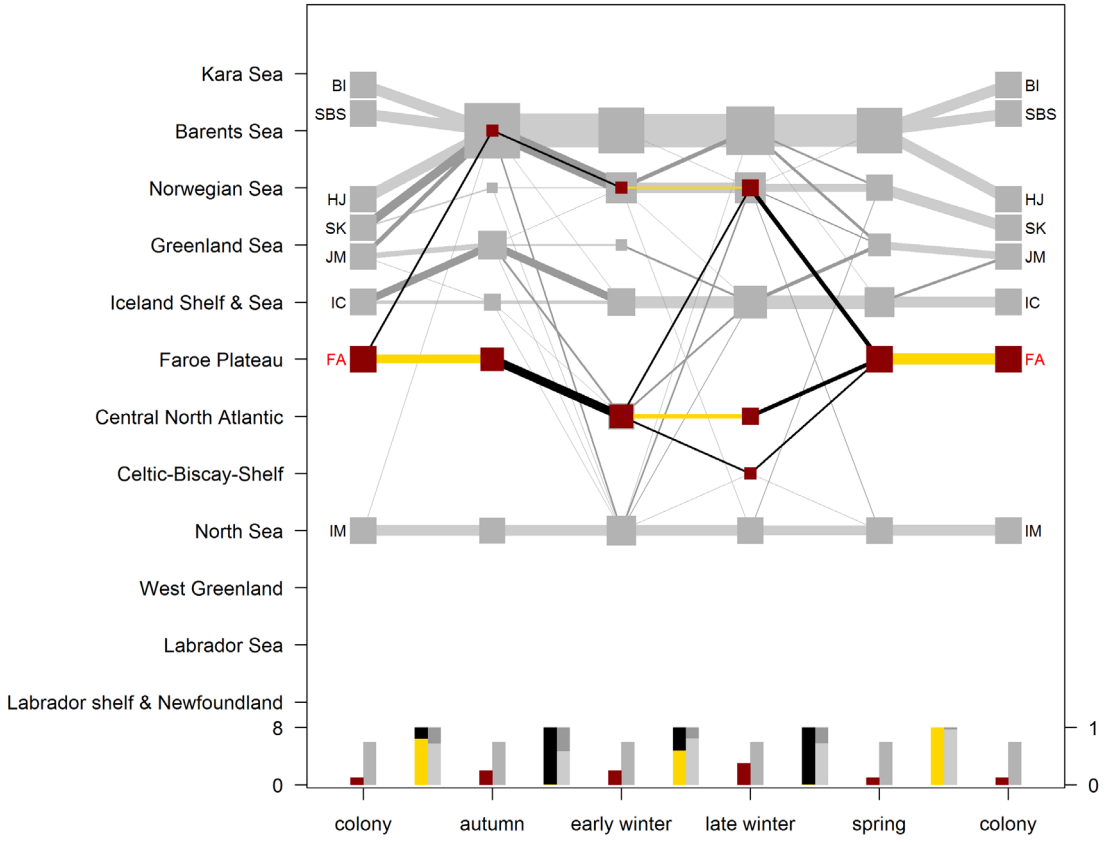

Figure S3.2. Common guillemots, Faroe Islands

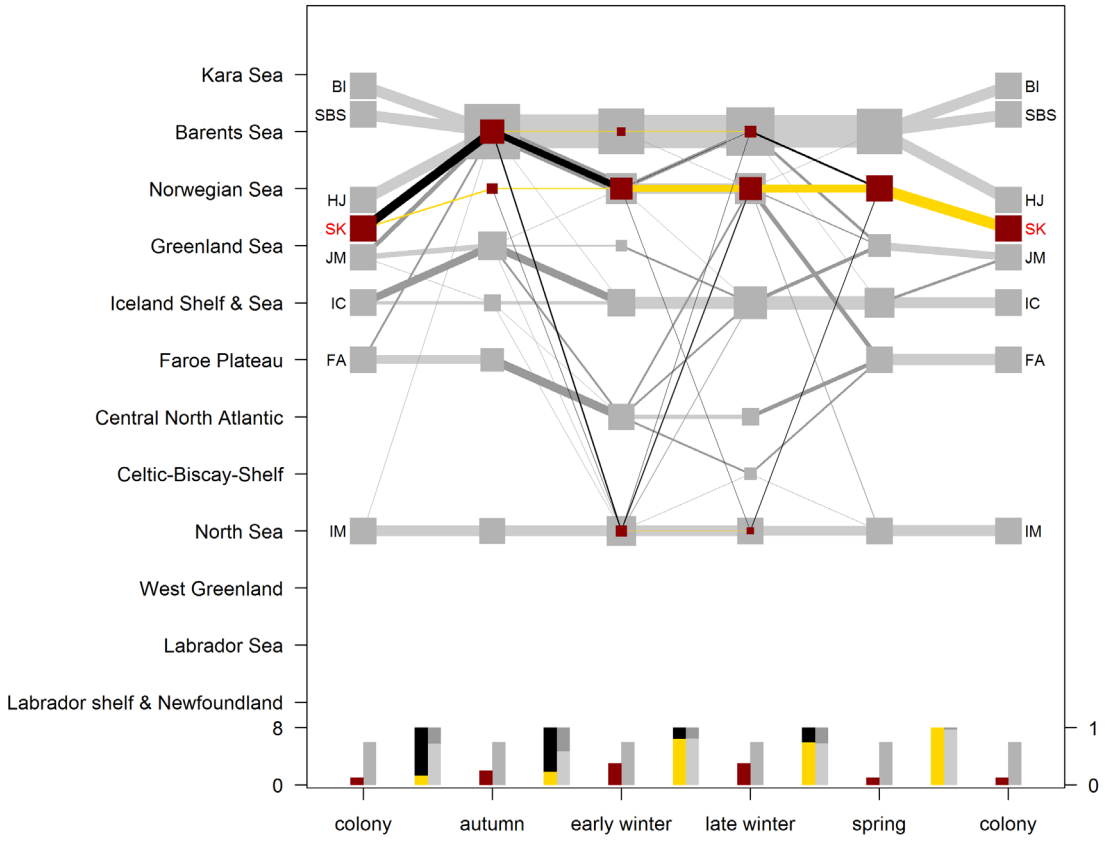

21

22 **Figure S3.3.** Common guillemots, Sklinna

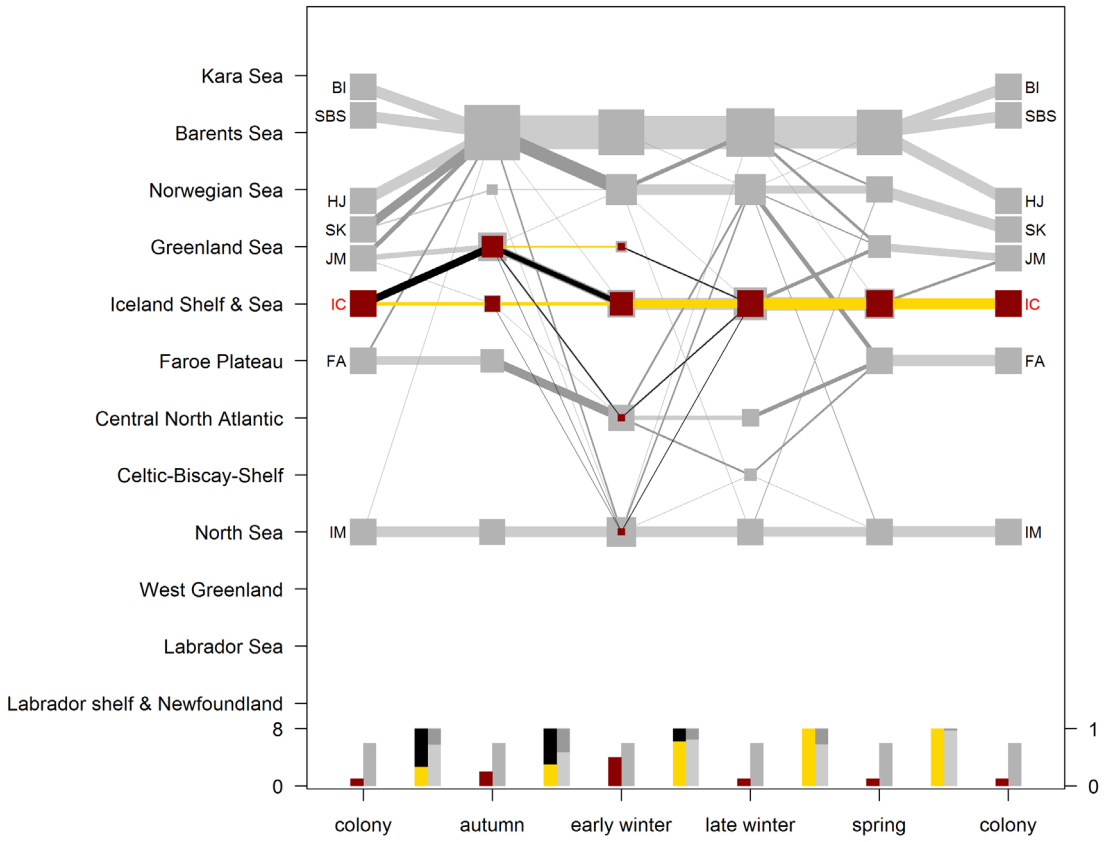

23

24 **Figure S3.4.** Common guillemots, North-East Iceland (Grimsey, Langanes)

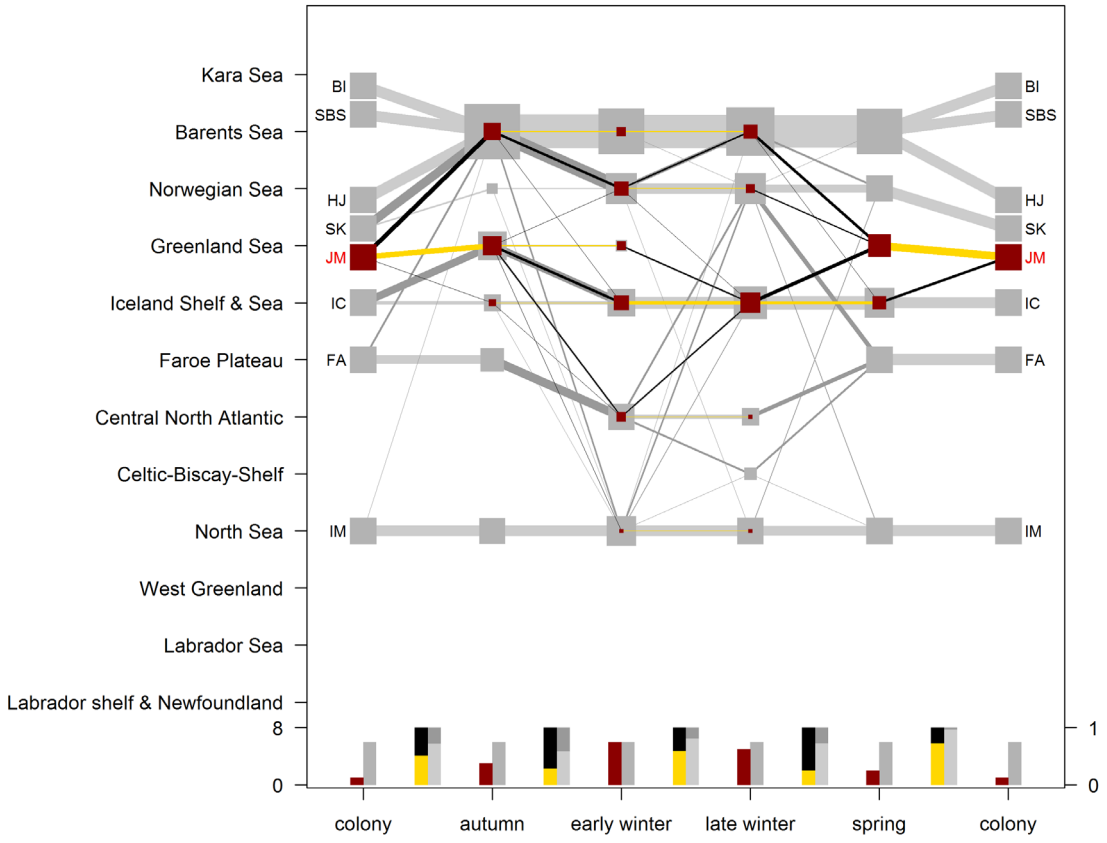

25

26 **Figure S3.5.** Common guillemots, Jan Mayen

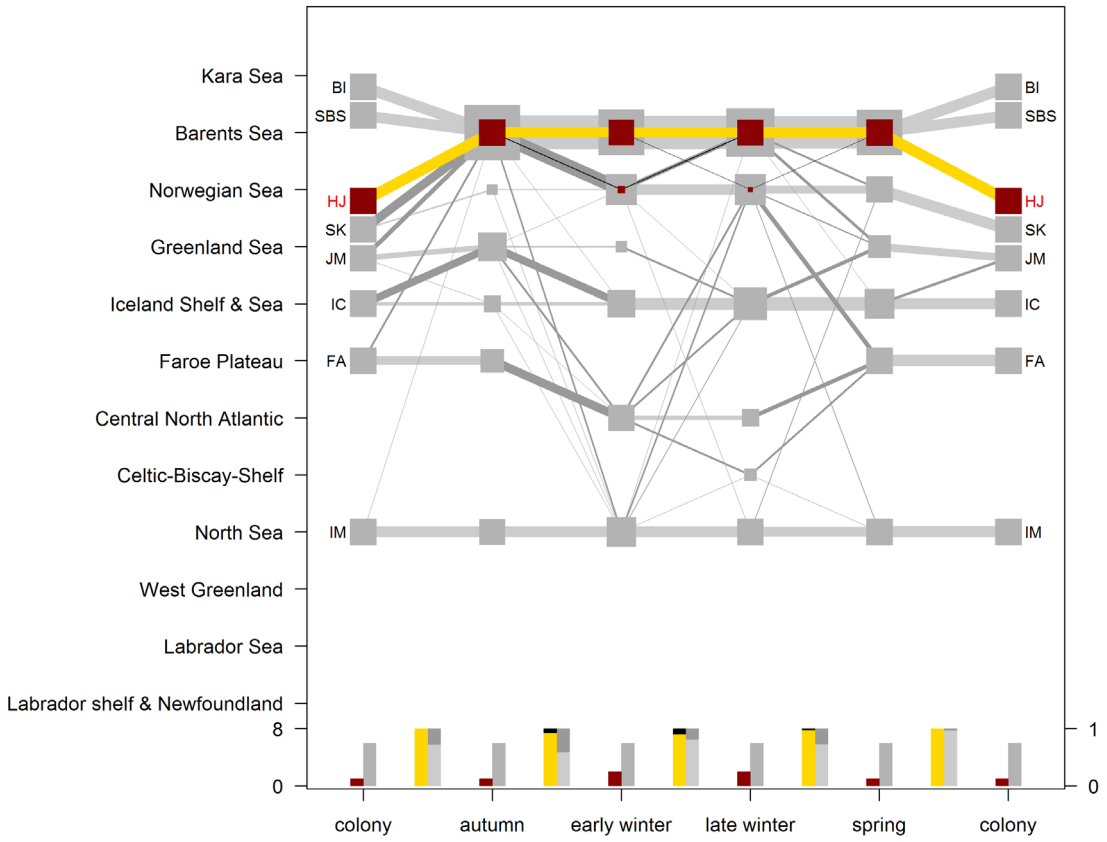

27

28 **Figure S3.6.** Common guillemots, Hjelmsøya

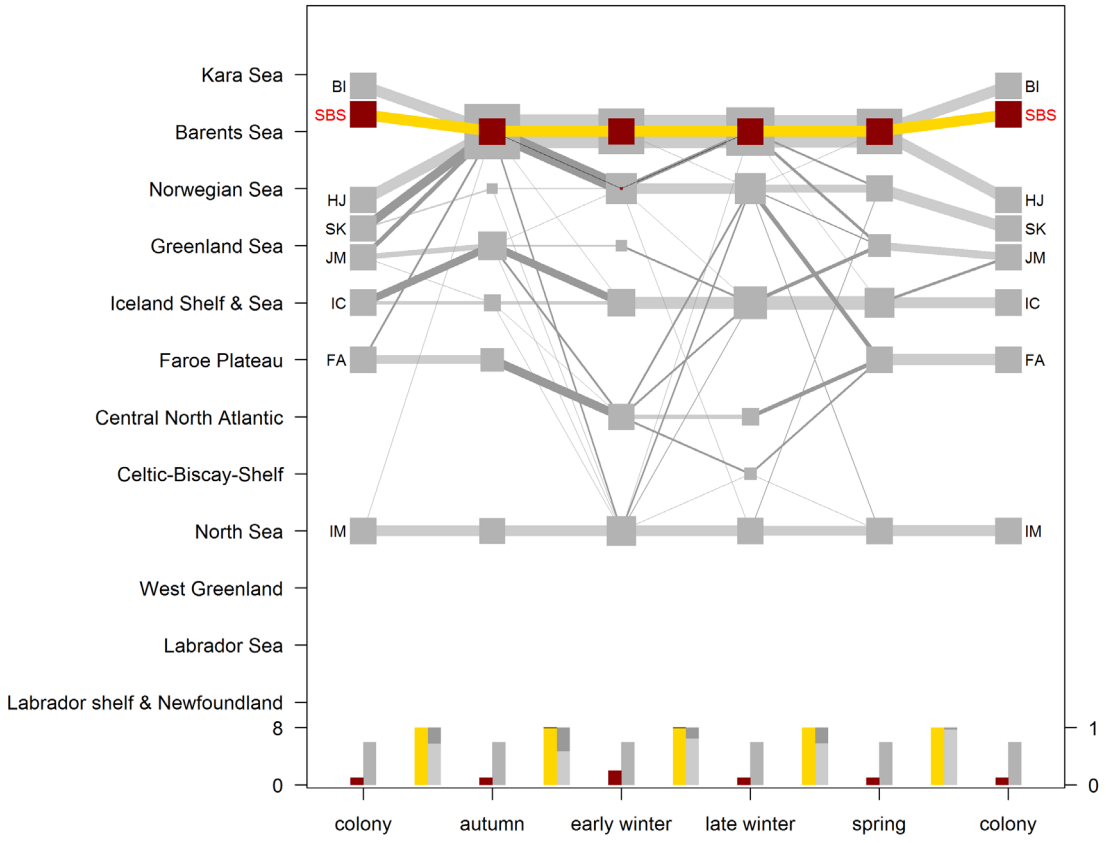

29

30 **Figure S3.7.** Common guillemots, Southern Barents Sea (Hornøya and Cape Gorodetskiy)

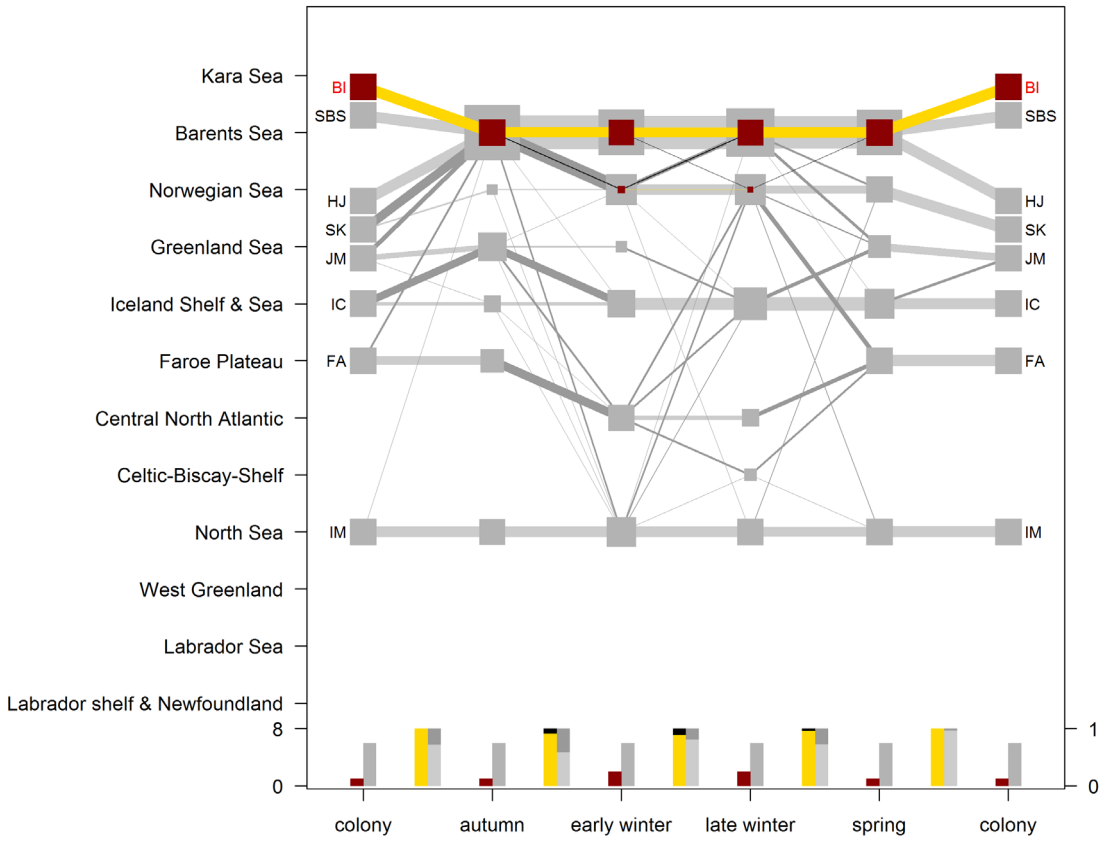

31

32 **Figure S3.8.** Common guillemots, Bjørnøya

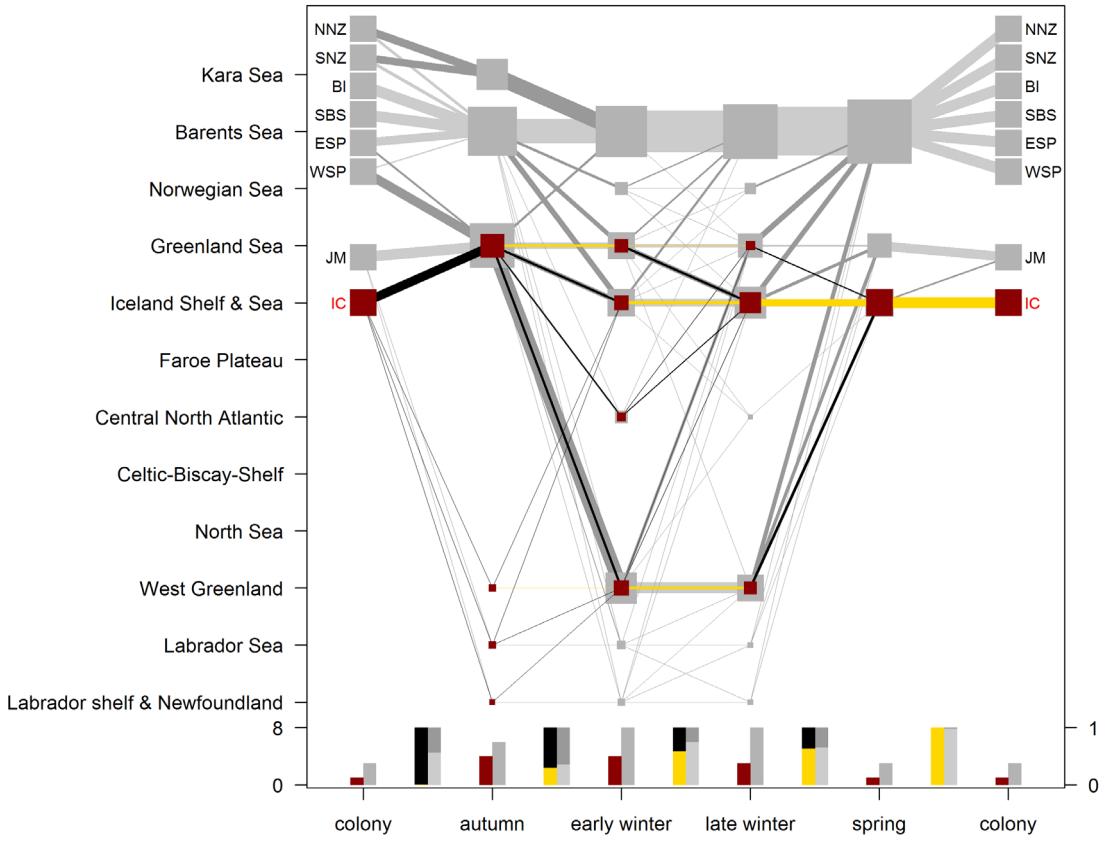

Figure S3.9. Brünnich's guillemots, North-East Iceland (Grimsey, Langanes)

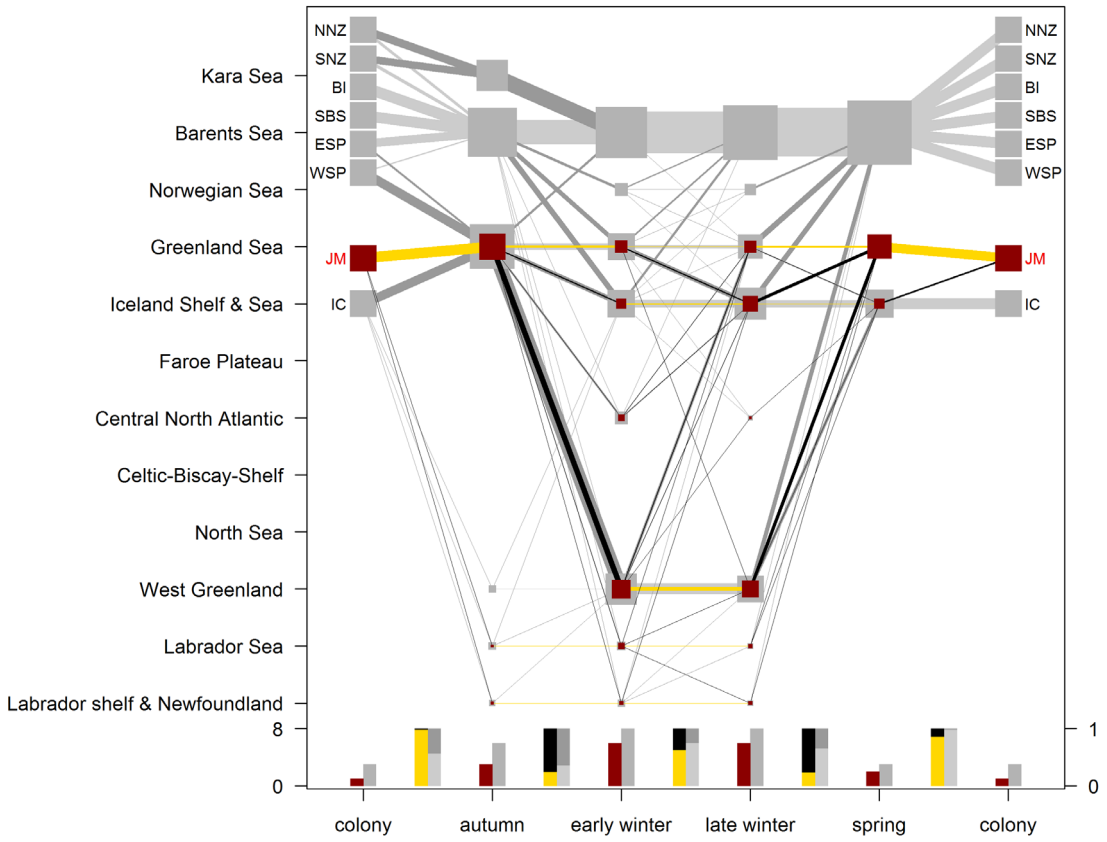

Figure S3.10. Brünnich's guillemots, Jan Mayen

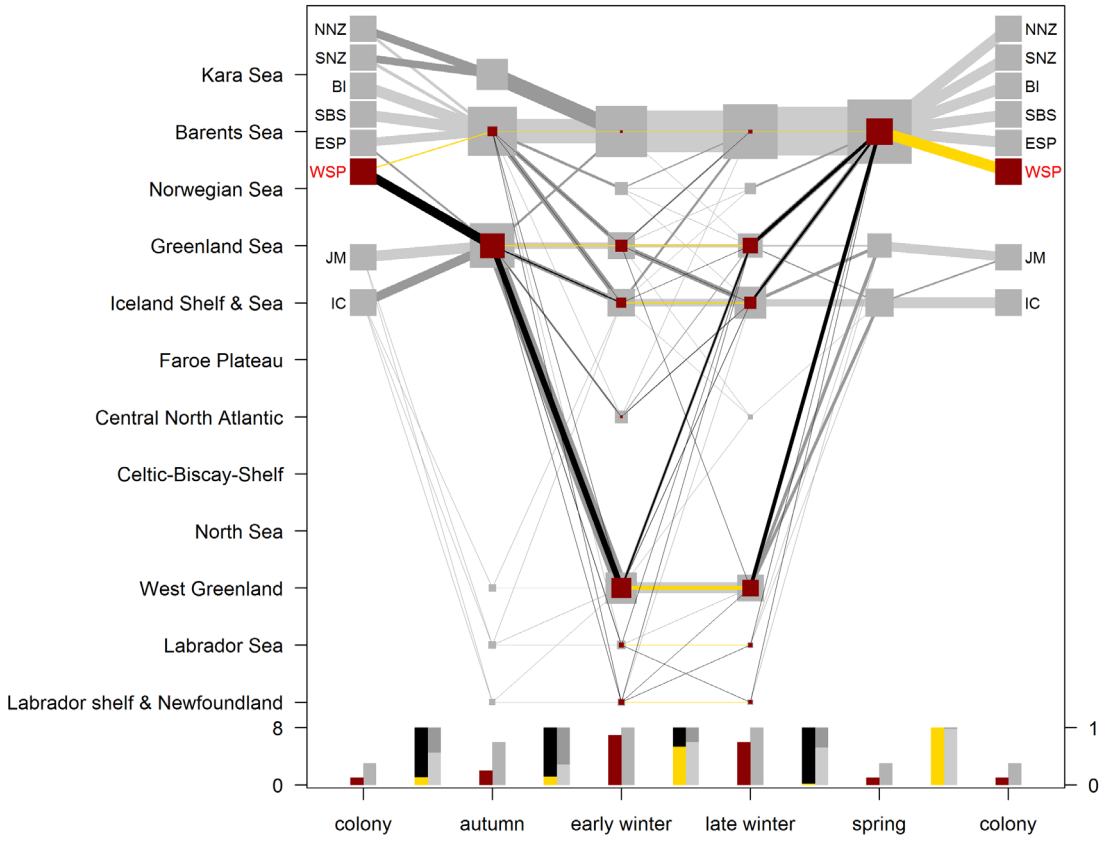

Figure S3.11. Brünnich's guillemots, Western Spitsbergen (Diabas, Ossian Sarsfjellet and John Scottfjellet)

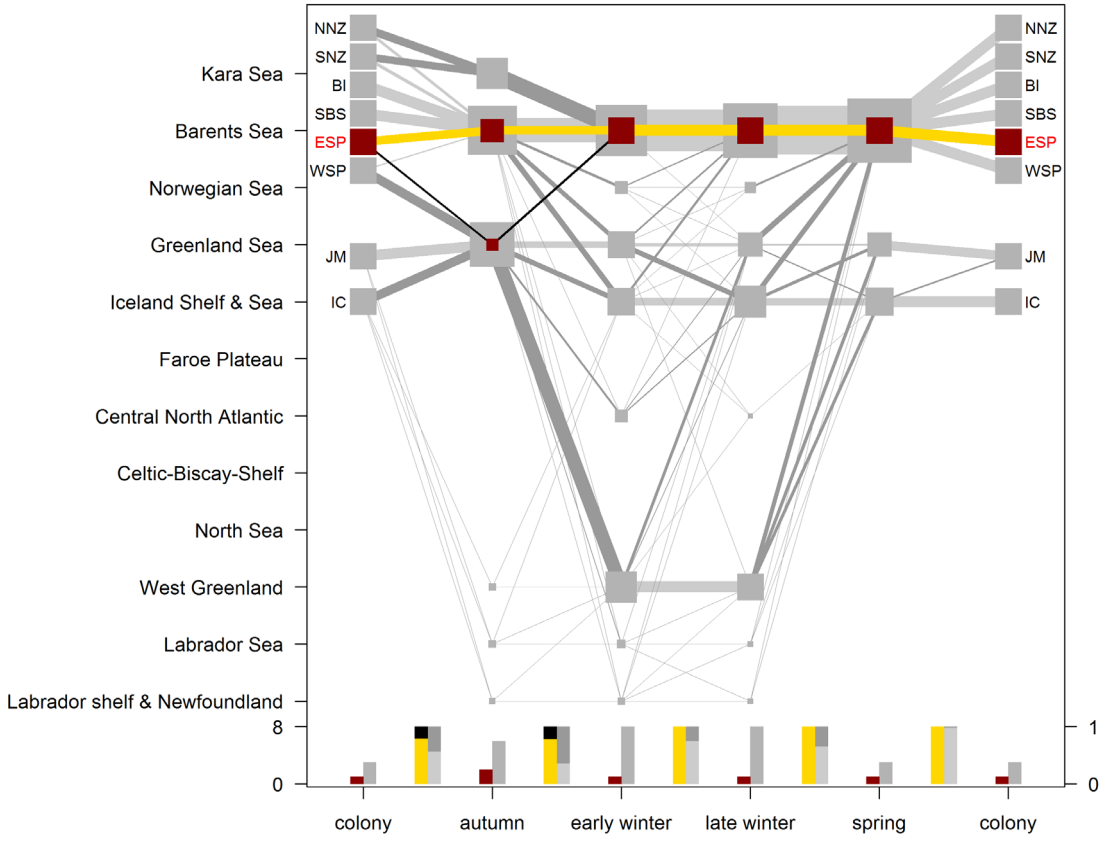

Figure S3.12. Brünnich's guillemots, Eastern Spitsbergen (Alkefjellet)

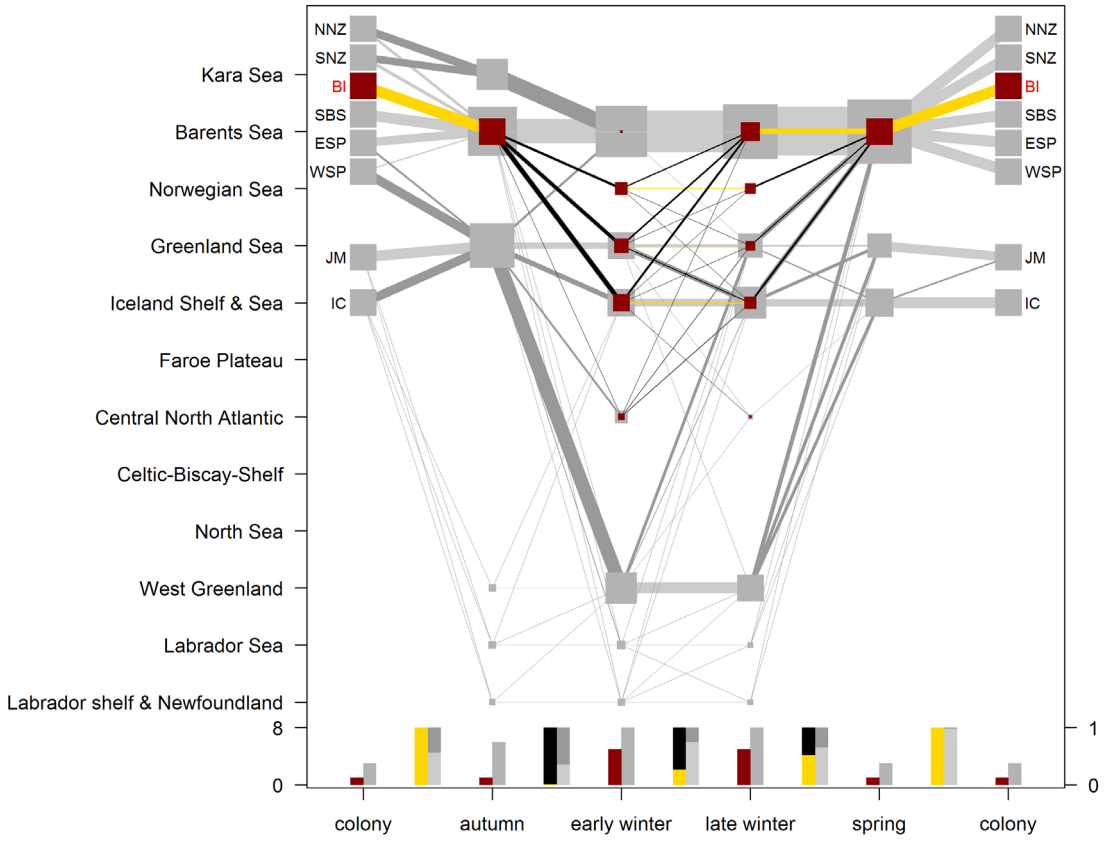

41

42 **Figure S3.13.** Brünnich's guillemots, Bjørnøya

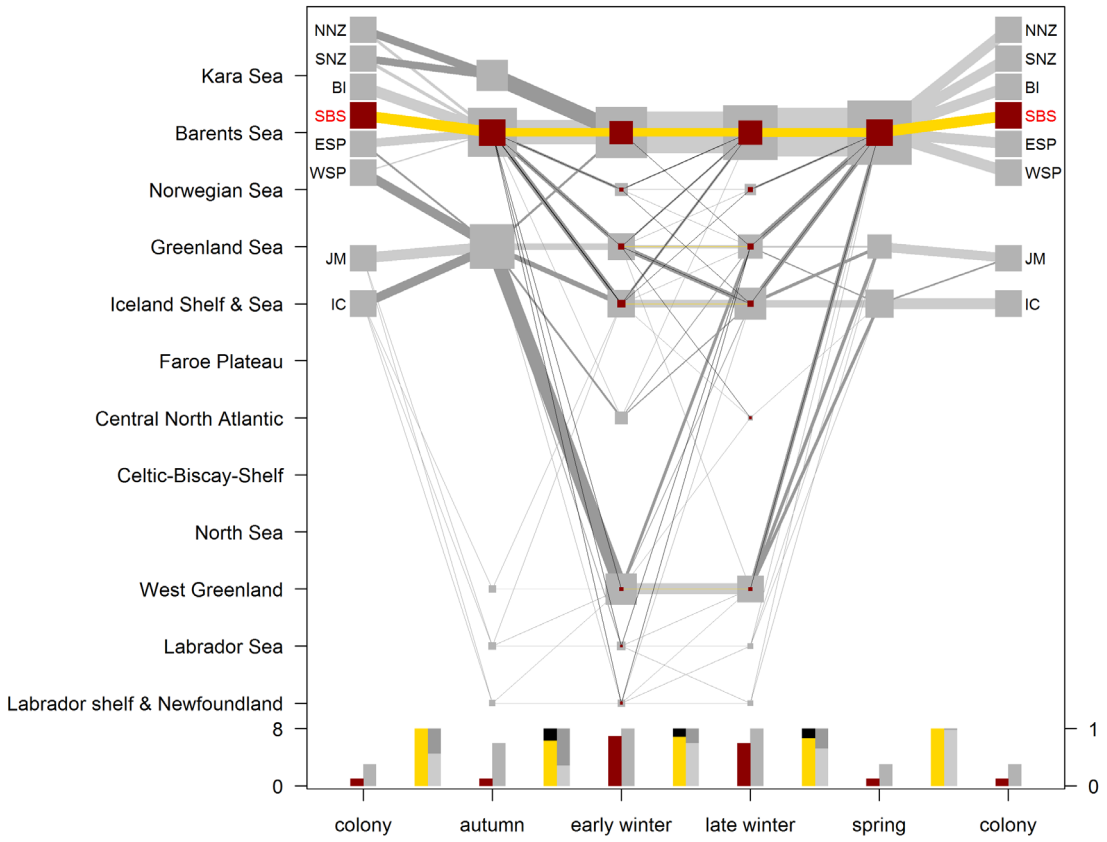

43

44 **Figure S3.14.** Brünnich's guillemots, Southern Barents Sea (Hornøya and Cape Gorodetskiy)

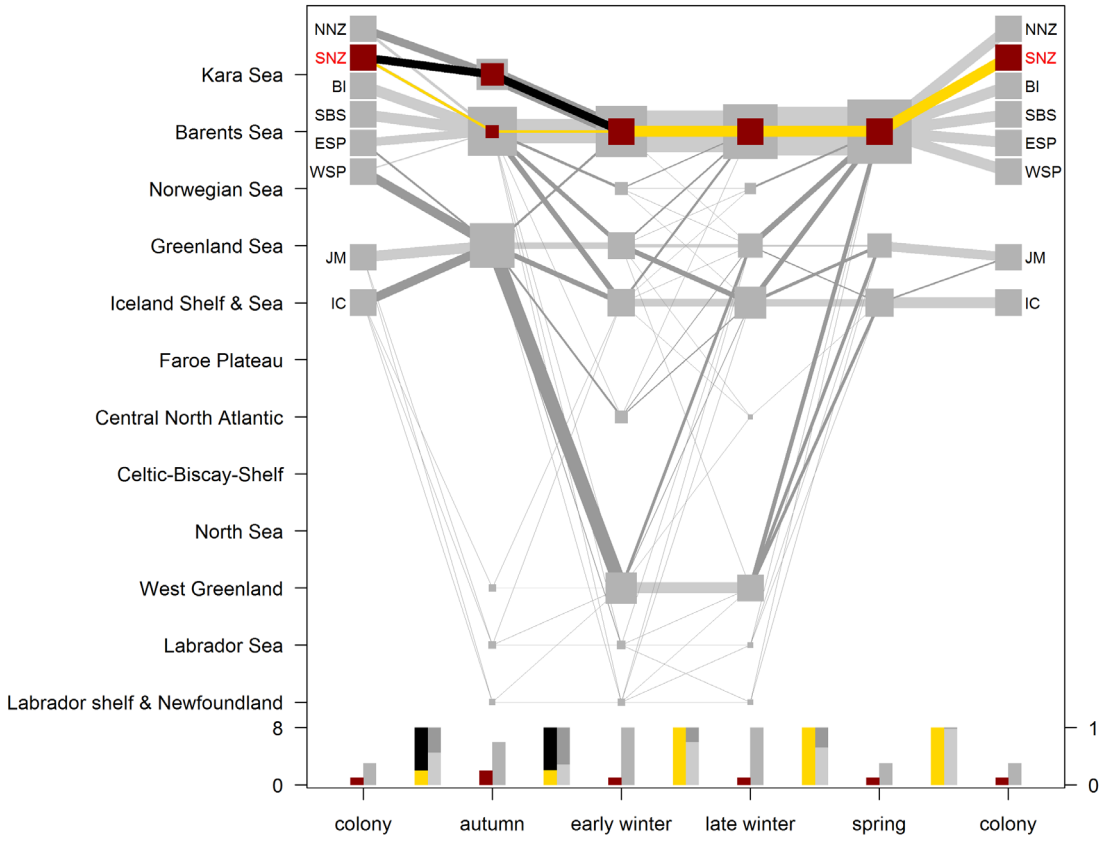

Figure S3.15. Brünnich's guillemots, Southern Novaya Zemlya (Kara Gate)

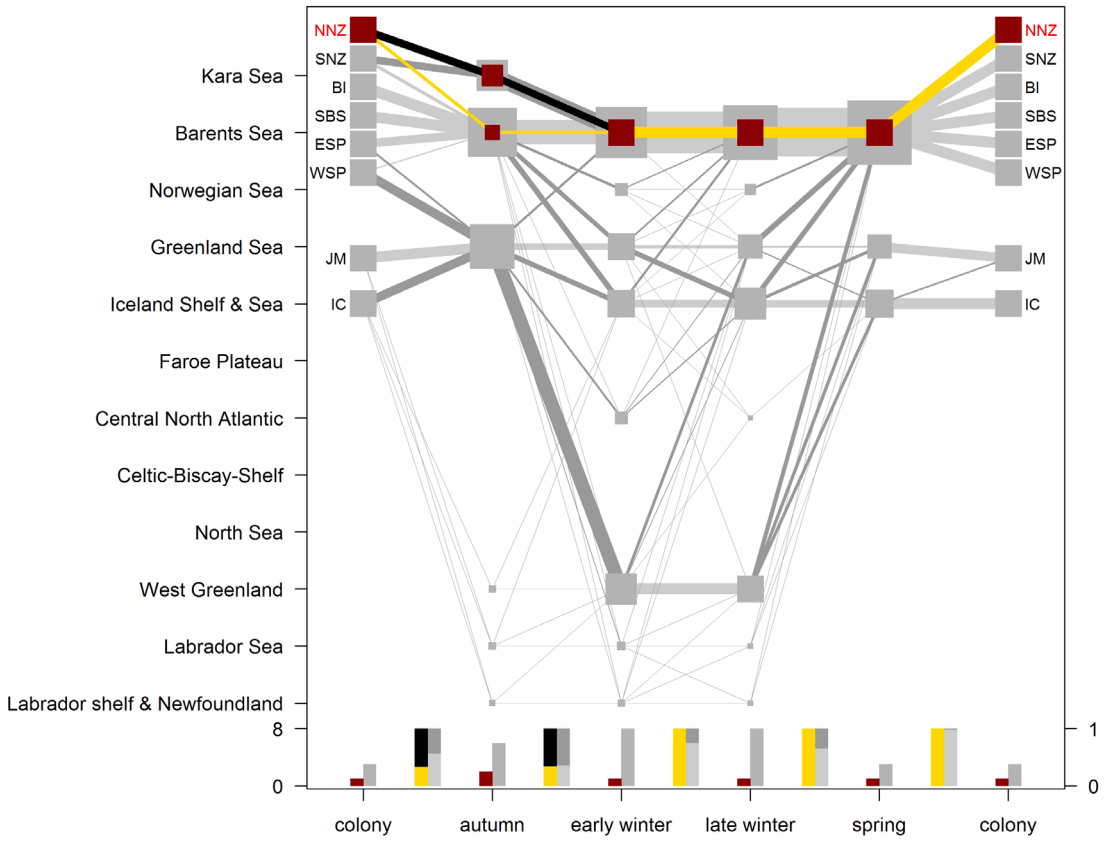

Figure S3.16. Brünnich's guillemots, Northern Novaya Zemlya (Oranskie islands)